GCIP water and energy budget synthesis (WEBS)

J. Roads,[1] R. Lawford,[2] E. Bainto,[1] E. Berbery,[3] S. Chen,[1] B. Fekete,[4] K. Gallo,[5] A. Grundstein,[6] W. Higgins,[7] M. Kanamitsu,[1] W. Krajewski,[8] V. Lakshmi,[9] D. Leathers,[10] D. Lettenmaier,[11] L. Luo,[12] E. Maurer,[11] T. Meyers,[13] D. Miller,[14] K. Mitchell,[7] T. Mote,[6] R. Pinker,[3] T. Reichler,[1] D. Robinson,[12] A. Robock,[12] J. Smith,[15] G. Srinivasan,[16] K. Verdin,[17] K. Vinnikov,[3] T. Vonder Haar,[18] C. Vörösmarty,[4] S. Williams,[19] and E. Yarosh[7]

Received 28 May 2002; revised 25 October 2002; accepted 10 December 2002; published 12 August 2003.

[1] As part of the World Climate Research Program's (WCRPs) Global Energy and Water-Cycle Experiment (GEWEX) Continental-scale International Project (GCIP), a preliminary water and energy budget synthesis (WEBS) was developed for the period 1996–1999 fromthe "best available" observations and models. Besides this summary paper, a companion CD-ROM with more extensive discussion, figures, tables, and raw data is available to the interested researcher from the GEWEX project office, the GAPP project office, or the first author. An updated online version of the CD-ROM is also available at http://ecpc.ucsd.edu/gcip/webs.htm/. Observations cannot adequately characterize or "close" budgets since too many fundamental processes are missing. Models that properly represent the many complicated atmospheric and near-surface interactions are also required. This preliminary synthesis therefore included a representative global general circulation model, regional climate model, and a macroscale hydrologic model as well as a global reanalysis and a regional analysis. By the qualitative agreement among the models and available observations, it did appear that we now qualitatively understand water and energy budgets of the Mississippi River Basin. However, there is still much quantitative uncertainty. In that regard, there did appear to be a clear advantage to using a regional analysis over a global analysis or a regional simulation over a global simulation to describe the Mississippi River Basin water and energy budgets. There also appeared to be some advantage to using a macroscale hydrologic model for at least the surface water budgets. *INDEX TERMS:* 1655 Global Change: Water cycles (1836); 3309 Meteorology and Atmospheric Dynamics: Climatology (1620); 3322 Meteorology and Atmospheric Dynamics: Land/atmosphere interactions; 1833 Hydrology: Hydroclimatology; *KEYWORDS:* hydrologic cycle, water cycle, water and energy budgets, regional models, land surface models

Citation: Roads, J. O., et al., GCIP water and energy budget synthesis (WEBS), *J. Geophys. Res.*, *108*(D16), 8609, doi:10.1029/2002JD002583, 2003.

[1]Scripps Institution of Oceanography, University of California, San Diego, La Jolla, California, USA.
[2]Office of Global Programs, National Oceanic and Atmospheric Administration, Silver Spring, Maryland, USA.
[3]Department of Meteorology, University of Maryland, College Park, Maryland, USA.
[4]Complex Systems Research Center, University of New Hampshire, Durham, New Hampshire, USA.
[5]National Environmental Satellite Data and Information Service, National Oceanic and Atmospheric Administration-U. S. Geological Survey EROS Data Center, Sioux Falls, South Dakota, USA.
[6]Department of Geography, University of Georgia, Athens, Georgia, USA.
[7]NOAA Science Center, Environmental Modeling Center-Climate Prediction Center, National Centers for Environmental Prediction, Camp Springs, Maryland, USA.
[8]IIHR-Hydroscience and Engineering, University of Iowa, Iowa City, Iowa, USA.
[9]Department Geological Sciences, University of South Carolina, Columbia, South Carolina, USA.
[10]Department of Geography, University of Delaware, Newark, Delaware, USA.
[11]Department of Civil and Environmental Engineering, University of Washington, Seattle, Washington, USA.
[12]Department of Environmental Sciences, Rutgers University, New Brunswick, New Jersey, USA.
[13]Air Turbulence and Diffusion Division, National Oceanic and Atmospheric Administration, Oak Ridge, Tennessee, USA.
[14]Environment Institute, College of Earth and Mineral Sciences, Pennsylvania State University, University Park, Pennsylvania, USA.
[15]Department of Civil and Environmental Engineering, Princeton University, Princeton, New Jersey, USA.
[16]Earth System Science Division, Department of Science and Technology, New Delhi, India.
[17]U. S. Geological Survey EROS Data Center, Sioux Falls, South Dakota, USA.
[18]Department of Atmospheric Science, Colorado State University, Fort Collins, Colorado, USA.
[19]University Corporation for Atmospheric Research, Boulder, Colorado, USA.

0148-0227/03/2002JD002583$09.00

1. Introduction

[2] The World Climate Research Program (WCRP) Global Energy and Water-Cycle Experiment (GEWEX) Continental-scale International Project (GCIP) was originally developed in the early 1990s for the purpose of assessing the accuracy to which water and energy budgets could be characterized and "closed" on a continental scale [*National Research Council (NRC)*, 1998]. GEWEX chose the Mississippi River Basin as the first Continental Scale Experiment (CSE), in part because the Mississippi River Basin is one of the major river systems of the world. It drains 41 percent of the Conterminous United States with a 3.2 million square kilometer basin, second largest river basin area in the world. At 3,705 km, the Mississippi is the longest river in North America and the third largest in the world. Its discharge of 17,300 cubic meters per second into the Gulf of Mexico ranks the Mississippi as the fifth largest in the world in this category (see Mississippi River Basin Alliance (MRBA) website at http://www.mrba.org and *Wiener et al.* [1998] (available online at http://biology.usgs.gov/s+t/SNT/noframe/ms137.htm). Elevations within the Mississippi River Basin range from sea level at the mouth of the Mississippi to some of the highest peaks in North America. The topography varies from low-lying swampland to undulating hills to craggy mountain peaks. Perhaps more importantly, however, no other identified basin at the time had the Mississippi River Basin's observational infrastructure and data richness as well as promise of future observing system development.

[3] There were a number of GCIP challenges. While the continental-scale Mississippi River Basin is large by hydrological standards, which have traditionally focused on hillslope to watershed scales, it is small by atmospheric standards, which have traditionally focused on continental to global atmospheric features. While the Mississippi River Basin has a great number of observations, available observations are still quite inadequate for characterizing, much less "closing" water and energy budgets. While the Mississippi River Basin has a number of distinct climate zones, it is not fully representative of all of the world's climate zones.

[4] Recognizing this latter challenge, a number of other CSEs in many different climate regimes began soon after GCIP. The CSEs and affiliated experiments are loosely coordinated by the GEWEX Hydrometeorology Panel (GHP) and include nine representative world climate regions. The regions over the Americas include the Mackenzie [*Stewart et al.*, 1998], Mississippi [*Lawford*, 1999], and Amazon (J. Marengo et al., On the atmospheric water budget and moisture cycling in the Amazon basin: Characteristics and space-time variability, submitted to *International Journal of Climatology*, 2002) river basins. In Europe, there is an experiment for the Baltic [*Raschke et al.*, 1998, 2001] and over Asia 4 GAME [*GAME International Science Panel*, 1998] sites over the Lena River Basin, HUBEX, Tibet, and tropical, regions. An affiliated experiment (CATCH) [*D'Amato and Lebel*, 1998] has begun over western equatorial Africa. About half of the CSEs are major river basins (Mackenzie, Mississippi, Amazon, Lena), one is an inland sea (Baltic), and the rest cover large-scale regions (CATCH, GAME-HUBEX, GAME-Tibet, GAME-Tropics). *Roads et al.* [2002a] describe some of the basic hydroclimatological characteristics of these CSEs.

[5] Following the pioneering work of *Rasmusson* [1967, 1968], continental-scale GCIP water and energy budget studies were undertaken by *Roads et al.* [1994, 1997, 1998, 1999, 2001, 2002a], *Roads* [2002], *Roads and Betts* [2000], *Roads and Chen* [2000], *Berbery et al.* [1996, 1999], *Berbery and Rasmusson* [1999], *Berbery* [2001], *Yarosh et al.* [1999], *Maurer et al.* [2001a, 2001b] with limited data and models. In this paper, the water and energy budgets of the Mississippi River Basin are again examined, but with a representative suite of models and observations developed, in part because of GCIP. In addition to global atmospheric models, there are now regional atmospheric and continental land surface models. In addition to operational global analyses there are now global reanalyses and operational regional analyses as well as a pending regional reanalysis. Additional satellite data is now available and can provide validation fields for a number of variables. Quality controlled gridded observations of precipitation, runoff, water vapor, and many radiation components are now available. High resolution Next Generation Radar (NEXRAD) [*NRC*, 1999] precipitation is beginning to become available. Soil moisture and tower flux measurements are also beginning to be measured at a number of sites.

[6] The goal of this community effort was to begin what might be vaguely thought of as the "best available" water and energy budget synthesis (WEBS) at the end of GCIP and start of the follow-on GEWEX Americas Prediction Project (GAPP). By necessity, WEBS must include models as well as observations and in this paper some representative global and regional analyses, global and regional simulations, are compared with a macroscale hydrologic model and available observations. It should be noted that the range of models used here only represents and does not summarize all of the modeling activities taking place during GCIP. It should also be noted that despite our best effort to include the best possible data and models, various model improvements and new observations and data sets have since been developed that could eventually help to improve our estimates. Again, our goal was to develop the "best available" rather than wait forever for the latest research refinements.

[7] There were a number of obvious questions. What is the relative contribution of moisture convergence and evaporation to the precipitation? Does the moisture convergence balance the surface runoff? What is the relative contribution of precipitation, evaporation to runoff? What is the relative contribution of the latent heat released by precipitation to the radiational cooling, sensible heating and dry static energy convergence? How is the surface radiation balanced by turbulent transfers of sensible and latent heat from the surface to the atmosphere? These questions can be answered, in part, by examination of the water and energy budget terms shown in this paper. In addition, there is a corresponding CD-ROM [*Roads et al.*, 2002b], which includes an expanded version of this summary paper, a more extensive set of tables, figures, and most of the monthly mean digital data. An updated online version of the CD-ROM is also available at http://ecpc.ucsd.edu/gcip/webs.htm/.

[8] This WEBS has focused for the most part on developing a seasonal climatology for the 1996–1999 period, when GCIP was fully active. Interannual variations during

this time period were minimal so the GCIP time period has been somewhat extended, mainly with the help of models, to also cover the 1988–1999 time period. Although long-term trends need to be better understood, only by studying interannual variations on much longer time scales will the confidence be gained to adequately describe these more subtle variations. In that regard, this WEBS could be the start of a longer-term effort in collaboration with WEBS activities in other CSEs to an eventual global synthesis. This GCIP WEBS also ignores diurnal variations, despite their potential importance to the moisture budgets. For example, there is a nocturnal jet in the Mississippi River Basin that appears to be related to nighttime precipitation maximum on the Rocky Mountain Front Range. Understanding better the character of the diurnal variations here as well as in other U.S. geographic regions will be one of the focuses of the new GEWEX Americas Prediction Project (GAPP).

[9] As will be shown, despite substantial progress during GCIP there is still much uncertainty. This uncertainty arises in part from the lack of adequate observations to fully characterize all of the processes. For example, soil moisture, evaporation and sensible heating, and various radiative components, are only measured in a few regions, water and energy transports can only be calculated from radiosondes over large-scale regions. Even a few of the variables that are inferred from remote sensing, such as surface skin temperature and solar radiation, must use a model tuned to only a few sites. Atmospheric and hydrologic models that attempt to synthesize this information are imperfect and even analysis output, which attempts to make use of all available data, is biased toward imperfections in the model.

[10] This paper is organized as follows. Section 2 provides an overview of the physiography (soils, topography, vegetation) of the Mississippi River Basin. Section 3 discusses characteristics of the observations. Section 4 discusses characteristics of the models and numerical analyses. Section 5 discusses the water and energy budgets. Section 6 summarizes the annual basin means. Section 7 summarizes the basin mean seasonal variations. Section 8 discusses interannual variations. A summary is provided in section 9.

2. Physiography

[11] Models, especially high-resolution hydrologic models are beginning to take advantage of the high-resolution physiography available for the Mississippi River Basin as well as the rest of the United States. To provide some background for the physiography increasingly being used for the models, topography, soils, and vegetation of the Mississippi River Basin are briefly described below.

[12] Although several scales of topographic data exist for most of the Mississippi Basin, the primary data set available for the entire basin is the U.S. Geological Survey HYDRO1k data set. The goal of the HYDRO1k data set (Data are available without restriction from the EROS Data Center's web site at http://edcwww.cr.usgs.gov/landdaac/gtopo30/hydro1k) was to develop hydrologically sound derivative data layers for the globe. On the basis of the USGS' GTOPO30 DEM, the HYDRO1k data set is an ensemble package, with a cell size of 1 km, containing eight data layers including elevations (Figure 1a), slope, aspect, compound topographic index, flow directions, flow accumulations, synthetic streamlines and drainage basins.

[13] The USDA-NRCS, through the National Cooperative Soil Survey (NCSS), is in the process of developing soil geographic databases for the United States. At the regional level, the State Soil Geographic Database (STATSGO) was released in 1992 for use in river basin, multicounty, multistate, and state resource planning. This database was created by generalizing available soil survey maps, including published and unpublished detailed soil surveys, county general soil maps, state general soil maps, state major land resource area maps, and, where no soil survey information was available, Landsat imagery [*Reybold and Tesselle*, 1988]. STATSGO consists of geo-referenced digital map data and associated digital tables of attribute data. The compiled soil maps were created using the USGS 1-degree by 2-degree topographic quadrangles (1:250,000 scale, Albers Equal Area projection) as base maps, which were then merged on a state basis. *Miller and White* [1998] developed a multilayer soil characteristics data set for the Conterminous United States http://www.essc.psu.edu/soil_info) from the separate STATSGO data sets. This data set (CONUS-Soil) provides soil physical and hydraulic properties for a set of standard layers extending to 2.5 m below the surface. Properties in CONUS-Soil include: soil texture class and particle-size fractions, bulk density, porosity, depth-to-bedrock, rock fragment volume, rock fragment class, available water capacity, permeability, plasticity, ph, K-factor (erosion), hydrologic soil group, and curve number (Figure 1b).

[14] Land cover information for the Mississippi River Basin (Figure 1c) was extracted from the IGBP Global Land Cover Characteristics Data set [*Loveland and Belward*, 1997]. The land cover classes were derived from monthly composites of a satellite-derived normalized difference vegetation index (NDVI) and include the most dominant land cover class per 20 km^2 grid cell as prepared for an analysis that links seasonal vegetation patterns to the three most dominant land cover classes within each 20 km^2 grid cell of the Conterminous United States [*Gallo et al.*, 2001]. The IGBP Land Cover Data set is available from the USGS EROS Data Center http://edcdaac.usgs.gov/glcc/glcc.html). Four IGBP land cover classes dominate the Mississippi River Basin. Over 75% of the land cover includes croplands (21.5% of the region), grasslands (21%), cropland/natural vegetation mosaic (20.8%), and deciduous broadleaf forest (16.5%). Urban and built-up areas represent <1% of the land cover within the region. The croplands dominate the North-Central part of the Basin; the grasslands dominate the West; deciduous forests dominate the Southeast portion of the region. The cropland/natural vegetation mixture includes clusters of homogeneous areas in the North and Western parts of the region.

[15] The satellite-derived NDVI data were also used to examine the seasonal characteristics of vegetation within the region. The NDVI data used in this analysis included biweekly composite products produced at the USGS EROS Data Center [*Eidenshink*, 1992; *Eidenshink and Faundeen*, 1994]. The composite products are based on daily, full resolution (1.1 km^2 at nadir) AVHRR scenes that were geometrically registered to a Lambert azimuthal equal-area map projection such that each map cell of the georegistered products represents 1 km^2. The daily scenes were compos-

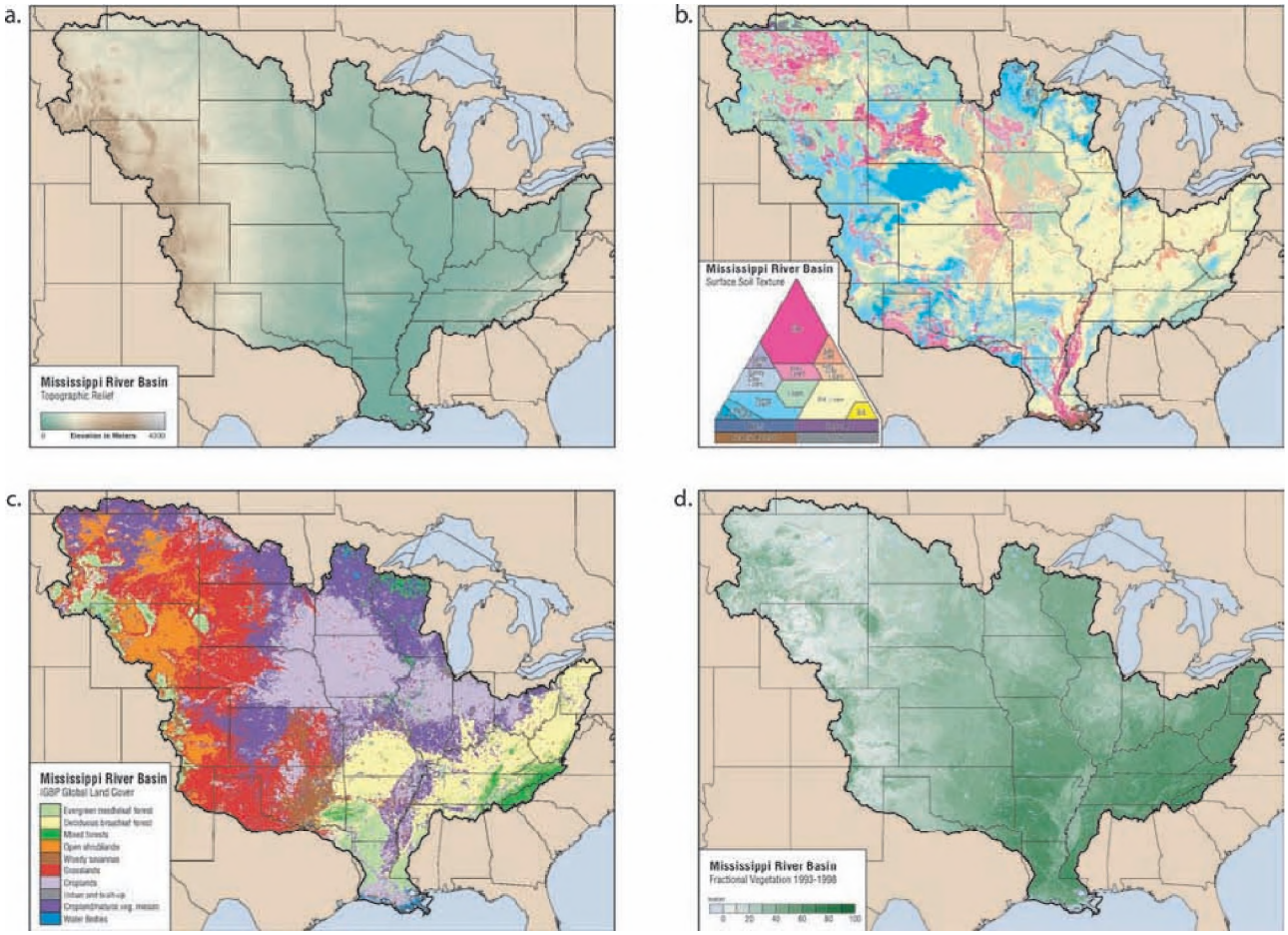

Figure 1. Physiographic characteristics of the Mississippi River Basin. (a) Topographic relief. (b) Surface soil texture. (c) Dominant IGBP land cover classes. (d) Annual mean fractional vegetation in the Mississippi River Basin.

ited on a biweekly basis such that the data value from the scene that exhibited the largest daily value of the NDVI was retained in the biweekly product. The composite process is a method for the removal of cloud-contaminated data from the biweekly data as clouds have very low NDVI values compared to vegetated land surfaces. The fractional green vegetation (Fgreen), defined as the fraction of horizontal area associated with the photosynthetically active green vegetation that occupies a specific area (e.g., 1 km × 1 km grid cell), was then computed from the NDVI values as described by *Gallo et al.* [2001].

[16] The annual mean (1993–1998, excluding 1994) Fgreen (Figure 1d) is greatest in the deciduous forest regions of the Mississippi River Basin where the duration of green vegetation is greatest. The cropland and croplands/natural vegetation regions display the next greatest levels of annual Fgreen. Each of the land cover classes displays unique seasonal trends in monthly Fgreen that depicts the spring green-up and autumn green-down observed for the region. The cropland class typically has the largest Fgreen value. The forests typically will green-up early compared to cultivated crops. All of the classes include some degree of green-up and green-down, an indication of the seasonality of the MRB region. Some of the classes, for example, the grassland class, may display bimodal green-up/green-down events, related to the rainfall within the region. In summary, there are four dominant land cover classes, all of which display patterns of green-up and green-down that reflect the seasonality of the region. The Fgreen and land cover information can be collectively used to monitor the seasonal progression of green-up and green-down throughout the region. Fgreen data are available at the UCAR/NOAA Joint Office for Science Support Data Management Center http://www.joss.ucar.edu/cgi-bin/codiac/dss?21.064).

3. Observations

[17] As described by *Higgins et al.* [2000] available meteorological observation networks have included the World Meteorological Organization (WMO) Global Telecommunication (GTS) sites, 24-hour reports from the River Forecast Centers, and NCDC cooperative stations [*National Oceanic and Atmospheric Administration* (*NOAA*), 1995], as well as many potential sites from SNOTEL and remote automated weather stations (RAWS). In addition, standard observations include the U. S. Geological Survey (USGS) streamflow measurements the upper air radiosonde network [*Eskridge et al.*, 1995] and aircraft measurements of

Table 1. Basic Observations Available for GCIP Water and Energy Budget Studies Along With a Subjective Evaluation of These Variables[a]

Variables	Measurement or Data Set	None/Poor/Good/Excellent
Precipitable Water	NVAP	Missing 1999; need higher resolution observations.
Surface Water	In situ, Illinois	Need more in situ observations.
Snow	Obs. plus SNWTHRM model	Need more months and combined satellite gauge.
Skin Temperature	*Janowiak et al.* [1999] gauge, *Lakshmi and Susskind* [2000] TOVS	Gauge only has T_{max}, T_{min}. Need combined satellite gauge skin temperature.
Precipitation	*Higgins et al.* [2000] gauge, *Smith et al.* [1996] NEXRAD	NEXRAD only has summer months. Undercatch issues not yet resolved for gauges.
Evaporation	2 Flux towers	Need more observations.
Moisture Conv.	A few radiosondes	Only basin means from observations.
Runoff	GRDC; see section 3.3	GRDC was not corrected for management effects and only included monthly means. *Maurer and Lettenmaier* [2001] only have basin-wide runoff values.
Dry Static Energy Conv.		
Sensible Heating	2 flux towers	Need more observations.
Atmospheric Radiative Cooling		
Surface Radiative Heating		
Radiation Fluxes	*Pinker et al.* [2003] solar, *Lakshmi and Susskind* [2000] olr (TOVS)	Need net surface longwave and more flux tower measurements.

[a]"None" indicates that no observations are available; "poor" indicates that there are some observations but not enough to develop a basin wide summary; "good" indicates that these variables are useful for basin means but that there are still some problems that prevent them from being fully utilized; and "excellent" indicates that no additional work is needed, at least in comparison to imperfect models.

temperature and wind [e.g., *DiMego et al.*, 1992]. New measurements begun during GCIP include the NEXRAD [*NRC*, 1999] radar network for precipitation [*Smith et al.*, 1996], various soil moisture measurements to complement the existing meager networks [*Robock et al.*, 2000], and flux tower measurements.

[18] Satellite measurements include the GEWEX NVAP water vapor [*Randel et al.*, 1996], the Pinker [*Pinker et al.*, 2003] solar radiation, and various other satellite products of standard variables derived from TOV [*Lakshmi and Susskind*, 2000] such as outgoing longwave radiation and surface skin temperature. Although GEWEX precipitation products such as the Global Precipitation Climatology Product [*Xie and Arkin*, 1997], and Tropical Rainfall Measuring Mission (TRMM, see *Adler et al.*, 2000) could have been utilized, standard products (2.5 × 2.5) are still relatively coarse in comparison to the standard higher resolution gauge [*Higgins et al.*, 2000] and NEXRAD [*Smith et al.*, 1996] products available to us.

[19] It should also be noted here that there are numerous plans for future satellite measurements, including: a cold seasons mission, which will attempt to develop algorithms for measuring snow equivalent water, a soil moisture mission, which will attempt to measure soil moisture in the upper few centimeters, a gravimetric mission, which will attempt to measure groundwater, and a satellite altimetry mission, which will measure river and lake levels. There are also plans to develop GEWEX radiation data sets. From our experience with this WEBS, it is recommended satellite products be transitioned into operational streams as soon as possible so that GAPP and other field measurement programs can take advantage of them.

[20] Finally, it should again be stressed that the water and energy budgets cannot be adequately characterized much less closed with observations, since many of the water and energy budget processes are not measured, in any meaningful way, on a continental scale. However, the available observations can at least be used to estimate how accurately the models and analyses to be discussed in the next chapter are simulating various terms. These comparisons, models with models, and models with limited observations, provide an estimate as to what error these models might have, which then provides clues as to how accurately the budgets are closed with models and analyses. Further details about some of the observations are provided below. A summary of the applicability of these observations is presented in Table 1 and in section 3.8.

3.1. Radiosondes

[21] Balloon borne radiosonde measurements provide our basic measurements for upper air measurements of temperature, humidity, winds, and pressure, as well as some derived quantities such as moisture and dry static energy fluxes and associated convergence and divergence. These expendable sensors are released twice daily (11Z and 23Z) at about 33 stations (the NCDC archives have about 169 stations at scattered global locations) within the Mississippi River Basin (Figure 2a). Although the number of locations and frequency of observations have been steadily decreasing, the analysis models have gotten better and have also been able to take advantage of a number of other observations (such as satellite measurements) that may ultimately have lower cost than the expensive radiosondes system. In that regard, it should be mentioned that modern analysis systems also have extensive quality control procedures to fix observation problems and analyses may therefore be producing superior artificial soundings. In fact, recent investigations of upper air moisture transports have tended to rely on the analysis products. Still, the analyses are a blend of coarse-scale numerical weather prediction forecasts and other observations, and just because an analysis method utilizes radiosondes, it

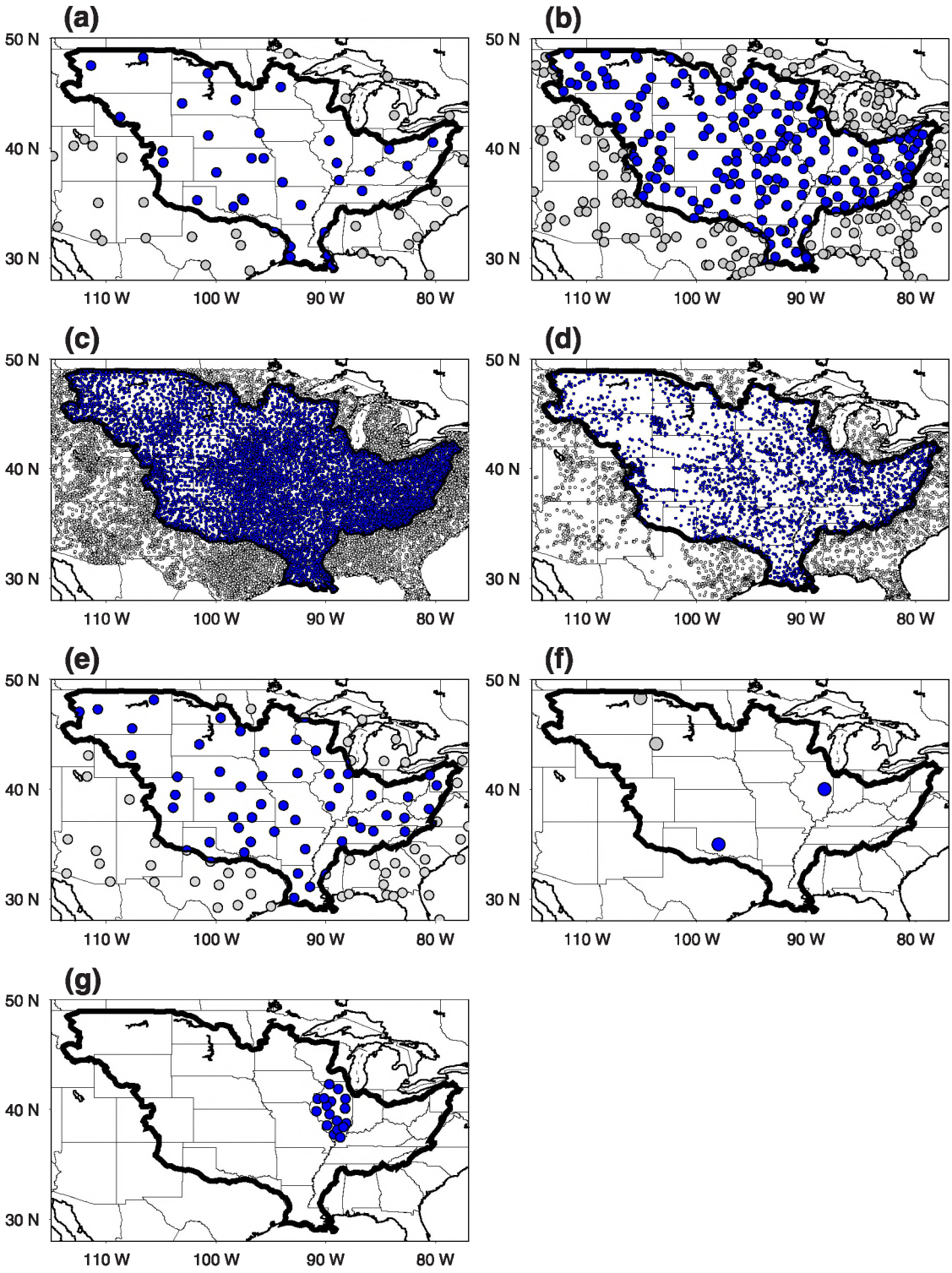

Figure 2. Mississippi River Basin observation networks for the period 1996–1999. (a) Radiosonde stations (34). (b) NCDC first-order stations (163). (c) NCDC COOP stations [8761]. (d) USGS streamflow gauges [2282]. (e) NEXRAD sites (51). (f) Flux tower sites (2). (g) In situ soil moisture measurements (19).

does not mean that these radiosonde observations will be identically emulated.

3.2. Surface Meteorology

[22] The principal surface stations used for the comparisons in this paper are the first-order stations at which temperature, relative humidity, wind speed and wind direction, and other meteorological observations are taken. There are about 300 such stations archived by NCDC; about 250 are present over the chosen domain (Figure 2b). These stations have hourly information from the many automatic recording instruments available at these sites. Radiosonde stations are usually close but independently located from surface stations. According to *DiMego et al.* [1992], an

advantage to the regional analysis, over the global analysis, performed at NCEP, is that it incorporates surface measurements of pressure, temperature, and humidity whereas the global analysis only includes surface pressure. Neither the global or regional analyses incorporate surface measurements of wind, since grid point winds are presumed not to be able to accurately represent surface wind measurements; at the same time surface wind measurements at the scattered first-order stations are not thought to be representative of the large-scale winds over large areas.

[23] In addition to these first-order stations where a number of meteorological variables are measured, the National Climatic Data Center [*NOAA*, 1995] maintains a huge network of cooperative stations (about 5000 in the Mississippi River Basin, Figure 2c), which measure daily max min temperature and precipitation (instrument shelters are 1.5 m above the surface) as a cooperation between NCDC and many volunteers. As stations change, because of ownership changes, deaths, etc., NCDC has attempted to locate sites in nearby regions, in order to maintain some climatic continuity. Many of these stations have been in existence for over 100 years. Hourly precipitation is also available from a number of stations maintained by the River Forecast Centers.

[24] The NCDC and first-order station network along with the precipitation network of the River Forecast Centers (not shown) was utilized by *Janowiak et al.* [1999] to develop gridded surface air temperature and by *Higgins et al.* [2000] to develop gridded daily precipitation. Gridding suffers somewhat from sampling errors associated with the sparse areal density of stations, particularly for convective rainfall. Additionally, systematic errors are associated with biases in the location of gauges (especially in areas of high topographic relief) and in the under catch of precipitation by individual gauges, especially for solid or intense precipitation. Nonetheless, is assumed that these gridded data sets provide the best available gridded set of observations available for temperature and precipitation. Comparison of precipitation with other products, including the NEXRAD based precipitation data set indicates small differences at the regional scales (25 km) examined here.

3.3. Runoff

[25] Streamflow is an integrator of surface runoff, and therefore (absent seepage or exfiltration from or to the river channel) the aggregate runoff (N) from a basin of any size can be estimated from stream discharge observations. In practice, discharge observations are made at gauging stations, where the direct observation is of stream water level, or stage, which is transformed to discharge via a rating curve, usually a curve fit through a set of discrete coincident observations of stage and discharge. The location of a stream gauge defines an upstream drainage area. The USGS stream-gauging network routinely collects streamflow data at more than 7000 locations in the U.S. (Figure 2d), and daily streamflow records totaling more than 400,000 station-years are held in USGS archives. Using this and other global observations as well as a climate-driven water balance model, *Fekete et al.* [2000] developed a global 0.5-degree climatological data set, which is the basis for some of the comparisons reported here. This data set uses discharge observations generally from the mid-1960s through the mid-1980s, which may not be wholly appropriate for comparison with the basic 1996–1999 GCIP period studied here.

[26] Groundwater flow divergence (that is, lateral flow) and changes in groundwater storage are not well observed except in areas of intensive groundwater management, and certainly not at continental or global scales. The location and density of groundwater monitoring wells is mostly determined by management concerns. Groundwater fluxes and storage changes are currently considered only in a cursory manner, if at all, by climate monitoring networks. Interpretation of monitoring well data is greatly complicated by local effects, such as pumping, which makes extraction of regional fluxes, and hence the surface water balance, difficult. In some cases, water balances can be conducted over regions (e.g., large river basins) for which geologic considerations dictate that groundwater flow across the boundaries is minimal. Even in these cases, however, changes in groundwater storage can complicate interpretation of regional water budgets. Present groundwater observation networks are unable to provide fundamental information about the amount and interannual variability of three critical fluxes. First, in systems ranging from large rivers to semiarid region riparian areas, groundwater-surface water interchange is not currently well characterized (and is largely ignored in the current generation of land-atmosphere models). Second, groundwater discharge to estuaries and oceans is largely unmeasured, even though some studies have shown that it can account for a substantial fraction of the net movement of fresh water from the continents to the oceans. Third, observation networks cannot discriminate among groundwater recharge mechanisms that may dominate over different time scales. For example, diffuse vadose zone recharge in undeveloped arid and semiarid zones may be important over decade-to-century times, while on shorter time scales water fluxes may involve net upward flow, not recharge, due to vapor transport. In some smaller subareas of the GCIP-WEBS region, such as arid areas where other water budget components are small, the groundwater discharge may be a factor. However, at the larger scale of the Mississippi River Basin or major subbasins, groundwater discharge is unlikely to be a significant component of the water budget.

[27] It is also important to appropriately adjust for management effects. In that regard, "undepleted" (water management effects removed) basin mean runoff for the WebS-GCIP study area was estimated using observed flows at the Vicksburg, Mississippi gauge, which is currently operated by the U.S. Army Corps of Engineers. The Vicksburg gauge has been in continuous operation since 1928, and is the best representative gauge for the entire Mississippi River Basin. Estimates of the "undepleted" or "naturalized flow" were made from estimated 1995 depletions from the Missouri River basin [*U. S. Army Corps of Engineers*, 1998] and the Ohio, Upper Mississippi, Arkansas-Red-White, and lower Mississippi River basins [*Solley et al.*, 1998]. Scaling the 1995 depletion by the ratio of VIC model annual evapotranspiration in each year to VIC model 1995 evapotranspiration produced a time series of depletions for each year in the WebS period. Because the distribution of runoff production is far from uniform over the Mississippi River Basin, with a concentration of much

greater values in the southeastern area, the basin-wide average for the area upstream of Vicksburg is substantially lower than that for the entire basin, and therefore must be corrected for the effect of the area in the basin downstream of Vicksburg. Therefore the undepleted runoff at Vicksburg was prorated for the entire basin using the ratio of runoff (per unit area) for the entire Mississippi River Basin to runoff from the area contributing to flow at Vicksburg as simulated by the VIC model.

3.4. NEXRAD

[28] The new network of WSR-88D [*NRC*, 1999] radars (Figure 2e) has the potential to improve precipitation estimates in the United States by vastly increasing the effective sampling density of precipitation. For GCIP, hourly rainfall accumulation maps on a 4km grid have been developed from WSR-88D "composite reflectivity" mosaics for the United States. The composite reflectivity data set has a 15 min time resolution and is created by merging composite reflectivity products from individual WSR-88D radars. WSR-88D radars have a nominal range of 230 km for rainfall products. The national composite is developed by WSI as part of the NEXRAD Information Dissemination Service program, which has been distributed by NASA through December 2000. The hourly rainfall accumulation fields were aggregated to produce monthly rainfall accumulation fields for June, July, and August during the years 1996–1999. Rain gauge observations from the COOP observer network were used to determine Z-R relationships used in developing the hourly rainfall accumulation fields. The June–August rainfall accumulation products are based on an interim precipitation product that has been developed by J. A. Smith (Princeton) and W. F. Krajewski (U. Iowa). The final data set will ultimately have a time resolution of 1 hour and a spatial resolution of ~4 km. The most significant changes to the warm season data set will result from additional quality control steps and incorporation of detailed regional gage-radar studies that are being carried out regionally for the Mississippi River Basin. Additional QC will mitigate problems of radar calibration at several radar sites (and for only a portion of the 5-year period). Although this product is still experimental, it was decided to at least compare it to the standard Higgins based product since it is likely to be more heavily utilized in the future as various problems are eliminated. In fact, *Higgins et al.* [2000] utilized the NEXRAD data to correct for the large number of incorrect reports of zero precipitation in the station measurements. That is when the station indicated zero precipitation, but the NEXRAD values were >2 mm, then the station was eliminated from the precipitation analysis. The NEXRAD data was also quality controlled using high resolution GOES-IR data to screen out heavy hourly radar precipitation estimates when collocated temperatures are warmer than a set threshold.

3.5. NOAA Tower Measurement Program

[29] In order to provide a long-term continuous record of the surface energy balance components for model testing and evaluation, a tower measurement program was initiated under the NOAA contribution to the United States GCIP program [*Meyers*, 2001; *Wilson and Baldocchi*, 2000]. In June of 1995, the first system was installed within the Little Washita Watershed, which is located in the GEWEX/GCIP large-scale areas (LSA) in the southwestern (SW) region. In August 1996, a second system was fully operational on a farm location near Champaign, Illinois, which is in the GEWEX/GCIP north central (NC) region. Using the eddy covariance technique, the average vertical turbulent eddy fluxes of sensible and latent heat (and other scalars) have been determined. Average vertical turbulent fluxes are computed in real time using a digital recursive filter (200 s time constant) for the determination of a running "mean" from which the instantaneous values are subtracted. An averaging period of 30 min is considered large enough for statistical confidence in the covariance quantity but is short enough to resolve the structure of the diurnal cycle. Additional measurements are being contemplated and will soon be available via the Web to interested parties. Figure 2f shows the location of the GCIP flux towers. Because of the timing at which various flux towers came on line, only the Little Washita and Illinois data sets could be used for this study (1996–1999).

3.6. Soil Moisture

[30] Only a few long time series of soil moisture observations in the Mississippi River Basin exist, but several new networks have been established in parts of the basin, and they provide detailed information for these regions. For evaluating the water budget of this region, its climatology and how it has changed for the past few decades, the currently existing database is clearly inadequate, even today. As the new data are used to develop better modeling and remote sensing capabilities, it should be possible to use data assimilation to produce basin-wide distributions of soil moisture. However, only the Illinois data (described by *Hollinger and Isard* [1994]) was available for this WEBS (Figure 2g). This data has also been used for evaluation of the Atmospheric Model Intercomparison Project (AMIP) [*Gates*, 1992] climate model simulations of soil moisture [*Robock et al.*, 1998, *Srinivasan et al.*, 2000], for evaluating the Global Soil Wetness Project [*Dirmeyer and Dolman*, 1998; *Dirmeyer et al.*, 1999] land surface schemes' calculations of soil moisture [*Entin et al.*, 1999], as ground truth for remote sensing by passive microwave observations of soil moisture [*Vinnikov et al.*, 1999a], for evaluating the temporal and spatial scales of soil moisture variations [*Entin*, 1998; *Entin et al.*, 2000], for designing new networks of soil moisture observations [*Vinnikov et al.*, 1999b], and for determining the dependence of the spatial averaging errors on network density [*Vinnikov et al.*, 1999b].

3.7. Satellite Products

3.7.1. Precipitation

[31] Considerable effort has been devoted previously to developing satellite-based remote sensing methods for precipitation [see *Adler et al.*, 2000; *Huffman et al.*, 1997; *Xie and Arkin*, 1997]. Infrared-based algorithms primarily based on cloud top temperature are really only meaningful in the case of deep penetrating convection (prevalent in the tropics). Microwave techniques are sensitive to the amount and distribution of precipitating ice particles and water drops present in the atmospheric column. These data sets have been combined with gauges over land, and although the gauges are currently given the greatest weight, due to

traditional problems with gauges more weight may be given to satellite measurements in the future. In that regard, it should be noted that the proposed Global Precipitation Mission (GPM) would provide 3-hourly 4 km precipitation coverage over the globe between 55°N and S and could be the cornerstone of future global observations over both ocean and land. Again, currently available satellite precipitation products are still too coarse in comparison to available station and NEXRAD products.

3.7.2. TOVS

[32] The TIROS Operational Vertical Sounder (TOVS) contains two instruments: the HIRS2 (High Resolution Infra-Red Sounder) and the MSU (Microwave Sounding Unit). TOVS has been operated on NOAA satellites from TIROS-N from 1978 to the present and has been used to derive outgoing longwave radiation and surface meteorological variables such as land surface temperature, air temperature, and specific humidity, as well as atmospheric profiles of air temperature, water vapor and ozone burden, and cloud fraction and height [*Susskind et al.*, 1984, 1997]. These variables are calculated separately for each (instantaneous) overpass (230am, 730am, 230pm and 730pm) and gridded to global 1° × 1° spatial resolution (land and ocean). The derived variables are aggregated into pentad (5-day) and monthly averages. Canopy air temperature and surface specific humidity are obtained by extrapolating the air temperature and water vapor profiles to the surface pressure. Land surface temperature is calculated directly using observations in the thermal and infrared regions (channels 8, 18 and 19: 11.14 μm, 3.98 μm and 3.74 μm, respectively) and inversion of the Planck function. Surface emissivity values of 0.95 (channel 8) and 0.85 (channel 18, 19) were assumed for the surface temperature calculations. For this WEBS the TOVS derived surface skin temperature and outgoing longwave radiation were used for comparison to model products.

3.7.3. Solar Radiation

[33] Surface short-wave radiation budget components are derived from a physical inference model [*Pinker et al.*, 2003], driven with satellite observations of reflected energy. The model requires clear column radiance, cloud top radiance, cloud fraction, precipitable water, snow cover, and composite clear sky radiance, as input. These model inputs are generated at NOAA/NESDIS where the satellite observations are received in real time (hourly), and preprocessed into the required quantities hourly for targets that are centered at 0.5 latitude/longitude intervals. The primary observing system is the visible channel (0.52–0.72 μm) on the GOES-8 satellite, which is a narrowband channel. To derive broadband fluxes requires development of narrow to broadband transformations of the spectral radiances, angularly dependent relationships between the broadband reflectance and the narrowband reflectance and the effects of surface types, aerosols, clouds and sun-viewing geometry. Coverage extends from 25° to 50°N latitude, and 70° to 125°W longitude. The targets consist of 9 × 8 arrays of 4 km center-to-center pixels (at nadir), where the visible data have been averaged up to 4 km resolution, to coincide with the 4 km resolution infrared pixels.

3.7.4. Water Vapor

[34] *Randel et al.* [1996] developed a blended, global, daily water vapor data set at 1° × 1° resolution. The data set is called the NASA Water Vapor Project (NVAP). The analysis combines water vapor retrievals from the Television and Infrared Operational Satellite (TIROS) Operational Vertical Sounder (TOVS), the Special Sensor Microwave/Imager, and radiosondes. The NVAP data is currently available for the time period 1988–1999, and is utilized here as the basic precipitable water observations. NVAP is being created in the post-1999 time period as well. NVAP contains total column water vapor as well as water vapor amounts from 1000 to 700, 700 to 500, 500 to 300, and 300 to 200 mb layers.

3.8. Summary of Hydroclimatic Observations

[35] There are certainly many measurements, but as summarized in Table 1, they are not yet adequate to close water and energy budgets on continental scales. We have inadequate observations of soil moisture, snow equivalent water, and tendencies in these variables are important components of the water budget. By contrast, water vapor is will observed but water vapor tendencies do not seem to be critical on seasonal time scales. Skin temperature and atmospheric tendencies are also probably not critically important on seasonal time scales but they along with atmospheric water vapor tendencies are important on shorter time scales. Satellite measurements are probably critical in that regard, but as will be shown probably need to be tied more closely to available observations of surface measurements. Surface flux measurements of latent and sensible heat as well as basic radiation components are exceedingly rare (there were only two tower sites available for the entire Mississippi River Basin). Satellite estimates of net radiation are useful, although only the outgoing radiation and the estimated downward solar flux at the bottom of the atmosphere were available for this time period and region. Moisture convergence was available only as a basin mean from radiosonde measurements and there were no estimates made for the energy convergence. In fact, only annual mean moisture convergence could be estimated from the climatological runoff. Streamflow can be measured at the outlet of the Mississippi but this measured streamflow, does not reflect the effects of water management, which had to be estimated here. Precipitation is probably our best measured variable, but attempts to go to higher resolution with NEXRAD have so far only been successful during the summer. In addition, there may be some undercatch issues associated with the raw observations. In short, the available observations really only allow us to characterize, rather than definitively close the water and energy budgets. Models, which automatically close their own false budgets, are needed to supplement observations and in effect help us to approximately close the true budgets.

4. GCIP Models

[36] Modern global and regional atmospheric and macroscale hydrologic models provide comprehensive hydroclimatological output and a means to supplement meager observations. There have been a number of different types of models used for GCIP studies, which are constrained in different ways to available observations. Global models are typically only constrained by observed sea surface temperatures (SSTs). However, they can be further constrained by

global atmospheric observations in atmospheric analysis. Regional models are also constrained by global atmospheric analyses and can be even further constrained through additional regional atmospheric observations in a regional analysis. Hydrologic models are constrained by the need to balance observed runoff using observed precipitation (and other forcings) as input. Some of these constraints, or lack thereof, are critically dependent upon their use. For example, to make long-range predictions, only global SSTs and other boundary conditions, including perhaps land surface boundary conditions, can be specified initially and then the boundary conditions can either be assumed to persist [see, e.g., *Roads et al.*, 2001, 2003] or a coupled model can be developed that predicts the behavior of the slowly varying boundary conditions. Coupled ocean atmosphere-land modeling is just beginning and may someday replace current long-range predictions that currently rely mainly upon persistent characteristics of the ocean and land surface conditions.

[37] Below, the models used for this WEBS are briefly described. Again these models only represent the types of models that were used for various GCIP investigations. Modeling studies with many other models were also developed during GCIP [see, e.g., *Tackle et al.*, 1999].

4.1. NCEP Global Spectral Model and Reanalysis

[38] The global spectral model (GSM) used for this study was based upon the Medium-Range Forecast (MRF) Model used at the NCEP for making the four-times-daily Global Data Assimilation System (GDAS) analysis and for making the medium-range (6–14 day) predictions. This GSM, which had undergone steady improvement for a number of years [see *Caplan et al.*, 1997], became on 10 January 1995, the basic global model used for the NCEP/NCAR reanalysis (hereafter referred to as REAN1; see *Kalnay et al.* [1996] for a description of the model). The REAN1 GSM used a primitive equation or hydrostatic system of virtual temperature, humidity, surface pressure, mass continuity, vorticity, and divergence prognostic equations on terrain- following sigma (sigma is defined as the ratio of the ambient pressure to surface pressure) coordinates. These levels (28) were concentrated near the lower boundary and tropopause.

[39] As discussed by *Hong and Leetmaa* [1999; see also *Hong and Pan*, 1996], the physics package for the GSM included longwave and short-wave radiation interactions between cloud and radiation; boundary layer processes, such as shallow clouds and convection; large-scale condensation; gravity wave drag; and enhanced topography. Vertical transfer throughout the troposphere, including the boundary layer, was related to eddy diffusion coefficients dependent upon a Richardson number-dependent diffusion process [*Kanamitsu*, 1989]. A major GSM development effort had been concerned with the cumulus convection parameterization, which currently used a simplified Arakawa-Schubert (SAS) parameterization [see *Grell*, 1993; *Pan and Wu*, 1995]. SAS removes large-scale instabilities by relaxing temperature and moisture profiles toward prescribed equilibrium values on a prescribed timescale. The convection scheme also allows entrainment into the updraft and detrainment from the downdraft between the level from which the updraft air originates and the level of free convection (LFC). An innovative land surface parameterization (LSP), which underwent a radical change from the former bucket model, was also developed for the GSM. The new LSP [see *Pan*, 1990] consists of two soil layers in which soil moisture and temperature as well as moisture present in the vegetation and snow are carried as dependent variables. Exchange between the two soil layers is modeled as a diffusion process. Evaporation occurs from bare soil, leaf canopy, as well as transpiration through leaf stomata. *Chen et al.* [1996] made further improvements [see also *Betts et al.*, 1997] to NCEP's associated Eta Model (described below), and these changes will soon be incorporated in later versions of the GSM.

[40] An upgraded version of the GSM was the basis for the NCEP/DOE AMIP Reanalysis II (hereafter referred to as REAN2; see *Kanamitsu et al.* [2002]) as well as the coarser-scale (T42) GSM continuous simulations forced by SST [*Reichler and Roads*, 2003] used here. Besides a few physical parameterization changes, a number of notable bugs in the REAN1 were also fixed. For example, REAN2 snow amount was prescribed from operational files instead of using a fixed climatology (which was mistakenly used in REAN1 for a few years). Horizontal diffusion is correctly applied to pressure surfaces, rather than sigma surfaces, which results in better diffusion at high latitudes and less spectral noise is now apparent in the precipitation and snowfields [see *Roads et al.*, 1999; *Roads*, 2003]. The radiation is now computed on the full model grid instead of a coarser grid. The cloudiness-relative humidity relationship was refined. There are some other important differences in the boundary layer. In the REAN1 boundary layer, vertical transfer is related to eddy diffusion coefficients dependent upon a Richardson number-dependent diffusion process [*Kanamitsu*, 1989]. In REAN2, a nonlocal diffusion concept is used for the mixed layer (diffusion coefficients are still applied above the boundary layer). Briefly, in the mixed layer, the turbulent diffusion coefficients are calculated from a prescribed profile shape as a function of boundary layer height and scale parameters derived from similarity requirements [*Troen and Mahrt*, 1986]. Finally, unlike REAN1, REAN2 does not force the soil moisture to an assumed climatology, which results in too large a seasonal cycle and too small interannual variations [*Roads et al.*, 1999; *Roads and Betts*, 2000; *Maurer et al.*, 2001a, 2001b]. This correction also contributed to some of the excessive precipitation noted in the U.S. Southeast. REAN2 corrects, instead, the model soil moisture by adding the previous pentad (5-day) difference between the reanalysis precipitation and observed precipitation to the soil moisture [see *Kanamitsu et al.*, 2002; *Roads et al.*, 2002a].

4.2. RSM

[41] The RSM used for this study was originally developed by *Juang and Kanamitsu* [1994] [see also *Juang et al.*, 1997]. This model has previously been used to simulate and analyze regional climate characteristics of precipitation [*Chen et al.*, 1999; *Hong and Leetmaa*, 1999], low-level winds and precipitation [*Anderson et al.*, 2000; *Anderson and Roads*, 2002] and Mississippi River Basin water and energy budgets [*Roads and Chen*, 2000]. The RSM is a regional extension to the GSM and in principle provides an almost seamless transition between the REAN1 (REAN2 is

not as available at high temporal resolution) and the higher resolution region of interest. Another advantage, according to *Hong and Leetmaa* [1999], is that the RSM does not have the same restrictions on nesting size that other regional climate models seem to have and smaller nests can be embedded within the large-scale reanalysis without noticeable errors or influences. Basically, the RSM use the same primitive hydrostatic system of virtual temperature, humidity, surface pressure and mass continuity prognostic equations on terrain-following sigma (sigma is defined as the ratio of the ambient pressure to surface pressure) coordinates as the GSM. Except for the scale dependence built into the horizontal diffusion and some other physical parameterizations, the GSM and RSM physical parameterizations should be, in principle, identical. Again, it is claimed, without too much justification that the RSM is representative of many of the other regional models, such as MM5, RAMS, MASS, etc. used for GCIP studies (see *Takle et al.* [1999] for a regional model intercomparison applicable to GCIP).

[42] In the absence of any regional forcing, (and intrinsic internal dynamics, any significant physical parameterization differences, and significant spatial resolution) the total RSM solution should be identical to the GSM solution. A minor structural difference is that the GSM utilizes vorticity, divergence equations, whereas the RSM utilizes momentum equations in order to have simpler lateral boundary conditions. The GSM and RSM horizontal basis functions are also different. The GSM uses spherical harmonics with a triangular truncation of 62 (T62) whereas the RSM uses cosine or sine waves to represent regional perturbations about the imposed global scale base fields on the regional grids. The double Fourier spectral representations are carefully chosen so that the normal wind perturbations are antisymmetric about the lateral boundary. Other model scalar variables (i.e., virtual temperature, specific humidity, and surface log pressure) are symmetric perturbations. Finally, the RSM usually uses a polar stereographic projection while the GSM uses Gaussian grid, and thus the geographical location of the grids do not match, requiring some interpolation from each grid.

4.3. NCEP Eta Model Analysis

[43] The NCEP regional Eta model (so named because of the vertical eta coordinate system, which has some advantage for mountainous terrain) was used for the basic regional analysis for GCIP [see *Berbery et al.*, 1996; *Berbery and Rasmusson*, 1999] (E. H. Berbery et al., A six year regional climatology of the atmospheric water balance, submitted to *Journal of Geophysical Research*, 2002). Although there are some similarities to the physical parameterizations of the GSM/RSM, there are some important differences, especially in the cumulus convection scheme, which uses the Betts Miller scheme versus the simplified Arakawa-Schubert scheme used in the GSM/RSM. The Eta model also has an upgraded land surface package [*Chen et al.*, 1996; *Betts et al.*, 1997] and an associated cloud prediction model [*Zhao et al.*, 1997]. Since April 1995 the Eta model operational forecasts were run from initial data resulting from the Eta Data Assimilation System (EDAS). This system began with a global model 6-hour forecast up to 12 hours prior to the Eta model forecast, and was followed by adjustments to observations by optimal interpolation at 3-hours intervals. Apart from synoptic observations the regional assimilation also ingests data from aircraft, wind profilers, and vertically integrated water vapor derived from satellite measurements at resolutions in accordance with those of the model [*Rogers et al.*, 1996]. Currently, the optimal interpolation has been replaced by a 3D-Var analysis. The advantages of computing surface energy balances from EDAS over those estimated from REAN-I are discussed by *Berbery et al.* [1999]; further discussion is given by *Yarosh et al.* [1999]. Since June 1998 EDAS has had its own soil moisture cycle, and global biases in soil moisture have been reduced.

[44] The success of the Eta model and EDAS to realistically reproduce mesoscale features of the circulation [see, e.g., *Berbery*, 2001] encouraged the development of an initiative to perform regional reanalyses for at least a 20-year period. The objective of the NCEP/EMC Regional Reanalysis (RR) project is to produce a long-term set of consistent climate data for the North American domain, at a regional scale. The RR product will probably be superior to the NCEP/NCAR Global Reanalysis (GR), over North America, in both resolution and accuracy. Intended resolution and domain size are those of the operational Eta prior to September 2000, 32-km/45 layer, North America and parts of Atlantic and Pacific. The intended regional reanalysis period is presently planned to be 1982–2003 [*Mesinger et al.*, 2002]. The work performed so far includes data gathering and processing, the design of a pilot reanalysis system, and running and analysis of a number of pilot runs. Besides the basic data used for the global reanalysis, additional data include Continental United States and Mexican rain gauge data (and CMAP pentad outside); TOVS-1b radiances, wind profilers, VAD winds, GOES radiances, and land surface temperature, wind and moisture data [*Mesinger et al.*, 2002].

4.4. Macroscale Hydrologic Model

[45] The macroscale hydrologic model used for this intercomparison was the variable infiltration capacity hydrologic model (VIC), which was described in detail by *Liang et al.* [1994] and at http://hydro.washington.edu; details on the application of the VIC model for WEBS were described by *Maurer et al.* [2001a, 2001b]. VIC is a macroscale hydrologic model that balances both energy and water over a grid mesh, in this application at a 1/8-degree resolution, using a 3-hourly time step. At the 1/8-degree resolution, the model represents about 23,000 computational grid cells within the Mississippi River Basin. The VIC model computed the vertical energy and moisture fluxes in a grid cell on the basis of a specification at each grid cell of soil properties and vegetation coverage. VIC included the representation of subgrid variability in soil infiltration capacity, and a mosaic of vegetation classes in any grid cell. Drainage between the soil layers (three were used in this application) is entirely gravity-driven, and the unsaturated hydraulic conductivity is a function of the degree of saturation of the soil, with base flow produced from the lowest soil layer using the nonlinear ARNO formulation [*Todini*, 1996]. To account for subgrid variability in infiltration, the VIC model used a variable infiltration capacity scheme based on *Zhao et al.* [1980, 1997]. This scheme uses a spatial probability distribution to

characterize available infiltration capacity as a function of the relative saturated area of the grid cell. Precipitation in excess of the available infiltration capacity forms surface runoff.

[46] The soil characteristics used in the VIC model for the Mississippi River Basin were based on the gridded 1/8-degree data sets that have been developed as part of the Land Data Assimilation system (LDAS) project. In this data set, specific soil characteristics (e.g., field capacity, wilting point, saturated hydraulic conductivity) were based on the work of *Cosby et al.* [1984] and *Rawls et al.* [1998], which used the 1-km resolution continental U.S. soil texture data set produced by Pennsylvania State University [*Miller and White*, 1998]. Land cover characterization was based on the data set described by *Hansen et al.* [2000], which has a resolution of 1 km, and a total of 14 different land cover classes. From this global data set, the land cover types present in each 1/8-degree grid cell in the model domain, and the proportion of the grid cell occupied by each were identified. The primary characteristic of the land cover that affects the hydrologic fluxes simulated by the VIC model is leaf area index (LAI). LAI is derived from the gridded (1/4 degree) monthly global LAI database of *Myneni et al.* [1997], which is combined with the land cover classification to derive the monthly LAI corresponding to each vegetation classification for each grid cell. Infiltration, moisture flux between the soil layers, and runoff all vary with vegetation cover type within a grid cell. Grid cell total surface runoff and base flow were computed for each vegetation type and then summed over the component vegetation covers within each grid cell for each time step.

[47] The VIC model was forced with observed, or derived from observed, meteorological data. The precipitation data consisted of daily totals from approximately 5000 NOAA Cooperative Observer (Co-op) Stations in the Mississippi River Basin. The raw precipitation data were gridded to a 1/8-degree grid and, as described by *Widmann and Bretherton* [2000], the gridded daily precipitation were then scaled so to match the long term average of the Parameter-elevation Regressions on Independent Slopes Model (PRISM) precipitation data set [*Daly et al.*, 1994], which is a comprehensive data set of monthly means for 1961–1990 that are statistically adjusted to capture local variations due to complex terrain. The daily precipitation total was distributed evenly over each time step. The minimum and maximum daily temperature data for the Mississippi River Basin, obtained from approximately 3000 Co-op stations in the basin, were combined with a digital elevation model and the temperatures lapsed to the grid cell mean elevation. Temperatures at each time step were interpolated by fitting an asymmetric spline through the daily maxima and minima. Dew point temperature was calculated using the method of *Kimball et al.* [1997], which relates the dew point to the daily minimum temperature, and downward short-wave radiation was calculated on the basis of the daily temperature range and the dew point temperature using a method described by *Thornton and Running* [1999]. Because surface observations of wind speed are very sparse and are biased toward certain geographical settings (e.g., airports), daily 10 m wind fields were obtained from the NCEP/NCAR reanalysis [*Kalnay et al.*, 1996], and regridded from the T62 Gaussian grid (approximately 1.9 degrees square) to the 1/8-degree grid using a linear interpolation.

5. Water and Energy Budget Equations

[48] Water and energy cycles are time varying 3-dimensional cycles involving various storages and processes. Taking vertical pressure weighted averages in the atmosphere and vertical averages in the subsurface, as well as monthly time means, this document is focused on 2-dimensional horizontal seasonal to interannual hydroclimatic variations.

[49] Consider first the atmospheric water (equation (1)) and surface water (equation (2)) mass conservation equations:

$$\frac{\partial Q}{\partial t} = E - P + MC + RESQ \tag{1}$$

$$\frac{\partial W}{\partial t} = P - E - N + RESW. \tag{2}$$

The two state variables for these water mass conservation equations are Q, the vertically (pressure weighted) integrated specific humidity or precipitable water W, the vertically integrated (2 m below the surface to the surface is used here) soil moisture (M) plus snow liquid water (S). The surface water, W = M + S, is computed only over land.

[50] As described by *Roads et al.* [2002a], the water cycle described by these equations can be viewed rather simplistically in five steps. Under suitable conditions, liquid and solid water evaporate (E) from the ocean and land surface (which includes snow and vegetation) into the atmosphere. Water vapor is transported by atmospheric winds to other regions, and the convergence of this mass flux, MC, will increase atmospheric water vapor over some regions while decreasing water vapor over other regions. Water vapor condenses into cloud particles, C. Cloud particles are formed (through nucleation), grow by condensation and coalescence and by accretion into large liquid and solid drops, which fall as precipitation to the surface, P. If there is no horizontal cloud advection in a vertical column, there is as much water condensed as is precipitated and in the rest of the paper, the identity, C = P, where C and P are the vertical integrals, was assumed. Although the contribution of cloud and precipitation evaporation to the total moisture budget is thought to be small, it could be important for influencing the dynamics and most models now take into account at least the evaporation of rain through unsaturated layers. In any event, surface water was eventually increased through snow cover and infiltration by liquid water and then decreased by evaporation. Some of this surface water was transported to rivers, which in turn transport the water to other locations; the net divergence of this transport or runoff, N, will increase surface water in low lying regions before discharging it into the oceans; in fact, most large and regional-scale atmospheric models simplistically assume that excess surface water is discharged immediately to the oceans. For a global long-term average, there is as much water precipitated as evaporated. For a long-term land average, there is as

much atmospheric water converged over the land as is discharged by rivers to the oceans.

[51] There are some additional artificial residual forcings, RESQ and RESW, which appear in 4-dimensional data assimilation (4DDA) analysis water budgets [e.g., *Kanamitsu and Saha*, 1996; *Roads et al.*, 1997]. RESQ and RESW are denoted as residual in part because they are deduced as a balance of all other terms and in part because they are not part of the natural processes and are only implicitly included in order to force the analyses' state variables close to observations. Unless some type of correction is done, current models will drift to their own model climate, instead of a climate close to the observations. In the atmospheric part of the analysis, this forcing was implicit by requiring the model to be adjusted to the available observations of atmospheric moisture, temperature and winds. At the surface, some implicit adjustment must occur for snow, part (areal coverage) of which is an observed quantity. Additional adjustment occurs for the surface water, which uses observed precipitation instead of model precipitation to keep the soil moisture realistic. Because of these residuals, one might think that reanalyses cannot be used to study hydrometeorological budgets. However, it is worth pointing out that since all models are designed to produce accurate budgets, and they will balance, independent of any residual, that there are many other dominant errors. For example, a continuous GCM, without any residual forcings and with perfect budgets, probably has larger errors in each of the individual terms, than an analysis with implicit residual forcings. An overall goal of an analysis system would therefore be to produce an analysis with small residuals and accurate estimates for each component of the budgets. In some sense these residuals also provide an estimate of the overall error in the budgets. It should also be noted that some of the residual may be due to the way we calculate moisture or heat convergence; however, *Roads et al.* [1998] previously discussed some of these possible influences and concluded that the analysis increment may be the most important contribution.

[52] Consider next the energy equations. The surface energy equation is simply the surface temperature equation:

$$Cv\frac{\partial Ts}{\partial t} = QRS - LE - SH + G' \tag{3}$$

The atmospheric energy equation to a good first approximation (neglecting kinetic energy) is the atmospheric dry static or temperature equation and was described previously by *Roads et al.* [1997]:

$$Cp\frac{\partial\{T\}}{\partial t} = SH + LP + HC + QR + REST' \tag{4}$$

The surface energy input comes mainly from incoming solar and downwelling infrared radiation, moderated by reflected solar radiation and outgoing infrared radiation, QRS. The net radiant energy that reaches the Earth's surface, QRS, is the source that controls temperature, drives evaporation and is affected by atmospheric humidity and clouds.

[53] Changes in the water phase can have a profound influence on the atmospheric and surface thermodynamic energy. Water cools its surroundings as liquid and solid water are converted into water vapor, LE. Globally averaged, this latent cooling must be balanced by the latent heat released when water vapor is converted to liquid and solid cloud particles, LC (again LC = LP is assumed here), which helps to balance the net radiative cooling of the atmosphere, QR. Because of the large latent heat involved in the condensation and evaporation of water molecules, water vapor is a very effective means of storing energy. The latent heat of fusion complicates the analysis. The latent heat required to melt snow should be balanced by the latent heat released when snow is formed initially. This exact relationship is usually not present in atmospheric models, which do not track the latent heat differences when snow is created from either the freezing of liquid drops or the conversion of vapor directly to ice. In particular, in the REAN2 model, snow at the surface is assumed when the temperature above the surface reaches a certain minimum, but no latent heat is released when this happens. However, the fusion energy release relationship is tracked at the surface, where the latent heat of fusion is included in the melt process.

[54] There are a number of other terms in the energy balance that are affected by the water phase change. The net equator-to-pole dry static energy transport or dry static energy convergence, HC, is positive and acts to balance the net atmospheric radiative cooling HC also acts to balance the latent heat released, especially in the tropical regions. Cooling of the surface and heating of the atmosphere by turbulent transfers of sensible heat, SH, in the planetary boundary layer, is also governed by the latent heat release since moist regions release more latent heat and thus require less sensible heat to achieve an energy balance.

[55] Again, there are some additional terms (REST′, G′) that appear in analysis energy budgets that are not wholly related to natural processes. Heat storage in the land surface is thought to be small, but not negligible. REAN2 includes a heat storage term, G′, that releases heat to the atmosphere during the colder part of the year and stores heat during the warmer part of the year. G′ also includes the energy needed to melt snow. These residual forcings are combined with the negative of the tendency terms although the tendency terms are thought to be small (REST = REST′-C_pdT/dt and G = G′-C_vdTs/dt). Again, only the global and regional analyses will have nonzero atmospheric residuals, although because of our not being able to access all of the heating terms in the Eta model the regional analysis residual could not be calculated. Still, given the similarity of the moisture and energy residuals to analysis increments [*Roads et al.*, 1998] and the additional argument by *Roads et al.* [2003] that this residual is mainly due to precipitation spinup and spindown and evaporation parameterization difficulties, one should expect the Eta analysis could have a similar residual. Finally, although it is not shown here, the surface-heating tendency would have a strong influence on the sea surface temperatures (SSTs) if it were not for the surface currents, upwelling, and heat capacity that act to maintain them. All of the WEBS variables are summarized in the notation section.

6. Annual and Seasonal Means

[56] Table 2 summarizes the annual areal (Mississippi River Basin) means of the various budget terms. Precipitable water ranges from 16–18 mm in the models, with the

Table 2. Mississippi River Basin Annual Mean (1996–1999) Water and Energy Budget Variables[a]

	OBS	REAN1	REAN2	GSM	RSM	ETA	VIC
Q, mm	16.847	16.523	16.836	18.845	16.776	16.139	NA
W, mm	NA	538.877	448.551	328.244	406.275	NA	413.131
Snow, mm	NA	NA	11.378	2.237	1.716	2.957	5.084
Ts, °C	10.455(J)						
9.422(L)	9.575	10.365	12.238	11.136	NA	11.129	
P, mm d^{-1}	2.153	2.319	2.316	2.172	2.318	2.096	2.255
E, mm d^{-1}	NA	2.372	2.423	1.941	2.039	1.980	1.612
MC, mm d^{-1}	−0.065	0.510	0.510	0.231	0.280	0.232	NA
N, mm d^{-1}	0.626(M)						
0.457(F)	0.539	0.148	0.207	0.212	0.355	0.664	
HC, K d^{-1}	NA	0.165	0.188	0.352	0.152	NA	NA
LP, K d^{-1}	0.538	0.577	0.598	0.561	0.596	0.524	0.564
LE, K d^{-1}	NA	0.590	0.632	0.503	0.524	0.530	0.389
SH, K d^{-1}	NA	0.099	0.077	0.113	0.194	0.285	0.206
QR, K d^{-1}	NA	−0.960	−0.827	−0.800	−0.903	NA	NA
QRS, K d^{-1}	NA	0.762	0.740	0.671	0.700	0.865	0.621
NSW Sfc, W m^{-2}	155.353	157.180	156.953	152.896	145.371	171.607	134.028
NSW TOA, W m^{-2}	226.115	213.486	223.266	225.581	201.966	NA	NA
NLW Sfc, W m^{-2}	NA	72.515	74.755	78.278	67.692	75.555	62.153
NLW TOA, W m^{-2}	232.970	235.479	232.930	239.786	224.493	NA	NA
RESQ, mm d^{-1}	NA	−0.563	−0.617	NA	NA	−0.116	NA
RESW, mm d^{-1}	NA	0.592	0.255	−0.024	−0.067	NA	NA
G, K d^{-1}	NA	−0.073	−0.031	−0.055	0.018	−0.050	−0.030
REST, K d^{-1}	NA	0.119	−0.036	NA	NA	NA	NA
LP, W m−^{2}	62.297	67.100	67.013	62.847	67.072	60.648	65.249
LE, W m^{-2}	NA	65.536	70.201	55.872	58.148	61.343	45.023
LMC, W m^{-2}	−1.881	14.757	14.757	6.684	8.102	6.713	NA
HC, W m^{-2}	NA	18.328	20.883	39.100	16.868	NA	NA
SH, W m^{-2}	NA	10.997	8.553	12.552	21.528	32.986	23.843
QR, W m^{-2}	NA	−106.658	−91.862	−88.862	−100.206	NA	NA
QRS, W m^{-2}	NA	84.665	82.198	74.533	77.679	96.052	71.875
LRESQ	NA	−16.291	−17.853	NA	NA	−3.356	NA
LRESW	NA	17.130	7.378	−0.694	−1.939	NA	NA
GG, W m^{-2}	NA	−8.132	−3.444	−6.109	1.997	−1.723	−3.009
RESTT, W m^{-2}	NA	10.233	−4.587	NA	NA	NA	NA
Ps g^{-1}	NA	9553.169	9553.169	9553.169	9543.942	NA	NA

[a]"NA" either means not available or not applicable. Observed runoff estimates come from the *Maurer and Lettenmaier* [2001], naturalized USGS streamflow observations, and the gridded climatological estimate from *Fekete et al.* [2000]. Temperature observations come from the *Lakshmi and Susskind* [2000] TOVS estimate and *Janowiak et al.* [1999] mean of T_{max} and T_{min}. Characteristics of other observations and models are provided in the text.

NVAP observations indicating a value of 16.8 mm. Surface water in the upper two meters, including snow liquid water, ranges from 400–500 mm in the available models with the VIC model having 413 mm. Snow contributes from 2–10 mm of this surface water in the models, with the VIC model having 5.1 mm. Surface skin temperature ranges from 8 to 11°C, with the satellite observations indicating 9.4°C and the *Janowiak et al.* [1999] average of T_{max} and T_{min} providing 7.9°C. Precipitation ranges from 2.1 to 3.0 mm d^{-1} in the models with the *Higgins et al.* [2000] observations indicating 2.1 mm d^{-1}. The evaporation is almost as large, with the models ranging from 1.6 to 2.4 mm d^{-1} and the VIC model having 1.6 mm d^{-1}, which is comparable to the difference between the *Higgins et al.* [2000] precipitation and the estimate of streamflow from the USGS gauges. Runoff ranges from 0.2 to 0.6 mm d^{-1} with observations estimated to be 0.6 mm d^{-1} (the *Fekete et al.* [2000] runoff is slightly lower at 0.46 mm d^{-1}). Moisture convergence ranges from 0.2 to 0.6 mm d^{-1} in the models; in order to balance the observed runoff, moisture convergence should be about0.6 mm/day. Note that the moisture convergence from the observations is actually negative, indicating that better estimates of moisture convergence may now be coming from models, or at least reanalyses, which have extensive quality control procedures for both wind and moisture. Sensible heating ranges from 0.01 to 0.19 K d^{-1} in the available models, which is much smaller than the associated latent heating (0.4 to 0.6 K d^{-1}) and the surface radiative heating (0.6 to 0.7 K d^{-1}). The ground heating, including energy needed for snowmelt) is much smaller but ranges from −0.1 to 0.1 K d^{-1} and obviously reflects model biases, which in comparison to other terms, are quite small. Atmospheric radiative cooling ranges from −0.72 to −0.94 K d^{-1} from the available models, which is balanced by the latent heat of condensation (0.5 to 0.75 K d^{-1}) and atmospheric heat convergence ranging from 0.05 to 0.19 K d^{-1} in the available models. Net solar radiation ranges from 134 to 172 W m^{-2} with observations indicating 155 W m^{-2} and the low value being provided by the VIC model and the high value being provided by the Eta model. Note that we have also provided the energy variables in W m^{-2}. Although the general character of the water and energy budgets seems clear, there are also quantitative problems. In the VIC model the solar and infrared radiative terms as well as the surface radiative heating appear to be too low. Also, in the atmospheric models, the moisture convergence appears to be too low whereas precipitation and evaporation appear to be too high.

[57] When it was possible to compute a complete budget in the analysis models, the residual forcing was large and

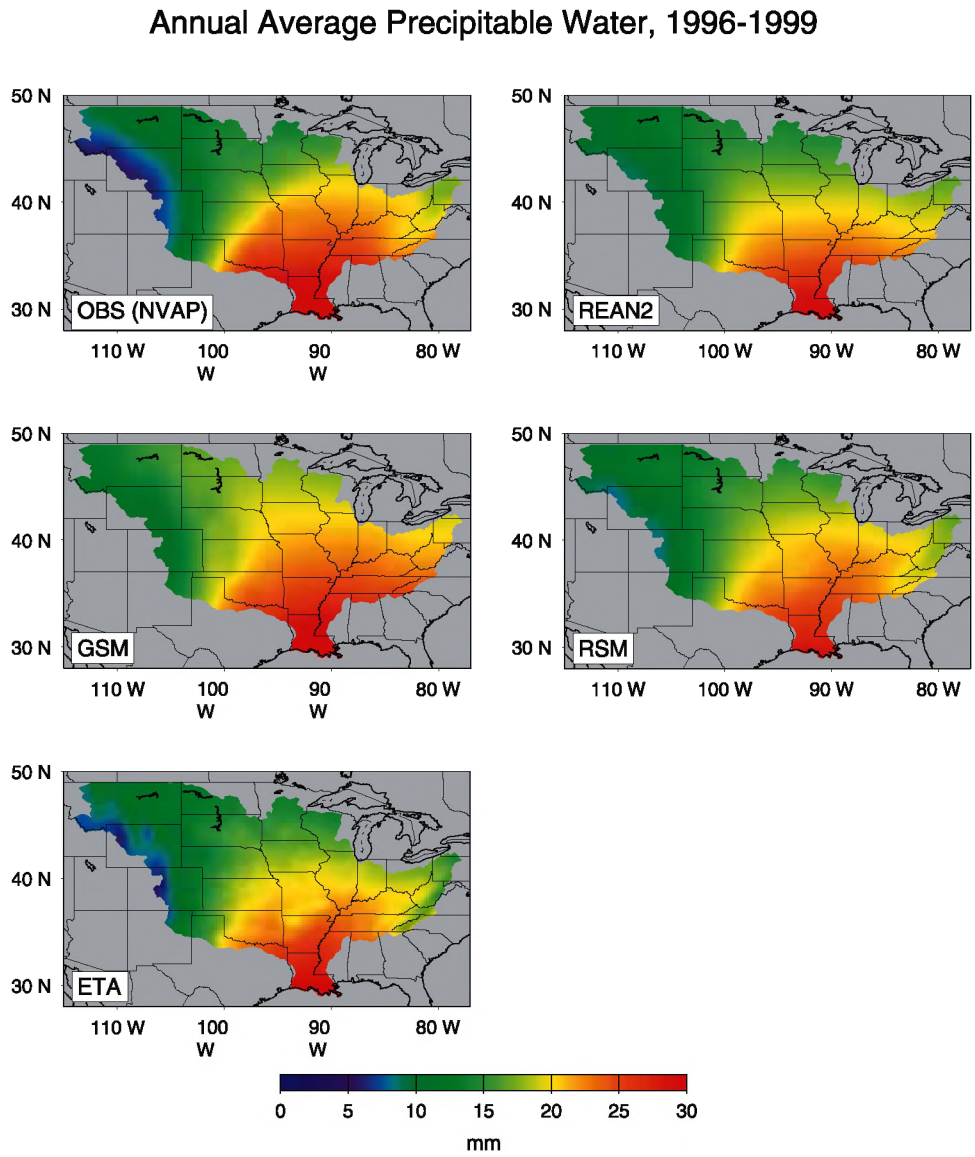

Figure 3. Annual average precipitable water (mm) from the observations (NVAP) and models and analyses (REAN2, GSM, RSM, Eta).

comparable to the other terms. In fact, the atmospheric residual was negative during the winter and positive during the summer in the atmospheric equation and the opposite in the surface equation, which might suggest that this residual is related to the precipitation spin-up and spin-down biases since precipitation acts differently in both equations and precipitation is known to have this spin-up and spin-down problem, [e.g., *Roads et al.*, 2002a] and also because the residual is of opposite sign in the atmospheric temperature equation. However, as pointed out by *Roads* [2002], errors in the evaporation field could also contribute to the error in the water equations and the evaporation errors may be as large as the precipitation errors. Again, the heat residual cannot be estimated from the Eta model since the atmospheric radiative heating was not available for this study. Also, since the heat convergence and moisture convergence were calculated as residuals in the RSM, it is not possible to calculate the contribution of the boundary forcing to the overall RSM budget. Despite the residual forcing, one may still expect that the analysis models and regional models provide the best estimate of individual processes. As the models get better, one can expect this residual to be reduced; in fact, this residual was reduced from a larger value in the first NCEP/NCAR analysis. This residual also provides a measure of uncertainty, which is at least consistent in magnitude with the uncertainty estimated from models and observation differences as well as differences among models.

6.1. Precipitable Water

[58] Precipitable water is an integrated measure of the amount of water within the atmosphere and is closely related to the temperature since the humidity is limited by the saturation humidity (moisture greater than saturation is converted to precipitation); local evaporation and moisture convergence in the basin usually results in the humidity usually being close to saturation. The geographic variations thus reflect the north south temperature gradient, as well as the decrease in temperature with elevation (Figure 3). The smallest amounts of precipitable water occurred during the winter in the Northwest and the largest amounts occurred

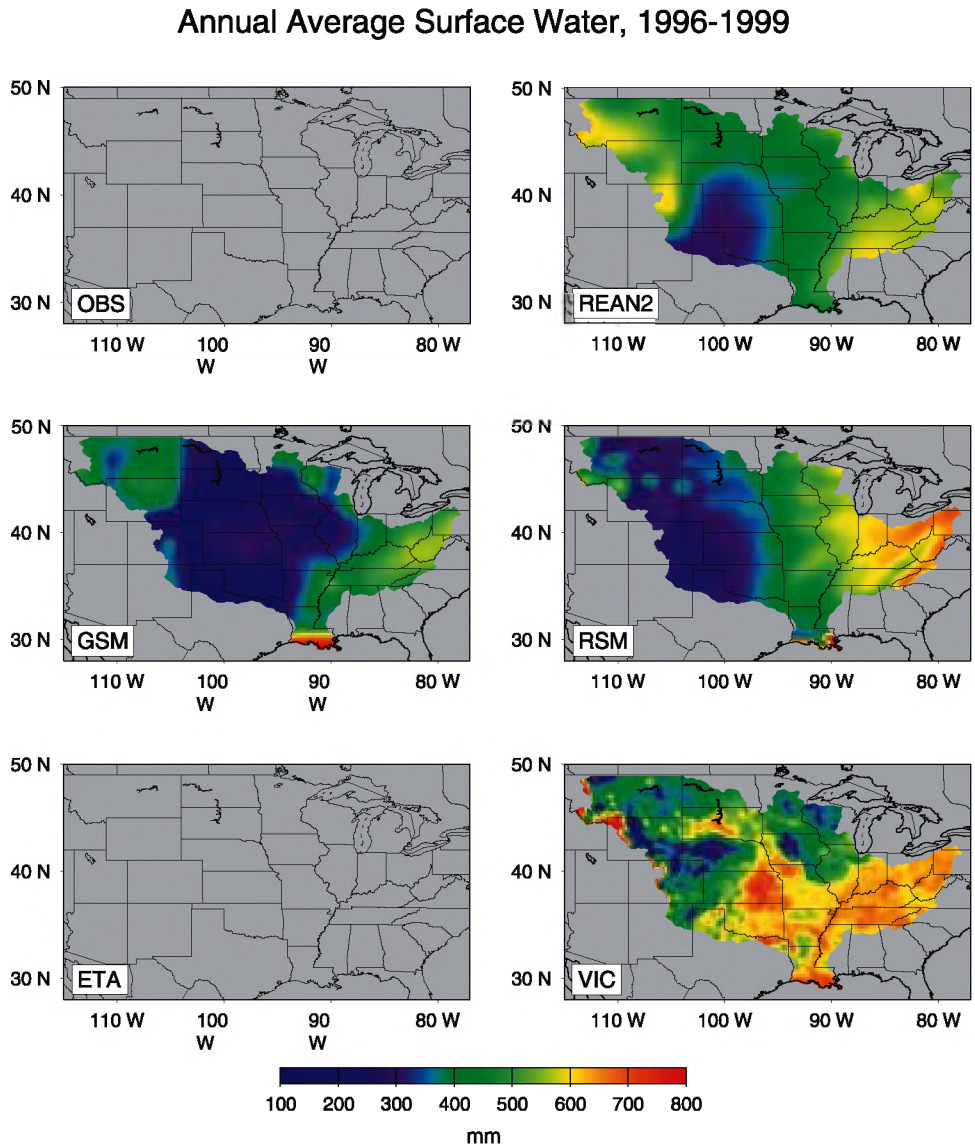

Figure 4. Annual average surface water (mm) from the observations (only in situ measurements available) and models and analyses (REAN2, GSM, RSM, Eta, VIC).

during the summer in the South. The driest part of the troposphere was the area over the Rocky Mountains with <8 mm of precipitable water in winter and about 16 mm in summer. The Eta model had the best minimum over the western Rocky mountain boundary. It should be noted that on monthly to seasonal time scales the precipitable water tendency only makes a small contribution to the atmospheric water budget and thus the small differences shown here are likely to have only a negligible impact (at least for the vertically integrated water budgets).

6.2. Surface Water

[59] Surface water measures the vertically integrated water below the surface and consists of both snow equivalent water and soil moisture. Figure 4 shows the geographic distribution of surface water, which is mainly soil moisture, although snow does provide a small contribution to the surface water in the northernmost regions. Surface water is less related to temperature and more to the relative magnitude of precipitation and evaporation, as well as the surface runoff. Surface water was a minimum in the West, especially in the RSM. By contrast the GSM and reanalysis had more surface water over the far western portion of the domain. This indicates that surface water characteristics were more sensitive to regional characteristics than atmospheric water vapor. All models (the Eta analysis was unavailable) had comparable surface water tendencies (not shown), with the smallest tendencies of corresponding to the VIC model, which had the smallest surface water seasonal cycle.

[60] There are few observations of soil moisture, as mentioned previously. However, it was possible to compare the soil moisture to direct measurements made by the Illinois Water Survey [*Hollinger et al.*, 1994; see also *Robock et al.*, 2000; *Kanamitsu et al.*, 2002] for Illinois (average of 19 stations) and these are shown in Figure 5. Again, only the REAN2, GSM, and RSM had values available for this comparison. The comparison was moder-

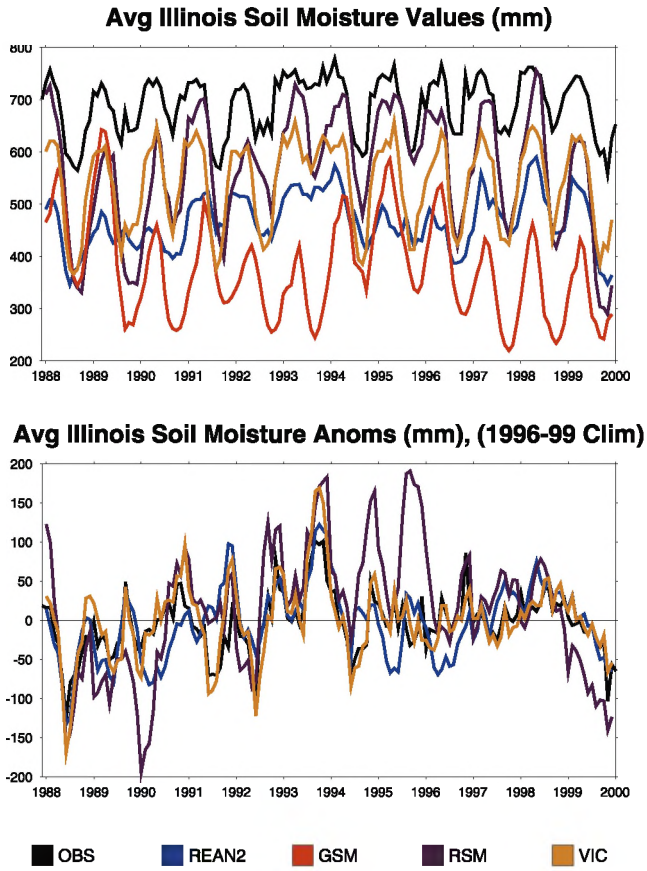

Figure 5. Average Illinois (19 stations) surface water (mm) from the observations (only in situ measurements available) and models and analyses (REAN2, GSM, RSM, VIC). (top) Seasonal cycle. (bottom) Monthly anomalies.

ately encouraging. Note that the models all had a maximum during the winter and a minimum during the late summer. The RSM compared most favorably during the winter but tended to have too large a seasonal variation, which was better emulated by the global models. The interannual variations were mostly above normal during the middle 90s and dryer in the late 80s and 90s, which had some similarity to the observations. This suggests that models may be able to explain some of the interannual soil moisture variations, even though seasonal values are still likely to be quite different from available observations.

6.3. Snow

[61] Although there is now a hybrid (model and observation) snow water equivalence (SWE) data set for a few months (DJF) the northern Plains [*Grundstein et al.*, 2003], the VIC model also provided a benchmark for comparison (for comparison of VIC snow cover extent with observations, see http://www.eewr.princeton.edu/~mpan/research/snow/snow_page.htm). As shown in Figure 6, the snow water equivalent was high near to the western boundaries, especially during the winter and spring. Snow water equivalent was also high during the winter in Minnesota and Wisconsin. The atmospheric models tended to spread this quantity more uniformly throughout the basin, which was related to the lower resolution, although the global model and analysis had especially large amounts during the winter. However, interestingly, the REAN2 did have interannual variations (not shown), comparable to the VIC model, suggesting that the large-scale anomalies in the coarse scale analysis may still be useful.

6.4. Temperature

[62] Surface skin temperature is another variable that was well simulated by all of the models (Figure 7). There was a realistic seasonal cycle in the domain and geographic variations consistent with the elevation of the underlying topography and latitude. The highest temperatures occurred in the GSM during the summer. Geographic variations were usually related to latitude or elevation and the lowest temperatures in the Northwest occurred in the models with highest resolution orography. In particular, the VIC model demonstrated much higher resolution features than could be simulated by the global or even regional models; it should also be noted that the VIC model was actually being forced (through parameterizations of radiation and turbulent heat transfer) with high resolution surface observations (e.g., temperature) as well as lower resolution observations for wind speed.

6.5. Precipitation

[63] Figure 8 shows that all models had less precipitation in the West and greater amounts in the Southeast. All models had a tendency to have more precipitation during the summer than during the winter, although the GSM, REAN1, and REAN2 shifted the precipitation maximum northward along the eastern boundary and also had a tendency to have too much precipitation in the east. By contrast, the Eta model had a good analysis of precipitation. Another gratifying feature was that the precipitation derived from NEXRAD (summer only) was close to the gridded gauge observations, although the NEXRAD precipitation was tuned to observed precipitation. Nonetheless, this NEXRAD product represented one of the hallmarks of GCIP research since for the first time radar climatologies, at least during the summer, are beginning to become available. In addition, it should be noted that NEXRAD precipitation could potentially provide much finer resolution precipitation observations than can be obtained from gauge observations.

6.6. Evaporation

[64] An estimate for the annual mean evaporation can be made by subtracting the *Fekete et al.* [2000] runoff from the *Higgins et al.* [2000] precipitation and these derived observations, along with all the models, had strong evaporation in the east and weaker evaporation in the west (Figure 9). The strong amounts at the outlet suggest that the large-scale models may have had ocean points instead of land points here and the boundaries for the large-scale models' diagnostics may need to be better defined. Except for the VIC, none of the models showed the relatively small evaporation in the North Central and North East. Seasonally, the RSM had the strongest summertime evaporation in the East although the other models were also strong in comparison to the VIC model. Since the VIC model was forced by observed precipitation and runoff and was in fairly good agreement with independent observations, its seasonal evap-

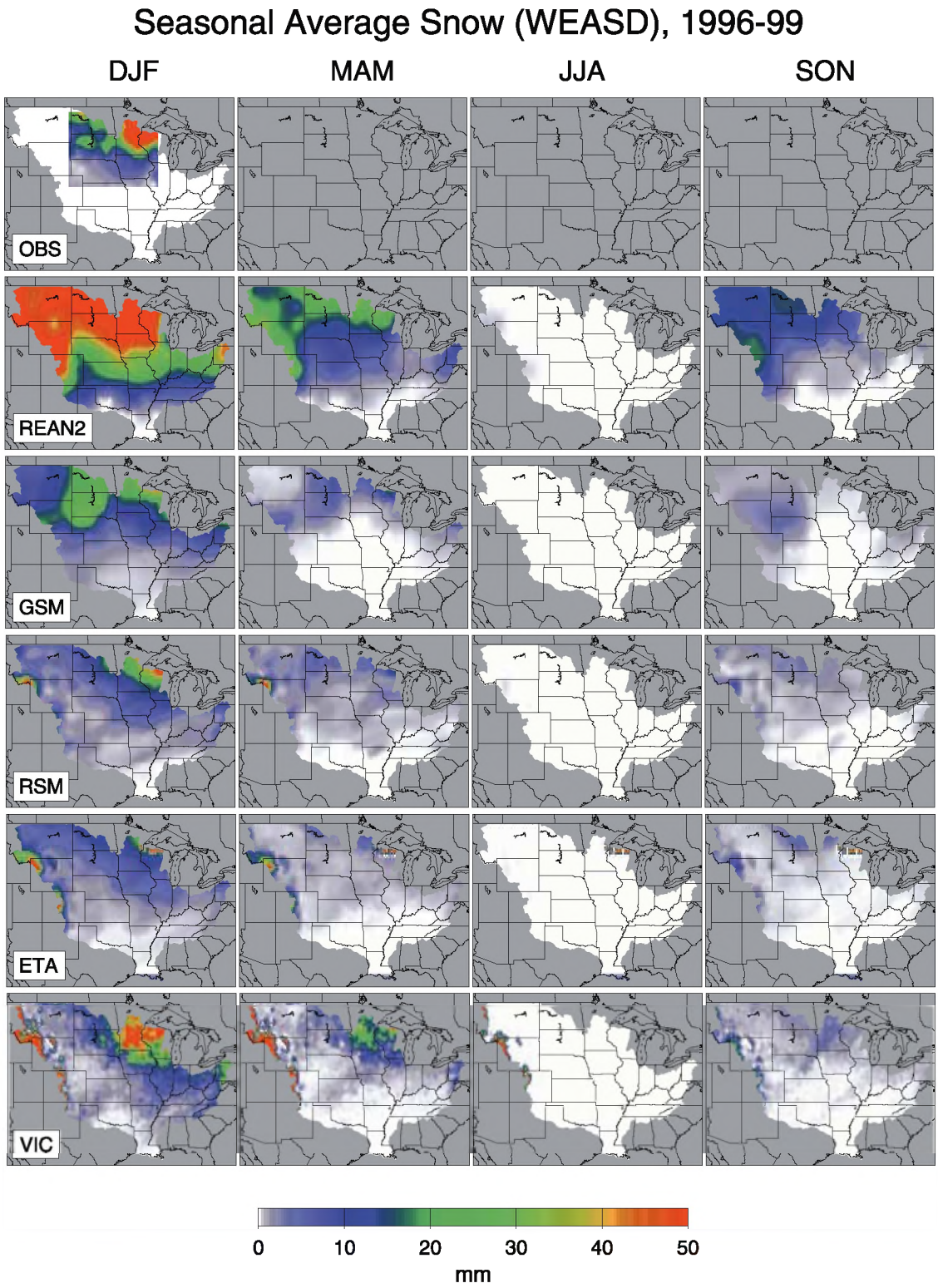

Figure 6. Seasonal average snow water equivalent (mm) from the observations and models and analyses (REAN2, GSM, RSM, Eta, VIC).

oration may be well modeled, although there were certainly major evaporation differences with the other models, especially during the spring to summer. There also may be some errors due to under catch of precipitation as well as unaccounted errors due to water management effects in the observed runoff.

[65] As shown in Figures 10a and 10b observed evaporation at the available tower sites (Little Washita and Champaign for 1997–1999) had much weaker seasonal variations than the models, and the values are especially lower during the summer. Still, one can see some similarities. Evaporation increased during the summer and decreased

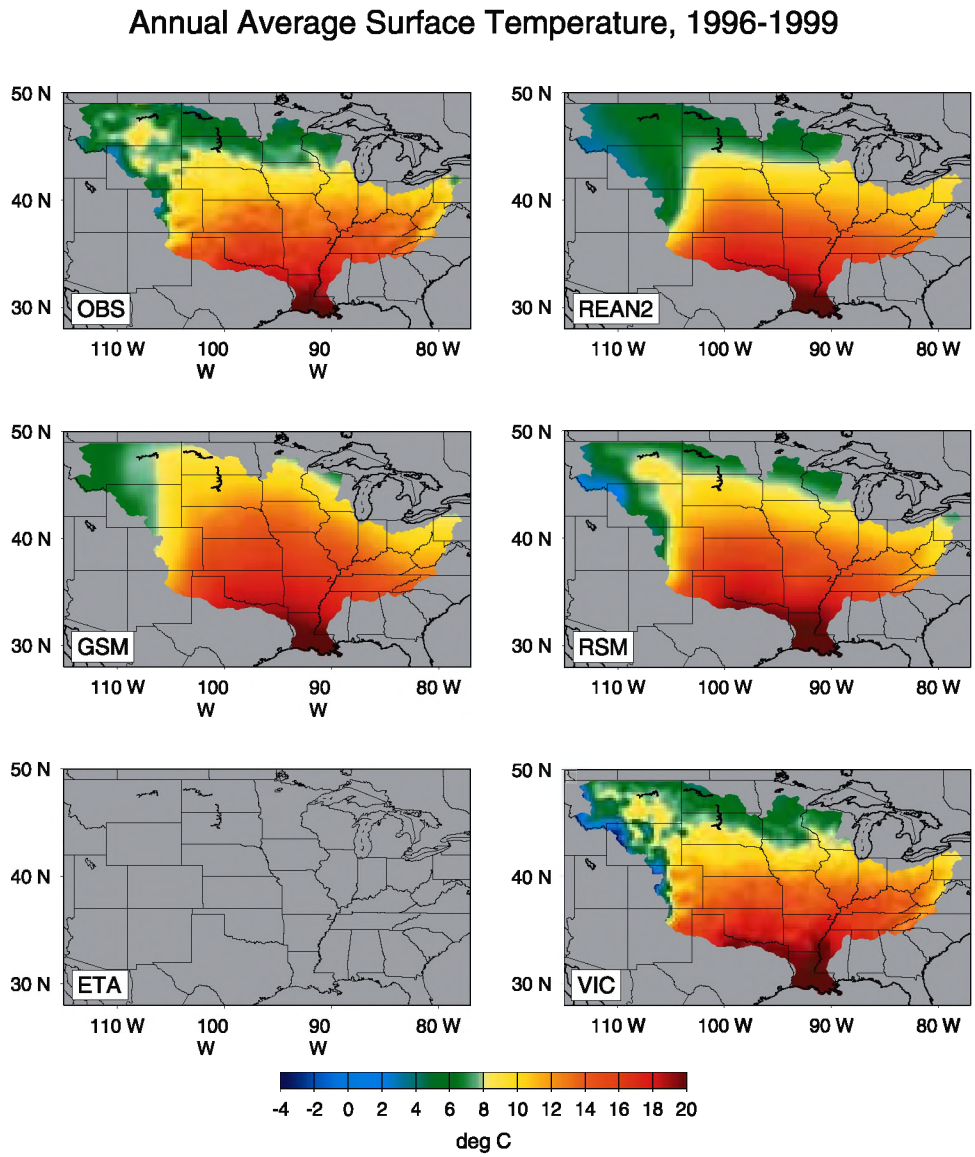

Figure 7. Annual average surface temperature (°C) from the observations [*Janowiak et al.*, 1999] and models and analyses (REAN2, GSM, RSM, Eta, VIC).

during the winter. Again, there is much work needed to develop appropriate models and observations of this inadequately observed variable.

6.7. Moisture Convergence

[66] Figure 11 shows the mean atmospheric moisture convergence for the 4 atmospheric models and the moisture fluxes for the atmospheric models (moisture fluxes were not saved in the GSM simulations). The average moisture convergence must balance the runoff and hence again the *Fekete et al.* [2000] runoff observations were used to estimate the observed moisture convergence. Moisture convergence is a direct calculation for the REAN1 [see *Roads et al.*, 2002a] and is used here for the REAN2 moisture convergence; the Eta model also had a direct calculation for the moisture convergence. All other atmospheric models' moisture convergences were estimated as a residual from $MC = dQ/dt + P - E$. Annually, there were some problems in that the annual mean moisture convergence should be positive and yet it was sometimes negative in some regions, especially for the Eta model in the West. The largest convergence occurred during the winter and spring and the largest divergence occurred during the summer and fall. This large divergence was disconcerting since it occurred at a time when the low-level jet is usually especially active and thought to be a strong contributor to moisture convergence in this region. Note the moisture convergence had the opposite seasonal behavior to precipitation in that the strongest convergence occurred during the wintertime when the evaporation was very small; as discussed by *Roads et al.* [2002a] this is a characteristic of midlatitude climates, which have increased summertime precipitation from increased surface evaporation in spite of the decreased moisture convergence.

6.8. Runoff

[67] Figure 12 shows the annual mean basin runoff. As discussed previously, the GRDC here refers to the *Fekete et*

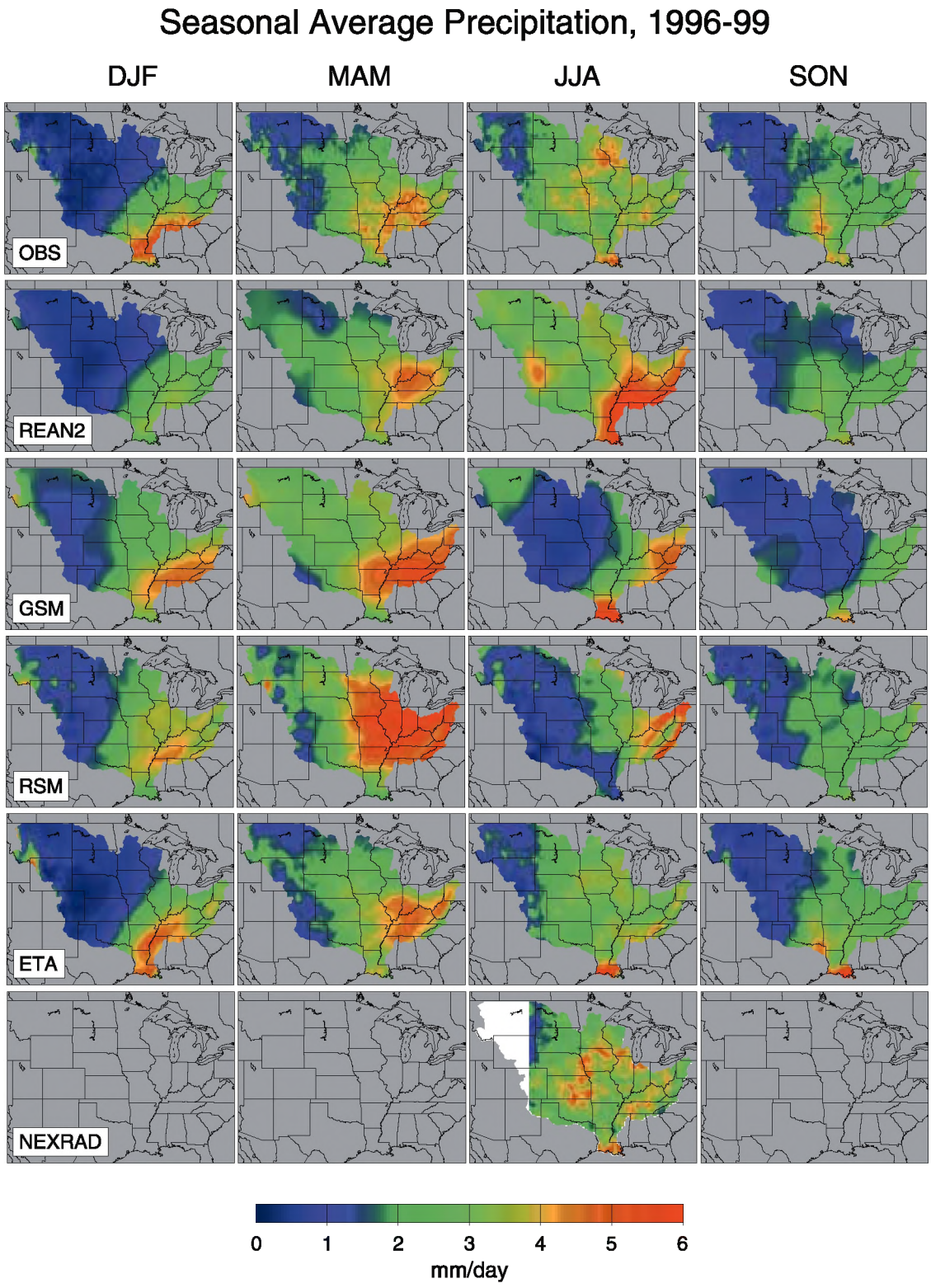

Figure 8. Seasonal average precipitation (mm d^{-1}) from the observations (*Higgins et al.* [2000] and *Smith et al.* [1996] NEXRAD) and models and analyses (REAN2, GSM, RSM, Eta).

al. [2000] climatology, which is primarily useful for understanding relative spatial variations in runoff. However, this gridded product certainly has some uncertainty associated with it, as discussed in section 3.3, and in that regard, the VIC model may actually provide the best geographic distribution of runoff, at least for the GCIP region, although it should be emphasized that the VIC model is tuned to produce the observed runoff only at the outlet of the major tributaries of the Mississippi and the VIC patterns do not seem all that realistic in the north central. The runoff was

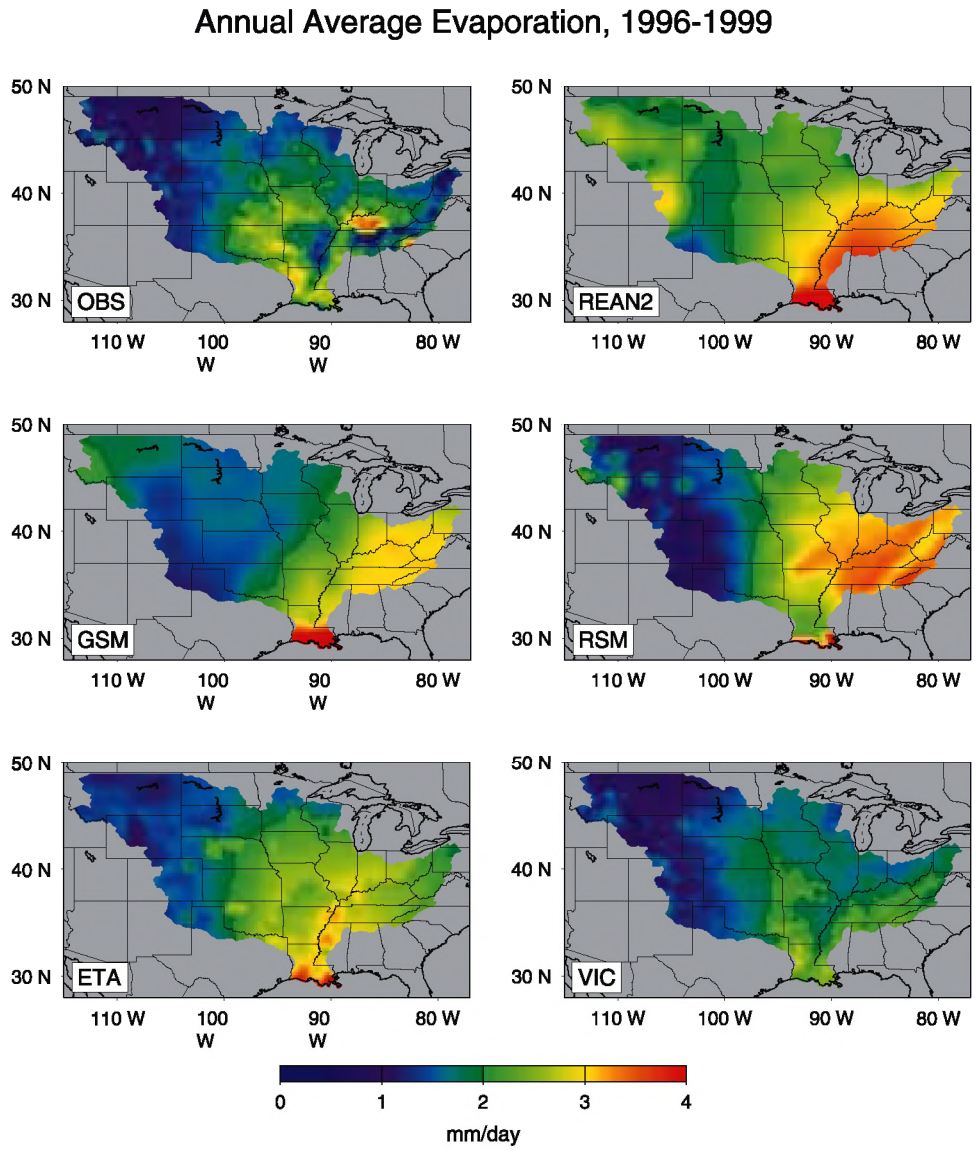

Figure 9. Annual average evaporation (mm d^{-1}) from the observations (estimated by the difference between the *Higgins et al.* [2000] precipitation and the *Fekete et al.* [2000] runoff) and models and analyses (REAN2, GSM, RSM, Eta, VIC).

much less realistic in the other models. However, at least the Eta and RSM showed somewhat comparable features, with the RSM being perhaps a bit more realistic during the spring and summer. The GSM also had surprisingly good features. The REAN2 on the other hand had too little runoff, which was consistent with its precipitation being closer to observations as well as its soil moisture being forced with observed rather than model precipitation.

6.9. Dry Static Energy Convergence

[68] There was some general correspondence among the available models with the dry static energy convergence (not shown here but please see GCIP WEBS CD-ROM) being positive during the winter and fall, when it balanced the atmospheric radiation cooling and negative during the spring and summer [see also *Roads et al.*, 2002a]. The geographic distribution was somewhat similar (but negative) to precipitation, since the adiabatic cooling and heating must balance the precipitation field as well as the radiation and sensible heating field. That is, atmospheric dry static energy flows from the surrounding areas to the Mississippi River Basin during the winter but during the summer when the precipitation is high, energy flows out of the basin. This was similar to the moisture convergence, which was also negative during the summer. The REAN2 had especially strong heat convergence during the winter and the GSM had the strongest divergence during the summer.

6.10. Sensible Heating

[69] The annual mean sensible heating (not shown here but please see GCIP WEBS CD-ROM) was similar among the models in that the strongest contributions occurred in the southwest where the evaporation was low; some disagreement occurred in the north where the REAN2 had strong negative values. This disagreement was apparently related to the various seasonal averages since in the winter, the

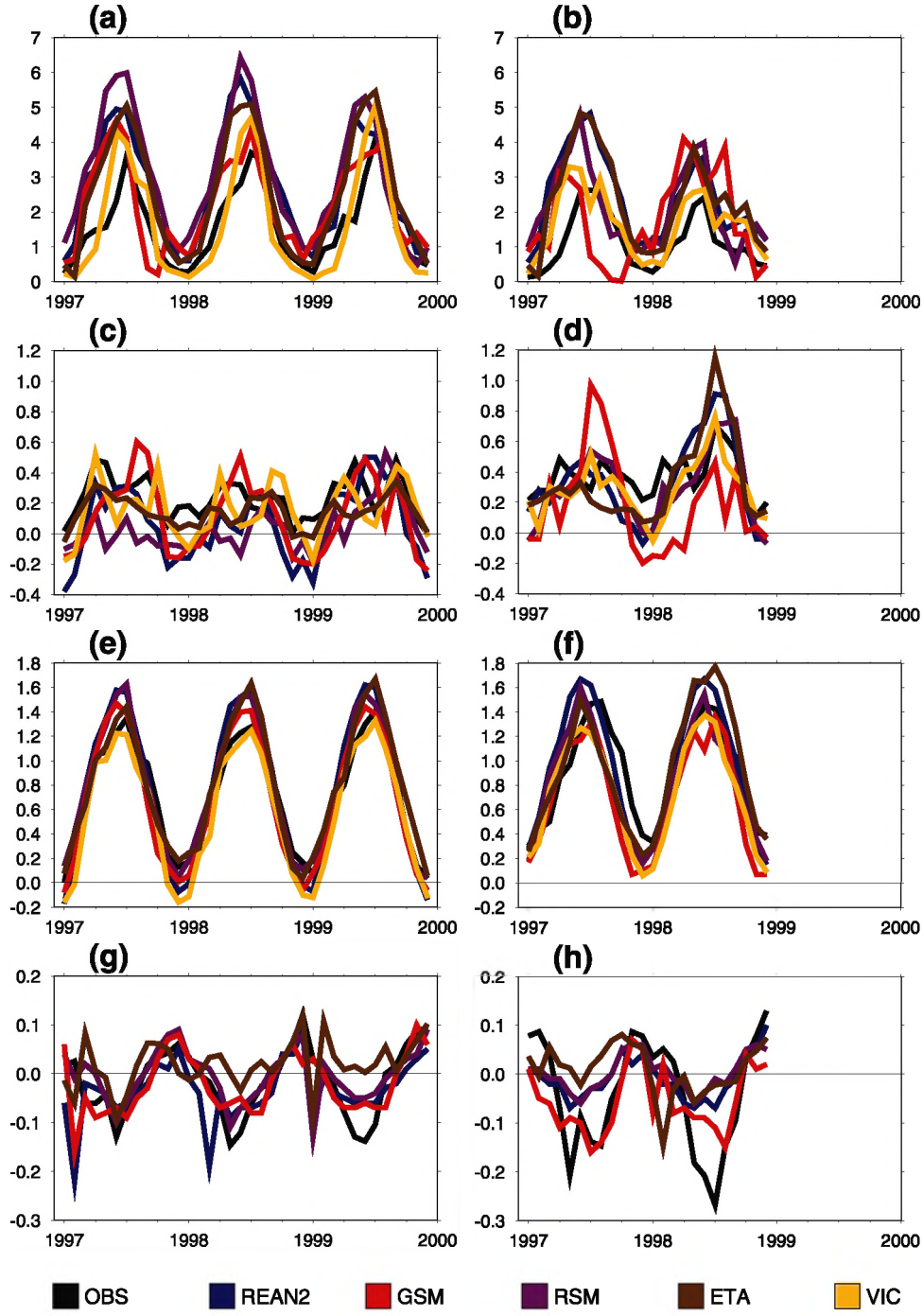

Figure 10. Comparisons of available models and analyses (REAN2, GSM, RSM) with the Meyer flux tower observations. (a) Champaign evaporation (mm d^{-1}). (b) Little Washita evaporation (mm d^{-1}). (c) Champaign sensible heating (K d^{-1}). (d) Little Washita sensible heating (K d^{-1}). (e) Champaign surface radiative heating (K d^{-1}). (f) Little Washita surface radiative heating (K d^{-1}). (g) Champaign subsurface heating G (K d^{-1}). (h) Little Washita subsurface heating G (K d^{-1}).

sensible heat in the northwest portion of the domain was negative in all models, and strongly negative in the REAN2. As shown in Figures 10c and 10d observed sensible heating at the available tower sites (Little Washita and Champaign) had much weaker seasonal variations than the models indicate. Still, one can see some similarities between the average model values at these stations. Sensible heating increased during the summer and decreased during the winter, although the observations never showed a flux of heat to the surface from the atmosphere, like the models.

6.11. Atmospheric Radiative Cooling

[70] The geographical variations in atmospheric radiative cooling (Figure 13) were fairly small but noticeably different among the various models, with the RSM having the greatest radiative cooling. All models did show that the atmospheric

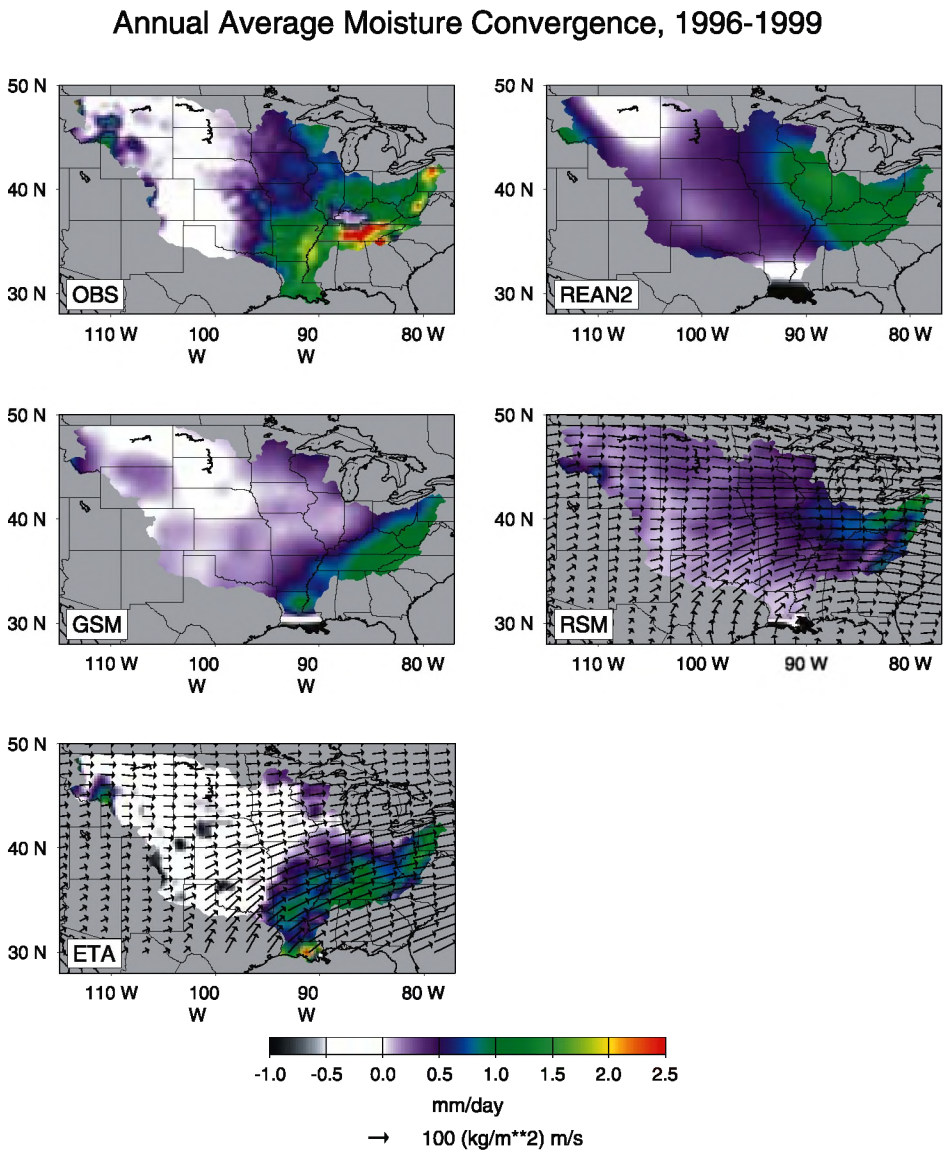

Figure 11. Annual average moisture convergence (mm d^{-1}) from the observations (*Fekete et al.* [2000] runoff) and models and analyses (REAN2, GSM, RSM, Eta).

radiative cooling was relatively strong during the winter and relatively weak during the summer, with the RSM perhaps having the greatest east-west gradient. Interannually (as shown later), the cooling was relatively weak during the early part of the period and beccame stronger at the end of GCIP.

6.12. Surface Radiative Heating

[71] The annual net surface radiative heating for the models was fairly consistent with the largest annual amounts occurring in the southeast and the smallest amounts in the northwest and north central, where the largest snow amounts occurred (Figure 14). The Eta model tended to have relatively large surface radiative heating whereas the VIC model's surface radiation was fairly weak. Seasonally all models showed the typical pattern of weak heating and even cooling (northwest) during the winter and strong heating during the summer. Interannually (as shown later), there were a number of differences, especially between the atmospheric models and the VIC model. It is important to note that the VIC model was forced with downward solar and longwave radiation derived from algorithms that are tuned to surface observations, whereas surface radiative heating from the atmospheric models was a product of the models' internal computations of cloud and water vapor. As shown in Figures 10e and 10f, the comparison to the observations at the available tower sites (Little Washita and Champaign) shows the models were quite good although the models had a larger seasonal cycle and provided larger values during the summer and smaller values during the winter. There is much work still needed for models as well as the development of observations of this important but inadequately observed variable.

6.13. Radiation Fluxes

[72] In addition to the basic hydroclimatic variables described above we also examined the individual radiation fluxes, and again the interested reader should refer to the WEBS CD-ROM for the relevant figures and discussion. One disappointing aspect of this synthesis is that we were unable to

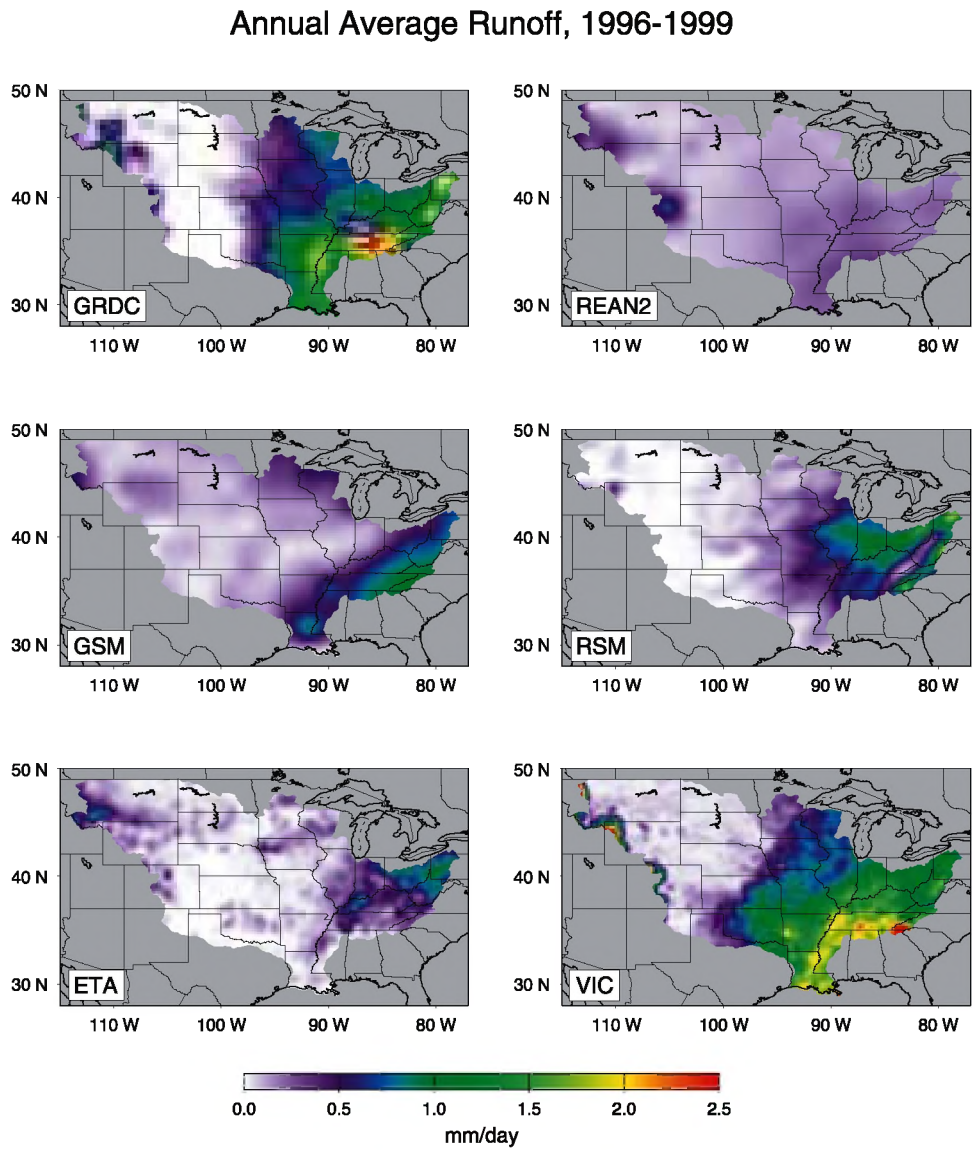

Figure 12. Annual average runoff (mm d^{-1}) from the gridded runoff product (labeled GRDC) [*Fekete et al.*, 2000] and models and analyses (REAN2, GSM, RSM, Eta, VIC).

acquire the net surface longwave flux to compute net surface radiation and the integrated atmospheric radiative cooling. However, some of the individual fluxes deserve comment.

[73] Annual mean bottom of the atmosphere (BOA or surface) net solar radiation drives the seasonal temperature variations and has a strong zonal component, with a tendency to be weakest in the northeast, consistent with the snow water. The net solar radiation is weakest in the VIC and strongest in the Eta models, which appear to be biased with respect to the observations. The VIC model is especially low during the summer, although as shown by *Maurer et al.* [2002], VIC surface solar radiation closely matches observations at SURFRAD sites. The RSM is also a bit low, indicating perhaps too much cloud cover, which is somewhat surprising given the fact that it is relatively dry in the RSM; however there may be a parameterization problem in that clouds need to be better tuned for the RSM.

[74] The net top of atmosphere (TOA) shortwave annual mean was fairly consistent among the available models, with the smallest amounts again occurring in the RSM, mainly because of low summertime radiation; again this may be a problem in either having overly reflective clouds or too many clouds. Perhaps the best comparison came from the REAN2, although the Eta analysis was unavailable for this variable. Interannually the various models show wide scatter, whereas the observations show a clear trend from decreased amounts at the beginning of GCIP [1996] to much larger amounts at the end [1999].

[75] Like the net solar radiation at the TOA, clouds strongly influence the net TOA longwave radiation and the available models may not be producing adequate clouds, especially during the summer. In that regard the RSM appeared to offer the best comparison, although again Eta variables were not available. The lowest TOA net longwave occurs over the Northwest, indicating fairly high clouds there. Interannual variations are quite consistent among all the models, and the largest amount of outgoing radiation occurs during the falls and winters of the 90s. Why there is

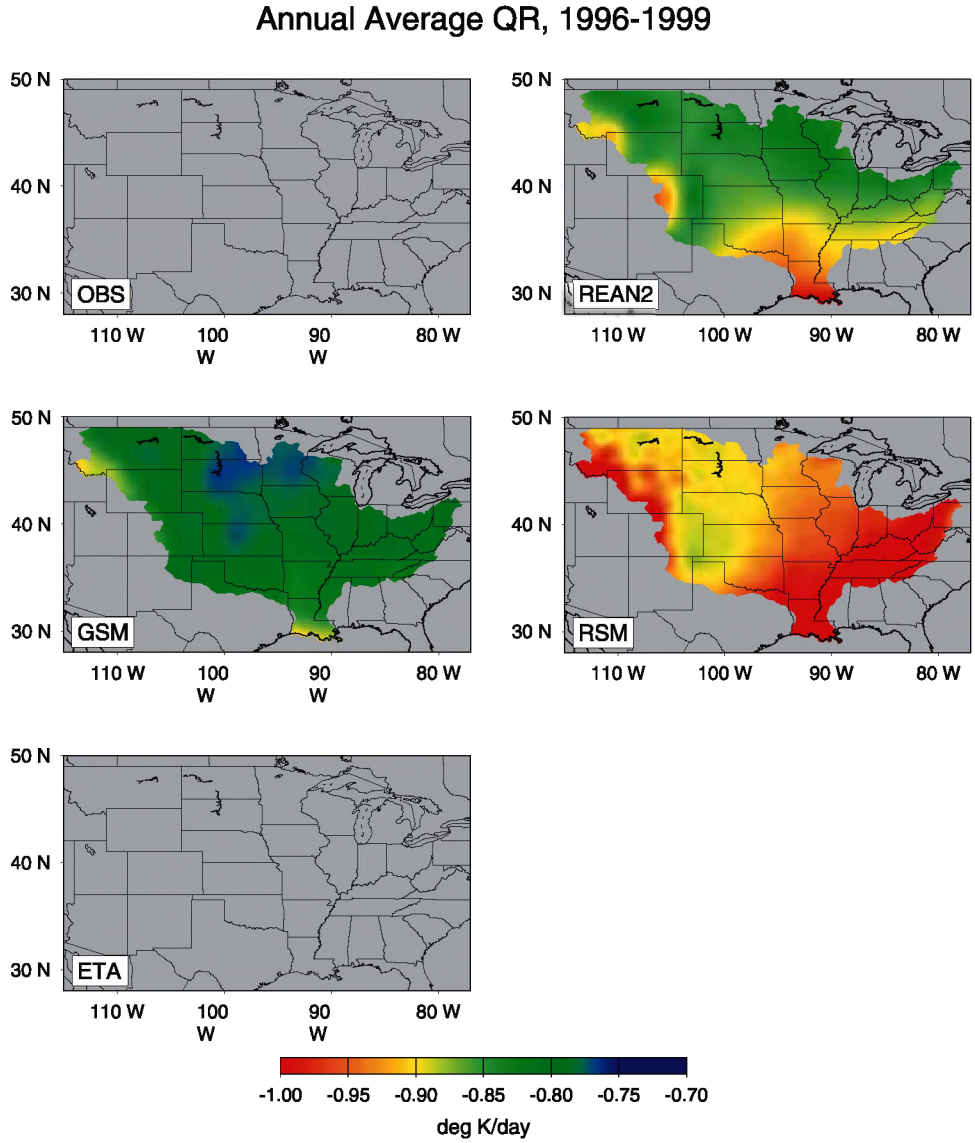

Figure 13. Annual average atmospheric radiative cooling (K d^{-1}) from the observations and models and analyses (REAN2, GSM, RSM, Eta).

this seemingly large amount of outgoing radiation when the precipitation is relatively high is quite curious.

[76] The surface net long wave radiation seasonal variations were fairly consistent among all the models. VIC had the largest discrepancy in that the net longwave radiation was weak in the southwest, especially during the summer (note that VIC comparisons with observations at SURFRAD sites did show good agreement, see *Maurer et al.* [2002]). By contrast, the Eta analysis had exceedingly large amounts during the summer and this may be related to erroneous surface temperatures, which were not available for this analysis. Unfortunately, without adequate observations of the net upward longwave flux, it is difficult to fully understand the discrepancies.

7. Seasonal Variations

[77] Figure 15 summarizes the seasonal mean atmospheric water budgets for the various models (except for the VIC model, of course). In comparison to NVAP observations, the precipitable water (Figure 15e) was fairly well simulated, with seasonal variations ranging from 7 to 30 mm; even though the tendency (Figure 15d) made only a small contribution to the budget, it was simulated well by all the models. The observed precipitation (Figure 15a) varied between 1 mm a day during the winter to 3 mm/d during the summer, and was basically the same in the NEXRAD and gauge observations. All models provided qualitatively similar seasonal variations, with perhaps the Eta model providing the best precipitation simulations. All other models had a positive precipitation bias, especially during the late winter early spring. This wet bias extended to the evaporation (Figure 15b). The RSM tended to be dryer but was still not as dry as the Eta model and not as dry as the VIC model. Note the moisture convergence (Figure 15c), had the opposite seasonal behavior to evaporation in that the strongest convergence occurred during the wintertime when the evaporation was very small; as discussed by *Roads et al.* [2002a] this is characteristic of midlatitude climates, which have increased summertime precipitation from increased

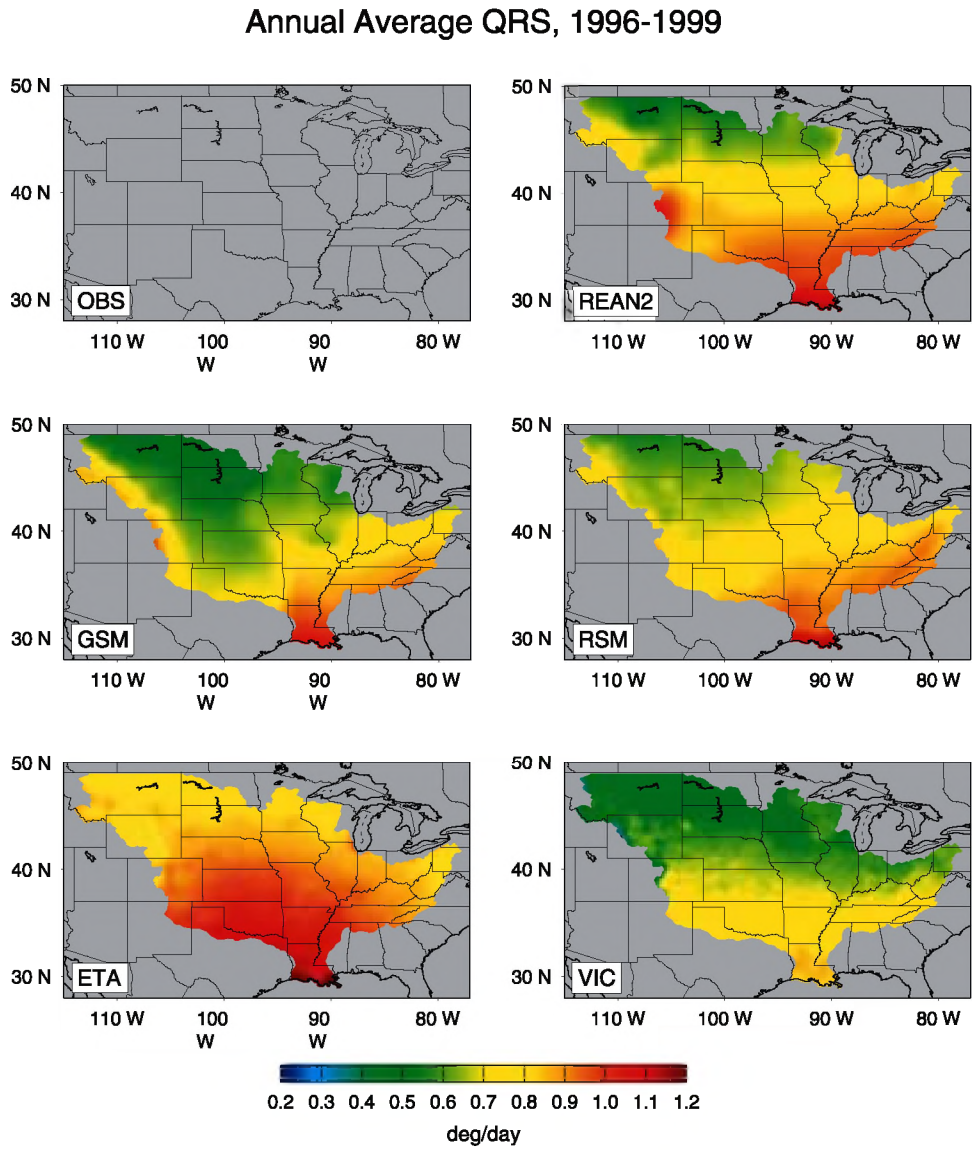

Figure 14. Annual average surface radiative heating (K d^{-1}) from the observations and models and analyses (REAN2, GSM, RSM, Eta, VIC).

surface evaporation in spite of the decreased moisture convergence. Finally, it should be noted that the REAN2 and Eta analyses had a residual RESQ (Figure 15f) that did not have a small seasonal cycle. Although the moisture convergence was not calculated explicitly for the other models, none of the other models probably had a similar large residual mainly because this residual is mainly a consequence of the constant correction analysis models go through in the analysis procedure. Despite the residual, we may still expect that the analysis models should provide the best estimate of individual processes. As the analysis models get better, we might expect this residual to be reduced; the magnitude of RESQ is one measure of our ability to close budgets (in fact, this residual was reduced from a larger value in the first NCEP/NCAR analysis). This residual also provided a measure of uncertainty, which was at least consistent in magnitude with the uncertainty estimated from other differences in the models. For example, 1 mm d^{-1} for a peak precipitation of 3–4 mm d^{-1} indicated about a 25–33% uncertainty in the atmospheric water budget. However, if this uncertainty was compared to other features of the water budget, like the moisture convergence, then the uncertainty can be almost 100%.

[78] Figure 16 summarizes the atmospheric energy budgets for the various models (mainly the REAN2, GSM, and RSM). The atmospheric radiative cooling (Figure 16d), was weakest during the spring and strongest during the winter. Note that the dry static energy convergence (Figure 16c) acted to balance the radiative cooling, except during the summer when it also balanced the sensible heating (Figure 16b) and latent heat of condensation (Figure 16a). That is, atmospheric dry static energy flowed from the surrounding areas to the Mississippi River Basin during the winter but during the summer when the precipitation was high, energy flowed out of the basin. This was similar to the moisture convergence, which was also negative during the summer. Besides the precipitation differences in the models discussed previously, there were some

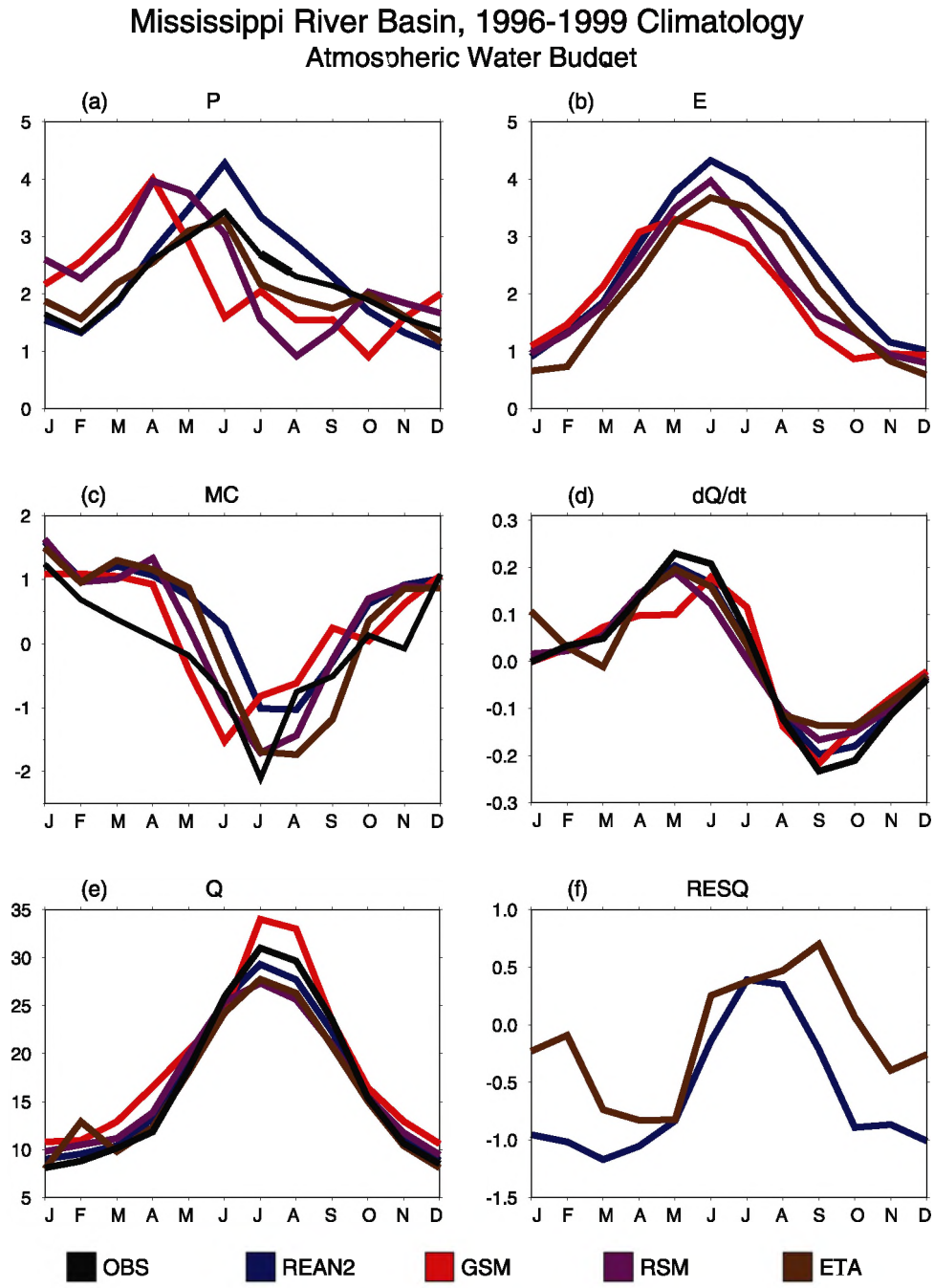

Figure 15. Mississippi River Basin seasonal atmospheric water budget from the observations and models and analyses (REAN2, GSM, RSM, Eta). (a) Precipitation (mm d^{-1}). (b) Evaporation (mm d^{-1}). (c) Moisture convergence (mm d^{-1}). (d) dQ/dt (mm d^{-1}).(e) Q (mm). (f) RESQ (mm d^{-1}).

differences in the dry static energy convergence (heat convergence), which was consistent with the precipitation differences. Note that the residual (Figure 16e) in this equation was positive during the winter and negative during the summer, and thus had the opposite behavior to the residual from the moisture equation. For this reason the residual was assumed to be largely related to the precipitation spin up and spin down biases since precipitation acted differently in both equations and precipitation is known to have this spin up and spin down problem [e.g., *Roads et al.*, 2001]. Again, we could not estimate the residual for the GSM and RSM since the dry static energy convergence (heat convergence) was deduced as a balance of the other terms, but it is presumably small. We also could not estimate the heat residual from the Eta model since we did not have the atmospheric radiative heating from the Eta analysis although since the residual is related to precipitation and there is a residual in the moisture equation there is also likely to be a temperature residual in the Eta operational analysis. The uncertainty measured by the residual or model differences was smaller than the latent heat of precipitation but as large as the sensible heating.

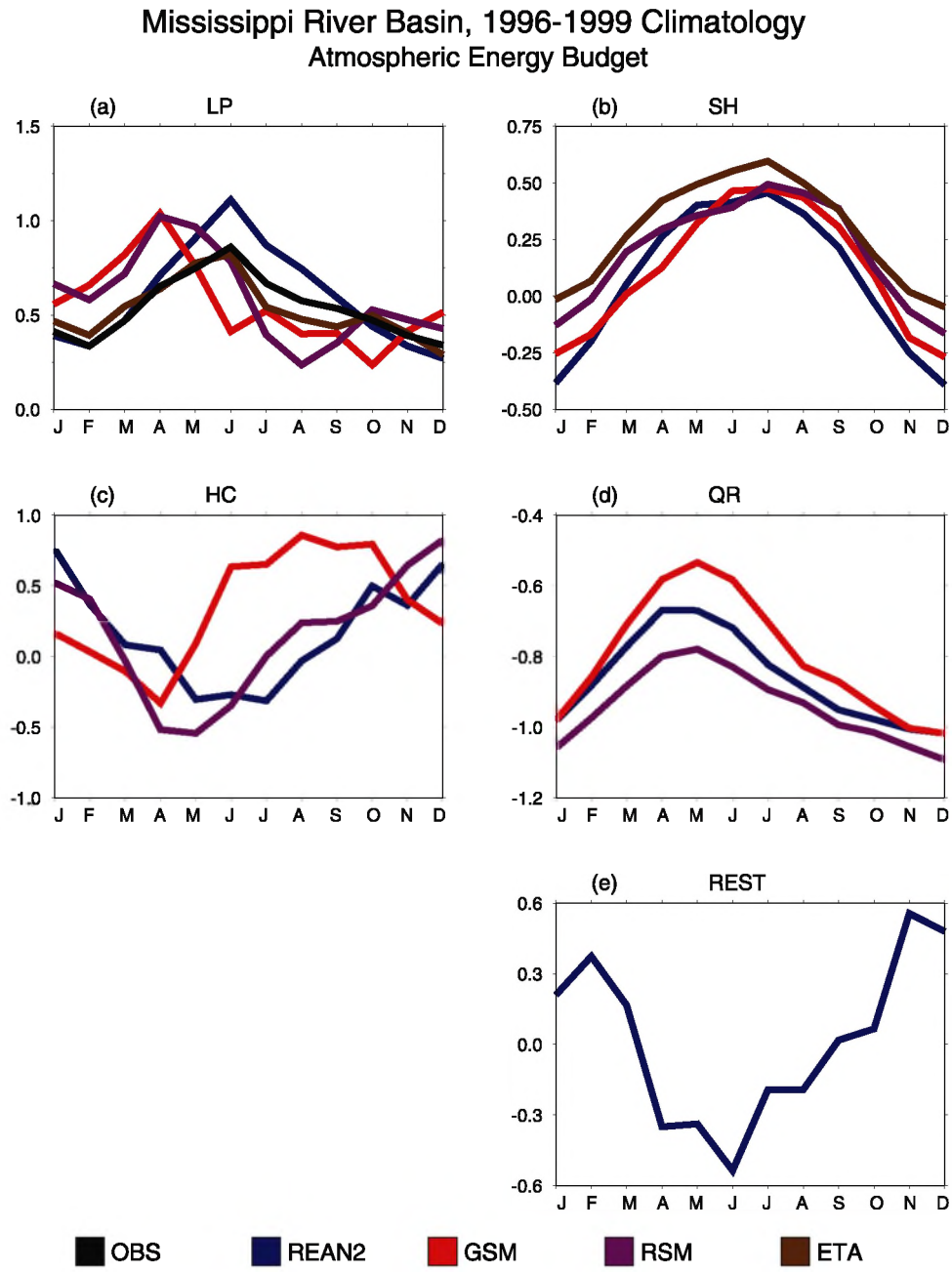

Figure 16. Mississippi River Basin seasonal atmospheric energy budget from the observations and models and analyses (REAN2, GSM, RSM, Eta). (a) Latent heat of condensation (K d^{-1}). (b) Sensible heating (K d^{-1}). (c) Dry static energy convergence (K d^{-1}). (d) Radiative cooling (K d^{-1}). (e) REST (mm d^{-1}).

[79] Figure 17 summarizes the surface water budgets for the various models. The precipitation (Figure 17a) and evaporation (Figure 17b) were discussed above, although here we also have the addition of the VIC products, which came from a macroscale hydrologic model simulation, forced by observed meteorology, that closely reproduced observed runoff (Figure 17c). Note that the runoff in the other models (except the GSM, which had erroneously high precipitation) was too low. The gridded monthly runoff from *Fekete et al.* [2000] was included for comparison with the monthly observations at the basin-wide scale, but as indicated in chapter 5, the basin-wide total runoff from *Fekete et al.* [2000] underestimated basin average observations on an annual basis. Since the VIC model was forced by observed precipitation and runoff was in fairly good agreement with independent observations, this might suggest that the evaporation (Figure 17b) was well modeled by the VIC, although there were certainly major evaporation differences with the other models, especially during the spring to summer. All models (the Eta analysis was unavailable) had comparable surface water (Figure 17e) and tendencies (Figure 17d), with the smallest tendencies of corresponding to the VIC model, which had the smallest surface water seasonal cycle and the largest tendencies

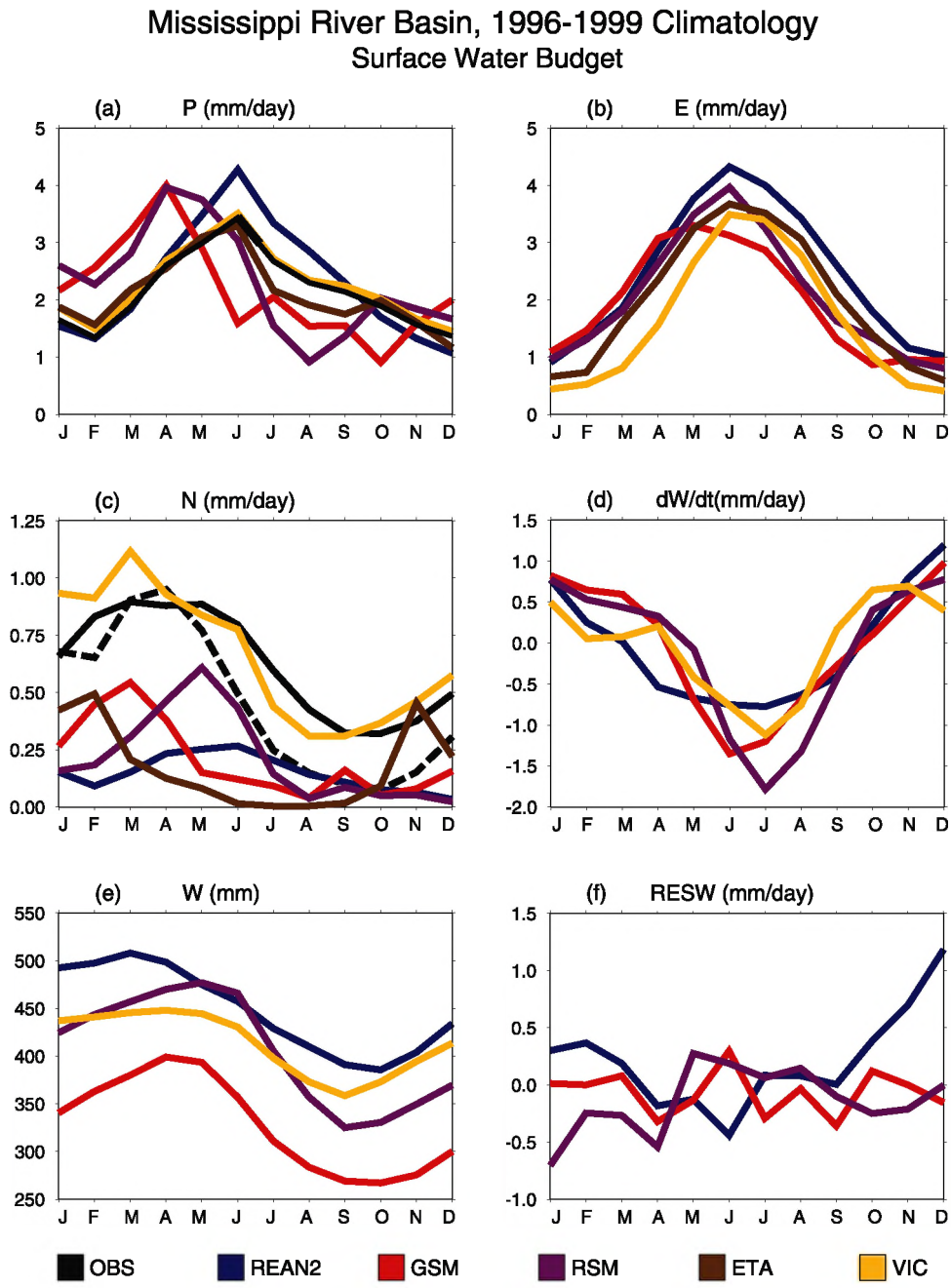

Figure 17. Mississippi River Basin seasonal surface water budget from the observations (*Higgins et al.* [2000] precipitation, solid line, and *Smith et al.* [1996] NEXRAD, dashed line; *Maurer and Lettenmaier* [2001] naturalized USGS runoff, solid line, and *Fekete et al.* [2000] gridded runoff product runoff, dashed line), and models and analyses (REAN2, GSM, RSM, Eta, VIC). (a) Precipitation (mm d^{-1}). (b) Evaporation (mm d^{-1}). (c) Runoff (mm d^{-1}). (d) dW/dt (mm d^{-1}). (e) W (mm). (f) RESW (mm d^{-1}).

corresponding to the RSM. The residual errors (Figure 17f) were largest in the REAN2, which externally forces the soil moisture with observed precipitation.

[80] Figure 18 summarizes the surface energy budgets for the various models. The net surface solar radiation (Figure 18c) drove the seasonal temperature variations (Figure 18e), and was balanced by the net long wave radiation (without long wave cooling, the surface radiative heating would have been significantly larger than that shown in Figure 18d) as well as the cooling generated by evaporation (Figure 18a) and sensible heat transfer (Figure 18b). The contributions by the ground heat flux (Figure 18f) were much smaller, although, perhaps somewhat surprisingly, largest in the VIC model, which had strong cooling during the spring and warming during the fall. Part of the relatively strong cooling in the GSM was related to the fact that energy was needed to melt the large accumulation of snow the GSM. Again, although it is certainly tempting to assume that the VIC model is producing the best evaporation, we can see here that the VIC model tended to have the smallest amount of net solar radiation (much smaller than the *Pinker et al.* [2003] observations), net longwave radiation, and sensible

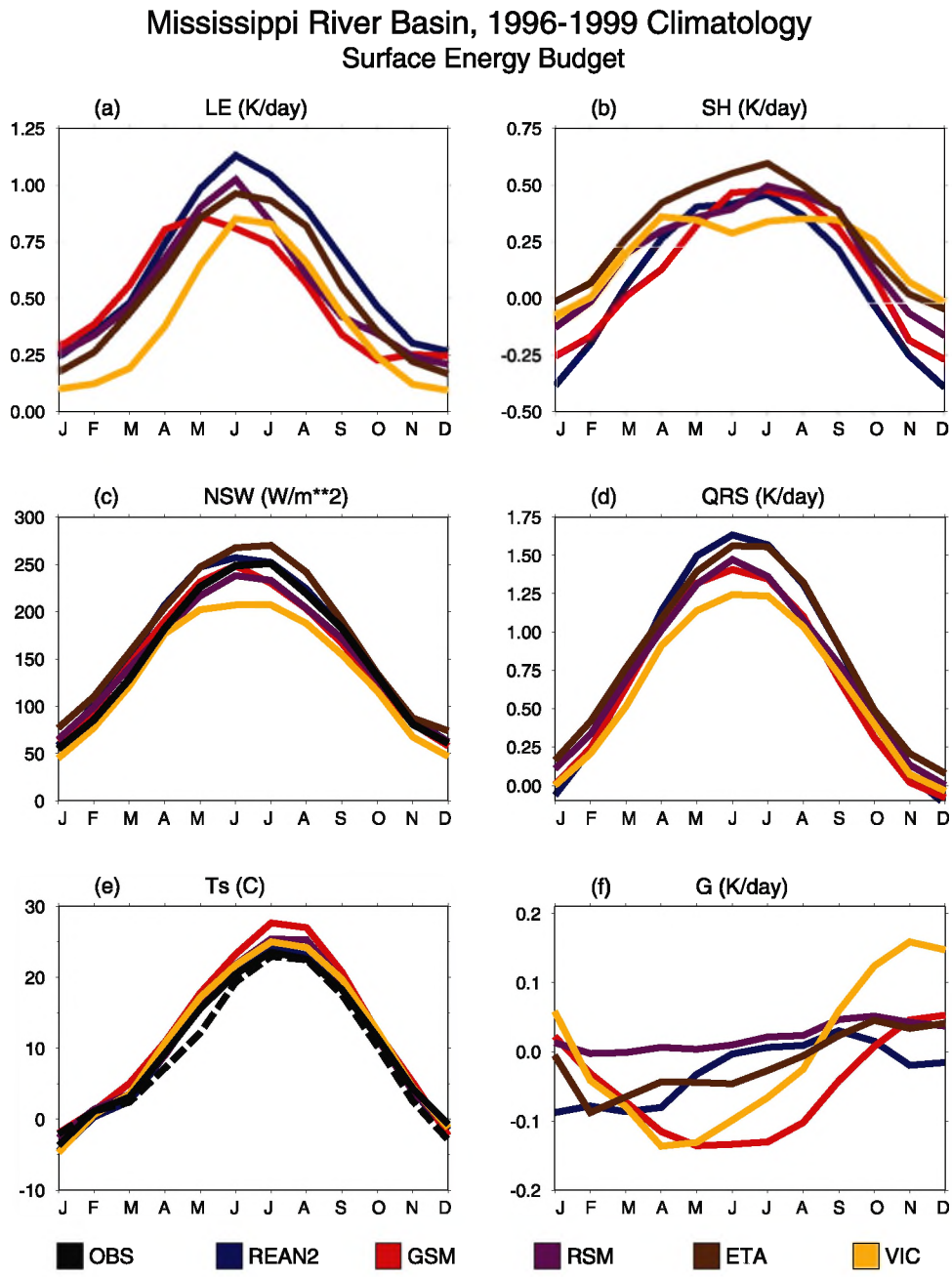

Figure 18. Mississippi River Basin seasonal surface energy budget from the observations (*Pinker et al.* [2003] radiation; *Janowiak et al.* [1999] temperature, solid line; *Lakshmi and Susskind* [2000] TOVS temperature, dashed line) and models and analyses (REAN2, GSM, RSM, Eta, VIC). (a) Latent heat of evaporation (K d^{-1}). (b) Sensible heating (K d^{-1}). (c) Surface net solar radiation (W m^{-2}) (d) Radiative heating (K d^{-1}). (e) T (°C). (f) Ground heating (K d^{-1}).

heating as well as latent heating. On the other hand, as shown by *Maurer and Lettenmaier* [2001] (available at http://www.cc.washington.edu/pub/HYDRO/cdm/WEBS_runoff/), the VIC model closely matched observed solar and downward longwave radiation, as well as net radiation, at SURFRAD sites. The largest differences in the sensible heating and net longwave radiation occurred between the VIC and Eta. The magnitudes of the differences were substantial, on the order of 0.25 to 0.5 K d^{-1} or 30–60 Watts m^{-2}. Finally, note that all models tended to have slightly higher temperatures (Figure 18a) than observations and also note that the satellite skin temperature observations appear to be too low in this region.

8. Interannual Variations

[81] Figure 19 summarizes the interannual atmospheric water budgets for the OBS, REAN2, RSM, and Eta. The monthly climatology removed was calculated from the 1996–1999 monthly means only. Also note that since only observed sea surface temperatures force the GSM, they did not provide the same verisimilitude as the other analysis

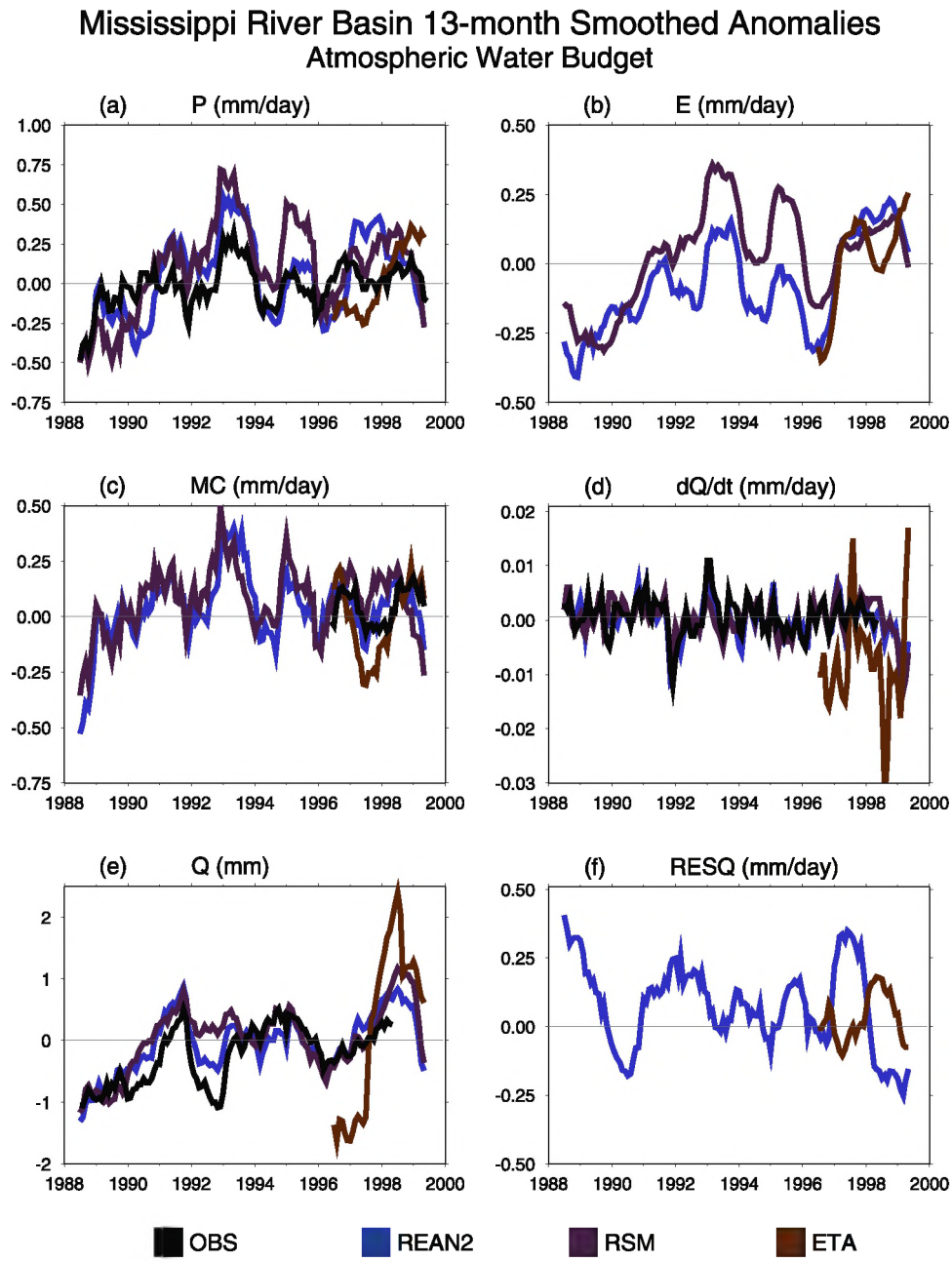

Figure 19. Mississippi River Basin interannual (monthly means removed and anomalies smoothed by running 13-month mean) atmospheric water budget from the observations and models and analyses (REAN2, GSM, RSM, Eta). (a) Precipitation (mm d^{-1}). (b) Evaporation (mm d^{-1}). (c) Moisture convergence (mm d^{-1}). (d) dQ/dt (mm d^{-1}). (e) Q (mm). (f) RESQ (mm d^{-1}).

based outputs and thus the GSM variations were not included in this comparison. Note also the fairly strong correspondence between the observed precipitation (Figure 19a) and REAN2 and RSM. Interannual precipitation variations tended to be best simulated in the REAN2, although the RSM also provided similar features. Interannually, all models and analyses tended to indicate larger divergence during the summer of 1988 and stronger convergence (Figure 19c) during the summer of 1993, consistent with the precipitation variations, although evaporation variations (Figure 19b) were also important. Precipitable water variations (Figure 19e) were somewhat related to the precipitation although interestingly, during the 1993 precipitation peak, the amount decreased. Also note that the precipitable water tendency (Figure 19d) is basically quite small in comparison to other processes. However, the residual forcing (Figure 19f) for the global reanalysis (REAN2) is not small. The residual is smaller for the Eta model, although the Eta model does not produce realistic interannual features in many other variables, in part because the model and analysis system changes during the course of GCIP swamp any naturally occurring variations. This again points out the importance of a reanalysis for interannual variations; in that regard it should be noted that there is a regional reanalysis is

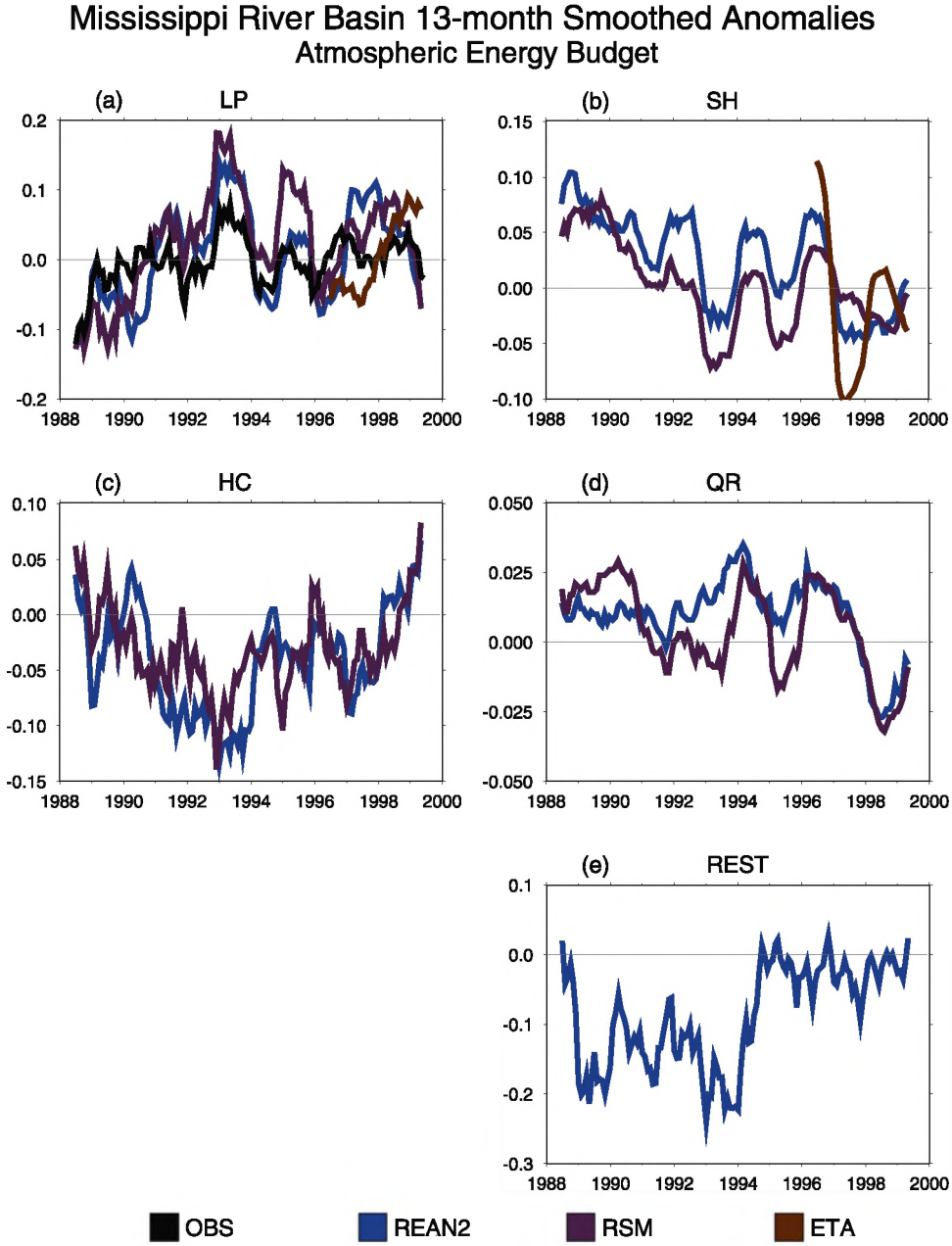

Figure 20. Mississippi River Basin interannual (monthly means removed and anomalies smoothed by running 13-month mean) atmospheric energy budget from the observations and models and analyses (REAN2, GSM, RSM, Eta). (a) Latent heat of condensation (K d^{-1}). (b) Sensible heating (K d^{-1}). (c) Dry static energy convergence (K d^{-1}). (d) Radiative cooling (K d^{-1}). (e) REST (K d^{-1}).

now underway [*Mesinger et al.*, 2002] with an updated version of the Eta operational products shown here.

[82] Figure 20 summarizes the interannual variations in the atmospheric energy budgets for the various models. Note the inverse relationship between the dry static energy convergence (Figure 20c) and the latent heat of condensation (Figure 20a). The sensible heat flux also contributed (Figure 20b), although more as a long-term trend, which can be related to the surface water variations (shown below). The atmospheric radiative cooling variations (Figure 20d) were much weaker although they tended to counteract the dry static energy convergence. Interannual variations in the sensible heating (Figure 20b) demonstrate an overall trend toward more sensible heating during the early dry period in comparison to the latter wet period described below. Again the residual term (Figure 20e) was as large as any of the other terms, especially during the early period of the reanalysis. Again note the erroneous Eta analysis interannual variations (sensible heating and possibly precipitation), were excessive and presumably caused by operational model changes.

[83] Figure 21 summarizes the interannual variations in the surface water budgets for the various models. Surface water (Figure 21e) tended to be low during the early part of the period and wet during the latter period, which was somewhat consistent with the precipitation (Figure 21a), although precipitations tended to lead the surface water

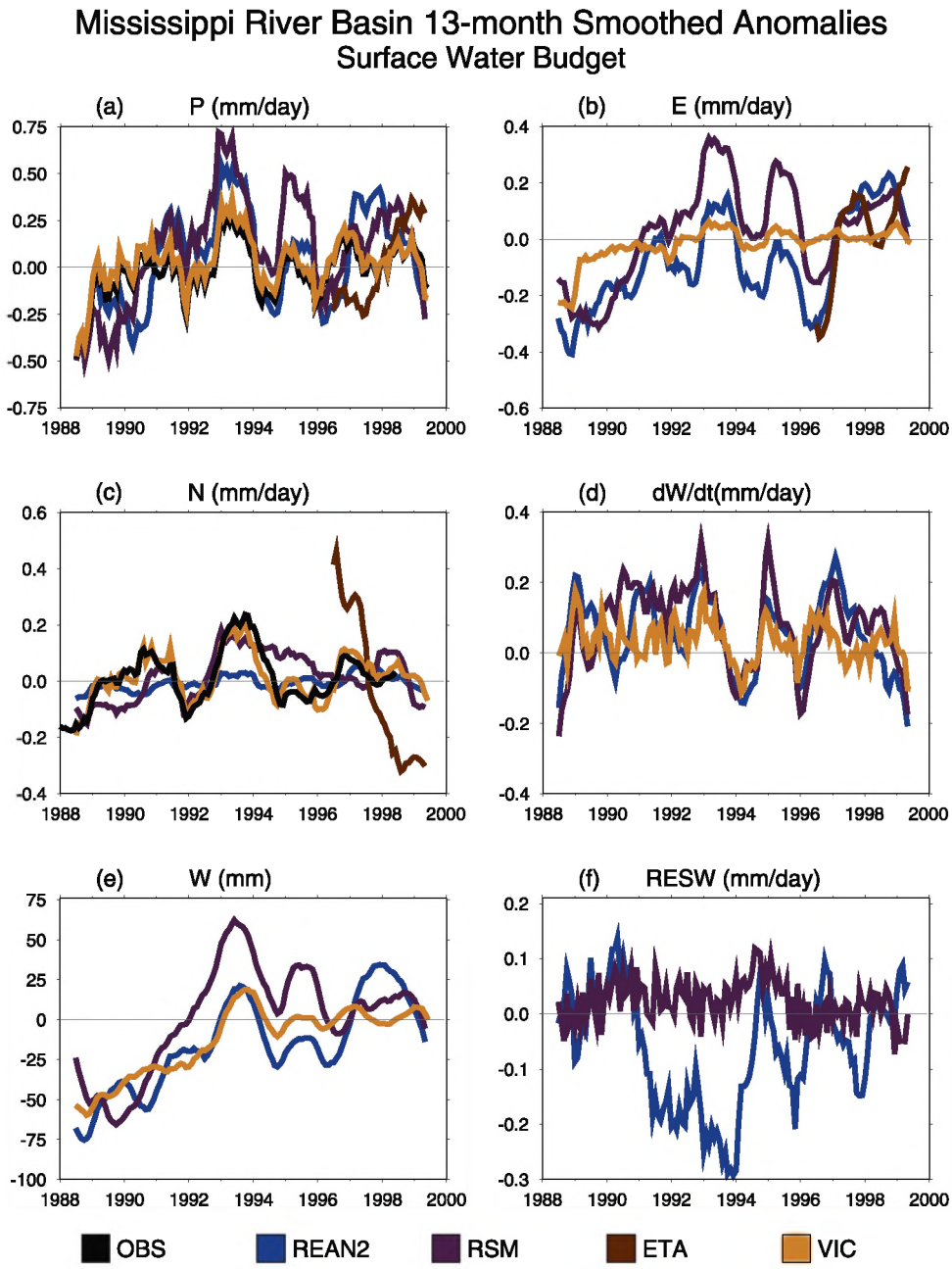

Figure 21. Mississippi River Basin interannual (monthly means removed and anomalies smoothed by running 13-month mean) surface water budget from the observations (*Higgins et al.* [2000] precipitation, solid line, and *Smith et al.* [1996] NEXRAD, dashed line; *Maurer and Lettenmaier* [2001] naturalized USGS runoff, solid line), and models and analyses (REAN2, GSM, RSM, Eta, VIC). (a) Precipitation (mm d^{-1}). (b) Evaporation (mm d^{-1}). (c) Runoff (mm d^{-1}). (d) dW/dt (mm d^{-1}). (e) W (mm). (f) RESW (mm d^{-1}).

variations. The observed runoff was somewhat larger than the runoff in the RSM and especially the REAN2 (Figure 21c). However, there was clearly a problem with the RSM runoff in that it tended to have a harder time changing from one state to another, reflecting perhaps a too large water reservoir in the model. Again there appears to be erroneous variations in Eta runoff, presumably because of analysis changes. By contrast note that the VIC had relatively small soil moisture variations (Figure 21d), but its runoff variations were comparable to the observed variations. A disquieting feature of the relatively small VIC surface water variations was that the evaporation variations (Figure 21b) were very small in comparison to the other models, indicating that evaporation did not play as an important role in VIC interannual variations as it does for the other models. The residuals (Figure 21f) were fairly small here, except for REAN2, which was actually forcing the soil moisture with observed rather than model precipitation.

[84] Figure 22 summarizes the interannual variations in the surface energy budgets for the various models. Note the fairly consistent trend in the surface energy variables, which can be related to the surface water variations.

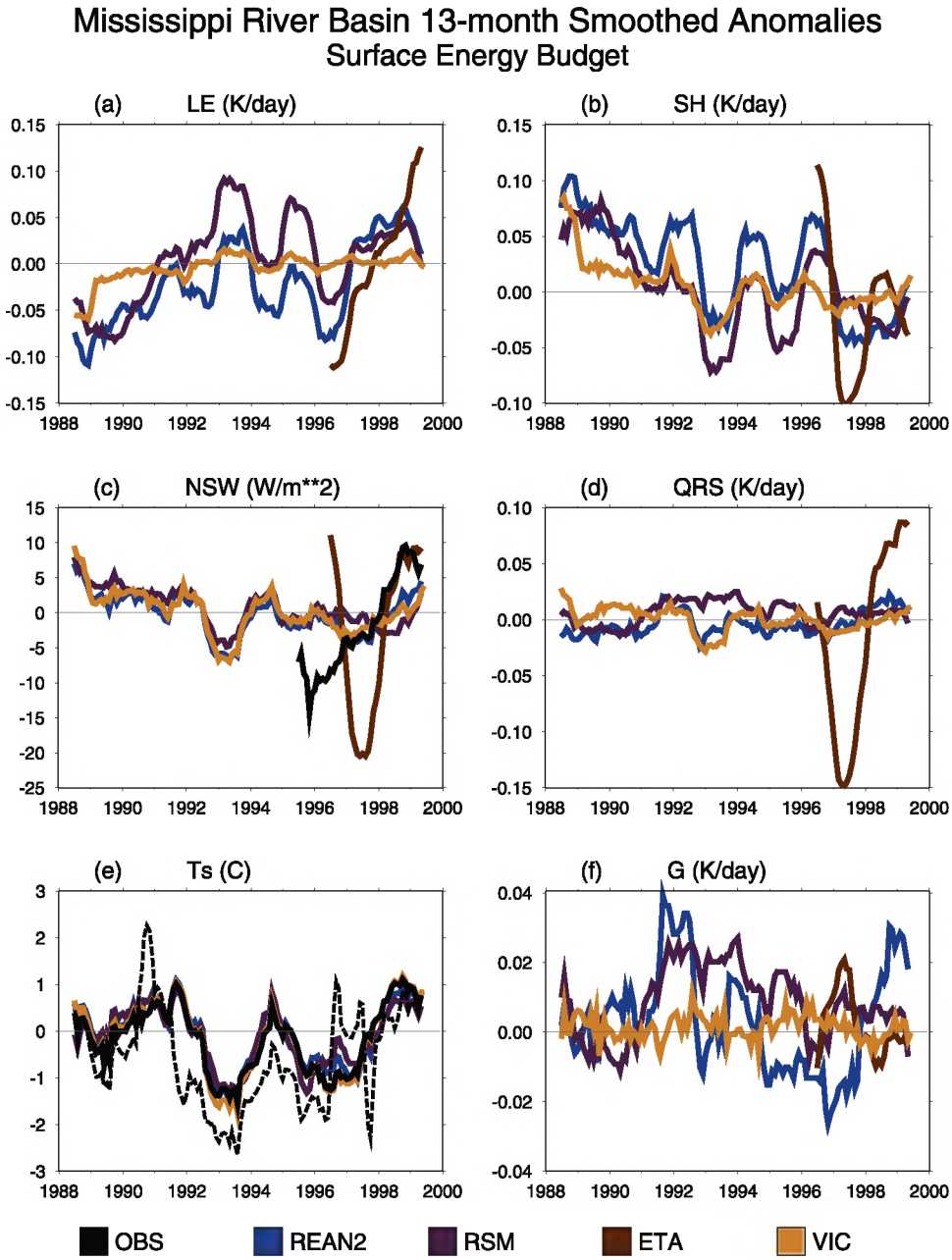

Figure 22. Mississippi River Basin interannual (monthly means removed and anomalies smoothed by running 13-month mean) surface energy budget from the observations (*Pinker et al.* [2003] radiation; *Janowiak et al.* [1999] temperature, solid line; *Lakshmi and Susskind* [2000] TOVS temperature, dashed line) and models and analyses (REAN2, GSM, RSM, Eta, VIC). (a) Latent heat of evaporation (K d^{-1}). (b) Sensible heating (K d^{-1}). (c) Surface net solar radiation (W m^{-2}). (d) Radiative heating (K d^{-1}). (e) T (°C). (f) Ground heating (K d^{-1}).

Besides the surface water variations, the early part of the period was characterized by above normal skin temperature (Figure 22e), low evaporation (Figure 22a), and increased sensible heating (Figure 22b). Net shortwave variations (Figure 22c) were consistent with this surface water trend (presumably because there were fewer clouds during dry periods) but were apparently largely balanced by net long wave variations resulting in only small contributions from the surface radiative heating (Figure 22d). The ground heating (Figure 22f) also contributed to this trend but was much smaller, especially in the VIC. Again the Eta model had some notably large spurious variations due to various analysis changes. It should also be noted here that the models might have produced more accurate variations in the temperature (Figure 22e) than the satellite observations although there was certainly great correspondence suggesting that the satellite observations may still be useful in regions where the surface network is not as extensive as the one over the Mississippi River Basin. Also note that the *Pinker et al.* [2003] net shortwave observations had a consistent change from lower values during the early part of the period to much larger values during the latter part of the period, which was

not found in the models. This noticeable discrepancy deserves future scrutiny.

9. Summary

[85] GCIP has provided new understanding of how water and energy processes interact on a continental scale by analysis of traditional measurements, development of new measurements, new models and analyses. This WEBS (paper and companion CD-ROM) attempted to provide a glimpse into some of these features and thus how one of the objectives of GCIP, which was to determine the water and energy budgets of the Mississippi River Basin, was partially satisfied.

[86] It is now clearer than ever that on a continental scale many of the observations needed to close the budgets cannot be obtained. There are currently inadequate soil moisture, snow equivalent water, evaporation, atmospheric moisture and dry static energy convergence, surface longwave radiation, and sensible heating observations. This inadequacy of comprehensive hydroclimatic measurements needs to be addressed in the future.

[87] Instead continental-scale depictions of these variables and processes have to be obtained from various coupled atmosphere and land surface models and their associated global, regional, and land surface analyses. Even some of these variables were not readily available from all of the models and analyses. For example, soil moisture, radiative cooling and dry static energy convergence apparently could not be easily obtained from the Eta model operational archives. Moisture convergence was only readily available from the NCEP/NCAR analysis.

[88] In that regard, it should be mentioned that the pending WCRP Coordinated Enhanced Observing Period (CEOP; see *World Climate Research Program* [2001]) has specifically requested that many of the world's numerical weather prediction centers explicitly provide these variables. CEOP may also be the stimulus for the development of more comprehensive observations of water and energy variables, including new satellite measurements.

[89] Clearly models and analyses have errors but at the same time they provide qualitative features that emulate many aspects of the observations and so one might expect that for those variables for which there are inadequate observations that these modeled processes may at least be qualitatively correct. However, there is still much uncertainty. Seasonal precipitation variations show large scatter among the models, especially during the spring to summer transition. This large scatter translates into large variations in runoff, as well as surface water tendencies. Interestingly, the atmospheric models with the best precipitation (Eta) tend to have the worst runoff. The atmospheric models also tend to produce too small a moisture convergence; although this is consistent with the subsequent model runoff, it is still too small to balance observed runoff. Direct observations of moisture convergence from radiosondes are not much help either. At the surface, the VIC hydrologic model produces a much better correspondence to mean observations (in part because it is tuned to observable surface parameters) suggesting that its surface water, evaporation and energy products might be superior. However, some of the surface energetics from the VIC are at odds with the other models as well as available observations (net solar radiation), suggesting that further examination is still needed.

[90] Interannually, there were many problems. The GSM interannual variations could not be included in the comparison, since the GSM was driven only by SSTs and the resulting forced simulations did not provide representative (at least in time) interannual variations. The Eta analysis had overly large interannual variations, which were presumably more reflective of analysis changes than natural variations. In this regard, the pending Eta reanalysis is likely to eventually provide a superior product. Runoff was obviously a problem for the atmospheric models and improvements in their land surface schemes are needed before using this product to drive hydrologic and water resource models. There seemed to be some relatively small interannual variations in the VIC energy parameterizations, which may be related in part to the smaller surface water variations in that model although this may also be related to the statistical nature of the forcing parameters. Finally, the satellite temperature and solar radiation observations, while certainly highly correlated with the models, seemed to have some spurious variations, indicating that further work may still needed for these remotely sensed "observations."

[91] The VIC model appeared to provide the best simulation of the mean surface water budget, suggesting, for example, that its evaporation provides a benchmark for comparison. However, the VIC surface radiation fluxes were noticeably different from other models and also observations of net solar radiation, and the VIC interannual variations were noticeably smaller than those from the other models. The Eta analysis provided the best precipitation of all the atmospheric models, although the RSM also had many realistic features, including a better agreement with the net solar radiation and various interannual variations that were clearly affected by various operational changes in the Eta output. Again, the pending Eta reanalysis should eventually provide the atmospheric model benchmark for interannual variations in the Mississippi River Basin. The global analysis and the GSM did not always capture some of the regional characteristics of the Mississippi River Basin, which suggests, but still does not prove, that current regional atmospheric models combined with macroscale hydrologic models will eventually provide the best regional predictions of water and energy processes.

[92] So, have the water and energy budgets been "closed?" All models had means and seasonal variations that resembled available observations and each other, meaning that qualitatively we probably understand the annual mean and seasonal and perhaps some of the major interannual variations in the water and energy budgets for the Mississippi River Basin. However, there were large quantitative differences. A number of errors were probably canceling, giving rise to smaller overall errors that were comparable to the residual errors calculated for the global and regional analyses [*Roads*, 2002]. Unfortunately, these errors can swamp interannual variations. In short, despite our best effort, it is clear that this current effort (this paper and the companion CD) should still be thought of as a preliminary synthesis and as new measurement systems and new models are developed as part of GAPP, it would be useful to once again examine just how well we can adequately characterize and close continental-scale water and energy budgets.

[93] Finally, besides developing the "best available" WEBS, another one of the original goals of GCIP was satisfied. Meteorologists and hydrologists had to come together to develop a better understanding of the coupled land atmosphere system at a scale much larger than typically studied by hydrologists and at a scale much smaller than traditionally studied by meteorologists. Such interdisciplinary understanding should help us to move forward toward eventually developing improved regional and global hydroclimatological analysis and prediction systems.

Appendix A: Variable Definitions

[94] In the water budget equations, all vertically integrated reanalysis water budget terms (kg m^{-2} s^{-1}) were multiplied by 8.64×10^4 s d^{-1}, which provided individual values in kg m^{-2} d^{-1} or mm d^{-1} (using a density of 1000 kg m^{-3} for water). In the atmospheric temperature or energy budget equation, all energy terms (W m^{-2}), were multiplied by $8.64 \times 10^4/(C_p p_s\, g^{-1})$, to provide normalized values in units of K d^{-1}. Here $C_p = 1.0046 \times 10^3$. It should be noted here that the p_s used for this normalization was taken from the monthly mean pressure files only although instantaneous calculations of fluxes did include the instantaneous pressure for the moisture and dry static energy convergences. The normalization was simply for presentation purposes.

[95] The surface energy terms were also multiplied by a constant atmospheric normalization in order to provide values in K d^{-1}. That is, $C_v H = C_p \frac{p_S}{g} \cong 10^7 W kg^{-1} K^{-1} kgm^{-2}$ This normalization definition was only a simplification in order to easily compare surface energy variations with atmospheric energy variations. The heat capacity of the surface is certainly different from the atmosphere and adequate accounting of this surface heat capacity is needed in order to properly represent diurnal and seasonal cycles. However, as is the case for many global climate models, the heat capacity of the surface was ignored since only a daily average heat balance was analyzed here.

[96] All the variables analyzed for this WEBS are summarized in the Notation.

Notation

Q	Atmospheric Precipitable Water, mm.
W	Surface Water (Soil Moisture + Snow) (M + S), mm.
S	Snow, mm.
Ts	Surface Temperature, °C.
P	precipitation, mm d^{-1}.
E	evaporation, mm d^{-1}.
MC	moisture convergence, mm d^{-1}.
N	runoff, mm d^{-1}.
HC	dry static energy convergence, K d^{-1}.
LP	latent heat of condensation, K d^{-1}.
LE	latent heat of evaporation, K d^{-1}.
SH	sensible heat (which is positive upward), K d^{-1}.
QR	atmospheric radiative heating (which is negative), K d^{-1}.
QRS = NSW + NLW	surface radiative heating, K d^{-1}.
NSW Sfc	net shortwave radiation at the bottom of atmosphere (BOA), W m^{-2}.
NSW TOA	net shortwave radiation at the top of atmosphere (TOA), W m^{-2}.
NLW Sfc	net longwave radiation at the bottom of atmosphere (BOA), W m^{-2}.
NLW TOA	net longwave radiation at the top of atmosphere (TOA), W m^{-2}.
RESQ	atmospheric residual water forcing, mm d^{-1}.
RESW	surface residual water forcing, mm d^{-1}.
G	surface residual temperature forcing, W m^{-2}.
REST	atmospheric residual dry static energy forcing, W m^{-2}.
LP	latent heat of condensation, W m^{-2}.
LE	latent heat of evaporation, W m^{-2}.
LMC	latent heat of moisture convergence, W m^{-2}.
HC	dry static energy convergence, W m^{-2}.
SH	sensible heat, W m^{-2}.
QR	radiative cooling, W m^{-2}.
QRS	surface radiative heating, W m^{-2}.
LRESQ	atmospheric residual water forcing, W m^{-2}.
LRESW	surface residual water forcing, W m^{-2}.
GG	surface residual temperature forcing, W m^{-2}.
RESTT	atmospheric residual temperature forcing, W m^{-2}.
Ps g^{-1}	atmospheric mass, kg m^{-2}.

[97] **Acknowledgments.** This research was funded mainly by NOAA and NASA grants to individual investigators working on the GCIP project. Grants include NASA-NAG81516, NAG5-4775, 11738, 11599, and cooperative agreements from NOAA-NA77RJ0453 and NA17R1231 to J. Roads and NOAA grants GC99-443b and support for the New Jersey Agricultural Experiment Station to A. Robock. The views expressed herein are those of the authors and do not necessarily reflect the views of NASA or NOAA. We would like to thank John Janowiak for providing us the station temperature data and Eugene Rasmusson for his comments on an earlier draft. Comments by R. Avissar, an anonymous reviewer, and editor S. Pawson helped to improve the summary presentation of this material.

References

Adler, R. F., G. J. Huffman, D. T. Bolvin, S. Curtis, and E. J. Nelkin, Tropical rainfall distributions determined using TRMM combined with other satellite and rain gauge information, *J. Appl. Meteorol.*, *39*, 2007–2023, 2000.

Anderson, B. T., and J. O. Roads, Regional simulation of summertime precipitation over the southwestern United States, *J. Clim.*, *15*, 3321–3342, 2002.

Anderson, B. T., J. Roads, S. Chen, and H. -M. Juang, Regional modeling of the low-level monsoon winds over the Gulf of California and southwest United States: Simulation and validation, *J. Geophys. Res.*, *105*, 17,955–17,969, 2000.

Berbery, E. H., Mesoscale moisture analysis of the North American monsoon, *J. Clim.*, *14*, 121–137, 2001.
Berbery, E. H., and E. M. Rasmusson, Mississippi moisture budgets on regional scales, *Mon. Weather Rev.*, *127*, 2654–2673, 1999.
Berbery, E. H., E. M. Rasmusson, and K. E. Mitchell, Studies of North American continental-scale hydrology using ETA model forecast products, *J. Geophys. Res.*, *101*, 7305–7319, 1996.
Berbery, E. H., K. E. Mitchell, S. Benjamin, T. Smirnova, H. Ritchie, R. Hogue, and E. Radeva, Assessment of land surface energy budgets from regional and global models, *J. Geophys. Res.*, *104*, 19,329–19,348, 1999.
Betts, A. K., F. Chen, K. Mitchell, and Z. Janjic, Assessment of land-surface and boundary layer models in 2 operational versions of the Eta Model using FIFE data, *Mon. Weather Rev.*, *125*, 2896–2915, 1997.
Caplan, P. J. Derber, W. Gemmil, S. Y. Hong, H. L. Pan, and D. Parrish, Changes to the 1995 NCEP operation medium-range forecast model analysis-forecast system, *Weather Forecast*, *12*, 581–594, 1997.
Chen, F., K. Mitchell, J. Schaake, Y. Xue, H. Pan, V. Koren, Q. Duan, and A. Betts, Modeling of land-surface evaporation by four schemes and comparison with FIFE observations, *J. Geophys. Res.*, *101*, 7251–7268, 1996.
Chen, S. C., J. O. Roads, H. M.-H. Juang, and M. Kanamitsu, Global to regional simulations of California wintertime precipitation, *J. Geophys. Res.*, *104*, 31,517–31,532, 1999.
Chen, T. H., et al., Cabuw experimental results from the Project for Intercomparison of Land-surface Parameterization Schemes (PILPS), *J. Clim.*, *10*, 1194–1215, 1997.
Cosby, B. J., G. M. Hornberger, R. B. Clapp, and T. R. Ginn, A statistical exploration of the relationships of soil moisture characteristics to the physical properties of soils, *Water Resour. Res.*, *20*, 682–690, 1984.
Daly, C., R. P. Neilson, and D. L. Phillips, A statistical-topographic model for mapping climatological precipitation over mountainous terrain, *J. Appl. Meteorol.*, *33*, 140–158, 1994.
D'Amato, N., and T. Lebel, On the characteristics of the rainfall events in the Sahel with a view to the analysis of climatic variability, *Int. J. Climatol.*, *18*, 955–974, 1998.
DiMego, G. J., K. E. Mitchell, R. A. Petersen, J. E. Hoke, J. P. Gerrity, J. J. Tuccillo, R. L. Wobus, and H.-M. Juang, Changes to NMC's regional analysis and forecast system, *Weather Forecast.*, *116*, 1977–2000, 1992.
Dirmeyer, P., and H. Dolman, Global Soil Wetness Project: Preliminary report on the pilot phase, *IGPO Publ. Ser. 29*, World Clim. Res. Program, Washington, D.C., 1998.
Dirmeyer, P., A. J. Dolman, and N. Sato, The pilot phase of the Global Soil Wetness Project, *Bull. Am. Meteorol. Soc.*, *80*, 851–878, 1999.
Eidenshink, J. C., and J. L. Faundeen, The 1 km AVHRR global land data set: First stages in implementation, *Intl. J. Remote Sens.*, *17*, 3443–3462, 1994.
Eidenshink, J. E., The 1990 conterminous U.S. AVHRR data set, *Photogramm. Eng. Remote Sens.*, *58*, 809–813, 1992.
Entin, J. K., Spatial and temporal scales of soil moisture variations, Ph.D. dissertation, Univ. of Maryland, College Park, 1998.
Entin, J., A. Robock, K. Y. Vinnikov, S. Qiu, V. Zabelin, S. Liu, A. Namkhai, and T. Adyasuren, Evaluation of Global Soil Wetness Project soil moisture simulations, *J. Meteorol. Soc. Jpn.*, *77*, 183–198, 1999.
Entin, J. K., A. Robock, K. Y. Vinnikov, S. E. Hollinger, S. Liu, and A. Namkhai, Temporal and spatial scales of observed soil moisture variations in the extratropics, *J. Geophys. Res.*, *105*, 11,865–11,877, 2000.
Eskridge, R. E., O. A. Alduchov, I. V. Chernykh, Z. Panmao, A. C. Polansky, and S. R. Doty, A Comprehensive Aerological Reference Data Set (CARDS): Rough and systematic errors, *Bull. Am. Meteorol. Soc.*, *76*, 1759–1776, 1995.
Fekete, B. M., C. J. Vörösmarty, and W. Grabs, Global, composite runoff fields based on observed river discharge and simulated water balances: Documentation for UNH-GRDC composite runoff fields, v. 1.0, Global Runoff Data Cent., Koblenz, Germany, 2000.
Gallo, K., D. Tarpley, K. Mitchell, I. Csiszar, T. Owen, and B. Reed, Monthly fractional green vegetation cover associated with land cover classes of the conterminous USA, *Geophys. Res. Lett.*, *28*, 2089–2092, 2001.
GAME International Science Panel, GEWEX Asian Monsoon Experiment (GAME) Implementation Plan, 136 pp., GAME Natl. Proj. Off., Tokyo, 1998.
Gates, W. L., AMIP: The Atmospheric Model Intercomparison Project, *Bull. Am. Meteorol. Soc.*, *73*, 1962–1970, 1992.
Greil, G., Prognostic evaluation of assumptions used by cumulus parameterization, *Mon. Weather Rev.*, *121*, 764–787, 1993.
Grundstein, A., T. Mote, and D. Leathers, A hybrid climatology of snow water equivalent over the northern Great Plains of the United States, *Polar Geogr.*, in press, 2003.
Hansen, M. C., R. S. DeFries, J. R. G. Townshend, and R. Sohlberg, Global land cover classification at 1 km spatial resolution using a classification tree approach, *Int. J. Remote Sens.*, *21*, 1331–1643, 2000.
Higgins, R. W., Y. Yao, E. S. Yarosh, J. E. Janowiak, and K. C. Mo, Influence of the Great Plains low-level jet on summertime precipitation and moisture transport over the central United States, *J. Clim.*, *10*, 481–507, 1997.
Higgins, R., W. Shi, E. Yarosh, and R. Joyce, Improved US precipitation quality control system and analysis, *NCEP/CPC Atlas 7*, Natl. Weather Serv., Natl. Oceanic and Atmos. Admin., Silver Spring, Md., 2000.
Hollinger, S. E., and S. A. Isard, A soil moisture climatology of Illinois, *J. Clim.*, *7*, 822–833, 1994.
Hollinger, S. E., B. C. Reinke, and R. A. Peppler, Illinois climate network: Site description, instrumentation, and data management, *Circ. Ill. State Water*, *178*, 1994.
Hong, S., and H. Pan, Nonlocal boundary layer vertical diffusion in a medium-range-forecast model, *Mon. Weather Rev.*, *124*, 2322–2339, 1996.
Hong, S. Y., and A. Leetmaa, An evaluation of the NCEP RSM for regional climate modeling, *J. Clim.*, *12*, 592–609, 1999.
Huffman, G. J., et al., The Global Precipitation Climatology Project (GPCP) combined precipitation data set, *Bull. Am. Meteorol. Soc.*, *78*, 5–20, 1997.
Janowiak, J., G. Bell, and M. Chelliah, A gridded data base of daily temperature maxima and minima for the conterminous US: 1948–1993, *NCEP/CPC Atlas 6*, Clim. Pred. Cent., Natl. Cent. for Environ. Predict., Camp Springs, Md., 1999.
Juang, H., and M. Kanamitsu, The NMC nested regional spectral model, *Mon. Weather Rev.*, *122*, 3–26, 1994.
Juang, H., S. Hong, and M. Kanamitsu, The NMC nested regional spectral model: An update, *Bull. Am. Meteorol. Soc.*, *78*, 2125–2143, 1997.
Kalnay, E., et al., NCEP/NCAR 40-year reanalysis project, *Bull. Am. Meteorol. Soc.*, *77*, 437–471, 1996.
Kanamitsu, M., Description of the NMC global data assimilation and forecast system, *Weather Forecast.*, *4*, 335–342, 1989.
Kanamitsu, M., and S. Saha, Systematic tendency error in budget calculations, *Mon. Weather Rev.*, *124*, 1145–1160, 1996.
Kanamitsu, M., W. Ebisuzaki, J. Woolen, J. Potter, and M. Fiorino, NCEP/DOE AMIP-II Reanalysis (R-2), *Bull. Am. Meteorol. Soc.*, *83*, 1631–1643, 2002.
Kimball, J. S., S. W. Running, and R. Nemani, An improved method for estimating surface humidity from daily minimum temperature, *Agric. For. Meteorol.*, *85*, 87–98, 1997.
Lakshmi, V., and J. Susskind, Comparison of TOVS derived land surface variables with ground observations, *J. Geophys. Res.*, *105*, 2001–2004, 2000.
Lawford, R. G., midterm report on the GEWEX Continental-Scale International Project, *J. Geophys. Res.*, *104*, 19,279–19,292, 1999.
Liang, X., D. P. Lettenmaier, E. Wood, and S. J. Burges, A simple hydrologically based model of land surface water and energy fluxes for general circulation models, *J. Geophys. Res.*, *99*, 14,415–14,428, 1994.
Loveland, T. R., and A. S. Belward, The IGBP-DIS global 1 km land cover data set, DISCover: First results, *Intl. J. Remote Sens.*, *18*, 3289–3295, 1997.
Maurer, E. P., and D. P. Lettenmaier, Calculation of undepleted runoff for the GCIP region, 1988–2000, Dep. of Civ. and Environ. Eng., Univ. of Washington, Seattle, 2001.
Maurer, E. P., G. M. O'Donnell, D. P. Lettenmaier, and J. O. Roads, Evaluation of NCEP/NCAR reanalysis water and energy budgets using macroscale hydrologic simulations, in *Land Surface Hydrology, Meteorology, and Climate: Observations and Modeling*, edited by V. Lakshmi, J. Albertson, and J. Schaake, pp. 137–158, AGU, Washington, D.C., 2001a.
Maurer, E. P., G. M. O'Donnell, D. P. Lettenmaier, and J. O. Roads, Evaluation of the land surface water budget in NCEP/NCAR and NCEP/DOE reanalyses using an off-line hydrologic model, *J. Geophys. Res.*, *106*, 17,841–17,862, 2001b.
Maurer, E. P., A. W. Wood, J. C. Adam, D. P. Lettenmaier, and B. Nijssen, A long-term hydrologically-based data set of land surface fluxes and states for the conterminous United States, *J. Clim.*, *15*, 3237–3251, 2002.
Mesinger, F., NCEP regional reanalysis, paper presented at Symposium on Observations, Data Assimilation, and Probabilistic Prediction and 16th Conference on Hydrology, Am. Meteorol. Soc., Orlando, Fla., 2002.
Meyers, T. P., A comparison of summertime water and CO_2 fluxes over rangeland for well watered and drought conditions, *Agric. For. Meteorol.*, *106*, 205–214, 2001.
Miller, D. A., and R. A. White, A conterminous United States multi-layer soil characteristics data set for regional climate and hydrology modeling, *Earth Interact.*, *2*(2), 1–26, 1998. (Available at http://EarthInteractions.org)
Myneni, R. B., R. R. Nemani, and S. W. Running, Estimation of global leaf area index and absorbed par using radiative transfer models, *IEEE Trans. Geosci. Remote Sens.*, *35*, 1380–1393, 1997.

National Oceanic and Atmospheric Administration (NOAA), Cooperative Summary of the Day, TD-3200-Period of record through 1993, http://www.ncdc.noaa.gov/oa/ncdc.html, Natl. Clim. Data Cent., Asheville, N.C., 1995.

National Research Council (NRC), *GCIP: Global Energy and Water Cycle Experiment (GEWEX) Continental-Scale International Project: A Review of Progress and Opportunities, Report of the Global Energy and Water Cycle Experiment (GEWEX) Panel Climate Research Committee Board on Atmospheric Sciences and Climate Commission on Geosciences, Environment and Resources*, 93 pp., Natl. Acad. Press, Washington, D.C., 1998.

National Research Council (NRC), *Enhancing Access to NEXRAD data: A Critical National Resource, Report of the Global Energy and Water Cycle Experiment (GEWEX) Panel Climate Research Committee Board on Atmospheric Sciences and Climate Commission on Geosciences, Environment and Resources*, 16 pp., Natl. Acad. Press, Washington, D.C., 1999.

Pan, H.-L., A simple parameterization of evapotranspiration over land for the NMC medium-range forecast model, *Mon. Weather Rev.*, *118*, 2500–2512, 1990.

Pan, H.-L., and W. Wu, Implementing a mass flux convective parameterization package for the NMC medium-range forecast model, 1995, *NMC Off. Note 409*, Environ. Model. Cent., Natl. Cent. for Environ. Predict., Camp Springs, Md., 1995.

Pinker, R., J. Tarpley, I. Laszlo, and K. Mitchell, Surface radiation budgets in support of the GEWEX Continental Scale International Project (GCIP), *J. Geophys. Res.*, *108*, doi:10.1029/2002JD003301, in press, 2003.

Randel, D. L., T. H. Vonder Haar, M. A. Ringerud, G. L. Stephens, T. J. Greenwald, and C. L. Combs, A new global water vapor data set, *Bull. Am. Meteorol. Soc.*, *77*, 1233–1246, 1996.

Raschke, E., U. Karstens, R. Nolte-Holube, R. Brandt, H.-J. Isemer, D. Lohmann, M. Lobmeyr, B. Rockel, and R. Stuhlmann, The Baltic Sea Experiment BALTEX: A brief overview and some selected results of the authors, *Surv. Geophys.*, *19*, 1–22, 1998.

Raschke, E., et al., Baltic Sea Experiment (BALTEX): A European contribution to the investigation of the energy and water cycle over a large drainage basin, *Bull. Am. Meteorol. Soc.*, *82*, 2389–2413, 2001.

Rasmusson, E. M., Atmospheric water vapor transport and the water balance of North America: Characteristics of the water vapor flux field, *I., Mon. Weather Rev.*, *95*, 403–426, 1967.

Rasmusson, E. M., Atmospheric water vapor transport and the water balance of North America: II. Large-scale water balance investigations, *Mon. Weather Rev.*, *95*, 720–734, 1968.

Rawls, W. J., D. Gimenez, and R. Grossman, Use of soil texture, bulk density, and slope of the water retention curve to predict saturated hydraulic conductivity, *Trans. ASAE*, *41*, 983–988, 1998.

Reichler, T. J., and J. O. Roads, The role of boundary and initial conditions for dynamical seasonal predictability, *Nonlinear Proc. Geophys.*, *10*(3), 1–22, 2003.

Reybold, W. U., and G. W. Tesselle, Soil geographic databases, J, *Soil Water Conserv.*, *43*, 226–229, 1988.

Roads, J., Closing the water cycle, *GEWEX News 12*, pp. 6–8, Int. GEWEX Proj. Off., Silver Spring, Md., 2002.

Roads, J., The NCEP/NCAR, NCEP/DOE, TRMM: Tropical atmosphere hydrologic cycles, *J. Hydrometeorol.*, in press, 2003.

Roads, J., and A. Betts, NCEP/NCAR and ECMWF reanalysis surface water and energy budgets for the Mississippi River Basin, *J. Hydrometeorol.*, *1*, 88–94, 2000.

Roads, J. O., and S.-C. Chen, Surface water and energy budgets in the NCEP regional spectral model, *J. Geophys. Res.*, *105*, 29,539–29,550, 2000.

Roads, J. O., S.-C. Chen, A. Guetter, and K. Georgakakos, Large-scale aspects of the United States hydrologic cycle, *Bull. Am. Meteorol. Soc.*, *75*, 1589–1610, 1994.

Roads, J. O., S.-C. Chen, M. Kanamitsu, and H. Juang, GDAS' GCIP energy budgets, *J. Atmos. Sci.*, *54*, 1776–1794, 1997.

Roads, J. O., S.-C. Chen, M. Kanamitsu, and H. Juang, Vertical structure of humidity and temperature budget residuals over the Mississippi River Basin, *J. Geophys. Res.*, *103*, 3741–3759, 1998.

Roads, J., S. Chen, M. Kanamitsu, and H. Juang, Surface water characteristics in NCEP global spectral model reanalysis, *J. Geophys. Res.*, *104*, 19,307–19,327, 1999.

Roads, J. O., S. C. Chen, and F. Fujioka, ECPC's weekly to seasonal global forecasts, *Bull. Am. Meteorol. Soc.*, *82*, 639–658, 2001.

Roads, J., M. Kanamitsu, and R. Stewart, CSE water and energy budgets in the NCEP-DOE reanalysis II, *J. Hydrometeorol.*, *3*, 128–165, 2002a.

Roads, J., et al., *GCIP Water and Energy Budget Synthesis (WEBS)* [CD-ROM], GAPP Program Off., Silver Spring, Md., 2002b.

Roads, J., S. Chen, and M. Kanamitsu, U.S. regional climate simulations and seasonal forecasts, *J. Geophys. Res.*, *108*(D16), 8606, doi:10.1029/2002JD002232, 2003.

Robock, A., C. A. Schlosser, K. Y. Vinnikov, N. A. Speranskaya, J. K. Entin, and S. Qiu, Evaluation of AMIP soil moisture simulations, *Global Planet. Change*, *19*, 181–208, 1998.

Robock, A., K. Y. Vinnikov, G. Srinivasan, J. K. Entin, S.E. Hollinger, N.A. Speranskaya, S. Liu, and A. Namkhai, The global soil moifssture data bank, *Bull. Am. Meteorol. Soc.*, *81*, 1281–1299, 2000.

Rogers, E., T. L. Black, D. G. Deaven, and G. J. DiMego, Changes to the operational "early" Eta analysis/forecast system at the National Centers for Environmental Prediction, *Weather Forecast.*, *11*, 391–413, 1996.

Smith, J. A., D. J. Seo, M. L. Baeck, and M. D. Hudlow, An intercomparison study of NEXRAD precipitation estimates, *Water Resour. Res.*, *32*, 2035–2045, 1996.

Solley, W. B., R. R. Pierce, and H. A. Perlman, Estimated use of water in the United States in 1995, *U.S. Geol. Surv. Circ.*, *1200*, 71 pp., 1998.

Srinivasan, G., A. Robock, J. K. Entin, L. Luo, K. Y. Vinnikov, P. Viterbo, and Participating AMIP Modeling Groups, Soil moisture simulations in revised AMIP models, *J. Geophys. Res.*, *105*, 26,635–26,644, 2000.

Stewart, R. E., H. G. Leighton, P. Marsh, G. W. K. Moore, H. Ritchie, W. R. Rouse, E. D. Soulis, G. S. Strong, R. W. Crawford, and B. Kochtubajda, The Mackenzie GEWEX Study: The water and energy cycles of a major North American river basin, *Bull. Am. Meteorol. Soc.*, *79*, 2665–2683, 1998.

Susskind, J., J. Rosenfield, and D. Reuter, Remote sensing of weather and climate parameters from HIRS2/MSU on Tiros-N, *J. Geophys. Res.*, *89*, 4677–4697, 1984.

Susskind, J., P. Piraino, L. Rokke, L. Iredell, and A. Mehta, Characteristics of the TOVS Pathfinder Path A data set, *Bull. Am. Meteorol. Soc.*, *78*, 1449–1472, 1997.

Tackle, E. S., et al., Project to Intercompare Regional Climate Simulations (PIRCS): Description and initial results, *J. Geophys. Res.*, *104*, 19,443–19,461, 1999.

Thornton, P. E., and S. W. Running, An improved algorithm for estimating incident daily solar radiation from measurements of temperature, humidity, and precipitation, *Agric. For. Meteorol.*, *93*, 211–228, 1999.

Todini, E., The ARNO rainfall-runoff model, *J. Hydrol.*, *175*, 339–382, 1996.

Troen, I., and L. Mahrt, A simple model of the atmospheric boundary layer: Sensitivity to surface evaporation, *Boundary Layer Meteorol.*, *37*, 129–148, 1986.

U.S. Army Corps of Engineers,, Reservoir regulation studies-daily routing model studies, Missouri River Master Water Control Manual Review and Update Study, Northwest Div., Omaha, Nebr., 1998.

Vinnikov, K. Y., A. Robock, S. Qiu, J. K. Entin, M. Owe, B. J. Choudhury, S. E. Hollinger, and E. G. Njoku, Satellite remote sensing of soil moisture in Illinois, USA, *J. Geophys. Res.*, *104*, 4145–4168, 1999a.

Vinnikov, K. Y., A. Robock, S. Qiu, and J. K. Entin, Optimal design of surface networks for observation of soil moisture, *J. Geophys. Res.*, *104*, 19,743–19,749, 1999b.

Widmann, M., and C. S. Bretherton, Validation of mesoscale precipitation in the NCEP reanalysis using a new grid-cell data set for the northwestern United States, *J. Clim.*, *13*, 1936–1950, 2000.

Wiener, J. G., C. R. Fremling, C. E. Korschgen, K. P. Kenow, E. M. Kirsch, S. J. Rogers, Y. Yin, and J. S. Sauer, Mississippi River Basin, in *Status and Trends of the Nation's Biological Resources*, vol. 1, pp. 351–384, U.S. Geol. Surv., Reston, Va., 1998.

Wilson, K. B., and D. D. Baldocchi, Seasonal and interannual variability of energy fluxes over a broadleaved temperate deciduous forest in North America, *Agric. For. Meteorol.*, *100*, 1–18, 2000.

World Climate Research Program, Coordinated Enhanced Observing Period (CEOP) implementation plan, *IGPO Publ. Ser. 36*, Int. GEWEX Proj. Off., Silver Spring, Md., 2001.

Xie, P., and P. A. Arkin, Analysis of global monthly precipitation using gauge observations, satellite estimates, and numerical model predictions, *J Clim.*, *9*, 840–858, 1997.

Yarosh, E. S., C. F. Ropelewski, and E. H. Berbery, Biases of the observed atmospheric water budgets over the central United States, *J. Geophys. Res.*, *104*, 19,349–19,360, 1999.

Zhao, R.-J., L.-R. Fang, X.-R. Liu, and Q.-S. Zhang, The Xinanjiang model, in *Hydrological Forecasting: Proceedings of the Oxford Symposium, IASH Publ.*, *129*, 351–356, 1980.

Zhao, Q., T. L. Black, and M. E. Baldwin, Implementation of cloud prediction scheme in the Eta model at NCEP, *Weather Forecast.*, *12*, 697–711, 1997.

E. Bainto, S. Chen, M. Kanamitsu, T. Reichler, and J. Roads, Scripps Institution of Oceanography, University of California San Diego, 441 Nierenberg Hall, 8605 La Jolla Shores Drive, La Jolla, CA 92093, USA. (jroads@ucsd.edu)

E. Berbery, R. Pinker, and K. Vinnikov, Department of Meteorology, University of Maryland, College Park, College Park, MD 20742, USA.

B. Fekete and C. Vörösmarty, Complex Systems Research Center, University of New Hampshire, Durham, NH 03824, USA.

K. Gallo and K. Verdin, U.S. Geological Survey EROS Data Center, 47914 252nd Street, Sioux Falls, SD 57198, USA.

A. Grundstein and T. Mote, Department of Geography, University of Georgia, Athens, GA 30602, USA.

W. Higgins, K. Mitchell, and E. Yarosh, NOAA Science Center, NCEP/EMC/CPC, World Weather Building, 5200 Auth Road, Camp Springs, MD 20746, USA.

W. Krajewski, IIHR-Hydroscience and Engineering, University of Iowa, Iowa City, IA 52242, USA.

V. Lakshmi, Department Geological Sciences, University of South Carolina, Columbia, SC 29208, USA.

R. Lawford, NOAA Office of Global Programs, Suite 1210, 1100 Wayne Avenue, Silver Spring, MD 20910, USA.

D. Leathers, Department of Geography, University of Delaware, Newark, DE 19716, USA.

D. Lettenmaier and E. Maurer, Department of Civil and Environmental Engineering, University of Washington, Seattle, WA 98195, USA.

L. Luo, D. Robinson, and A. Robock, Department of Environmental Sciences, Rutgers University, New Brunswick, NJ 08901, USA.

T. Meyers, NOAA/ATDD, P. O. Box 2456, Oak Ridge, TN 37830, USA.

D. Miller, EMS Environment Institute, Penn State, University Park, PA 16802, USA.

J. Smith, Department of Civil and Environmental Engineering, Princeton University, Princeton, NJ 08544, USA.

G. Srinivasan, Earth System Science Division, Department of Science and Technology, New Delhi 110016, India.

T. Vonder Haar, Department of Atmospheric Science, Colorado State University, Fort Collins, CO 80523, USA.

S. Williams, UCAR, P. O. Box 3000, Boulder, CO 80307, USA.